GROWTH RESPONSE OF THE GREEN ALGA *PICOCHLORUM OKLAHOMENSIS* TO NUTRIENT LIMITATION AND SALINITY STRESS

By

JOSEPH NANA ANNAN

Bachelor of Science (Hons) in Botany and Zoology
Diploma in Education
University of Cape Coast
Cape Coast, Ghana
1992

Master of Philosophy in Botany
University of Cape Coast
Cape Coast, Ghana
1999

Submitted to the Faculty of the
Graduate College of the
Oklahoma State University
in partial fulfillment of
the requirements for
the Degree of
DOCTOR OF PHILOSOPHY
July, 2008

GROWTH RESPONSE OF THE GREEN ALGA

PICOCHLORUM OKLAHOMENSIS TO NUTRIENT

LIMITATION AND SALINITY STRESS

Dissertation Approved:

Dr. William J. Henley

Dissertation Adviser

Dr. Robert L. Burnap

Dr. Robert V. Miller

Dr. Gerald F. Schönknecht

Dr. A. Gordon Emslie

Dean of the Graduate College

ACKNOWLEDGEMENTS

I am grateful to Dr. William J. Henley for being a great adviser, mentor and friend to me. I have gained valuable experiences through his guidance, insightful knowledge, patience, suggestions and encouragement. Words cannot express how grateful I am. I would also like to thank the other members of my committee, Dr. Robert L. Burnap, Dr. Robert V. Miller and Dr. Gerald F. Schönknecht for their time, assistance and encouragement. I am particularly grateful to Dr. Burnap for allowing me to use his lab for the fluorescence measurements.

I am also grateful for the opportunity of knowing and working with other faculty members and staff of the Department of Botany as well as past and present members of Dr. Henley's Lab.

I am thankful for financial support in the form of research assistantship, chemicals and materials through National Science Foundation Microbial Observatories grant MCB-0132097 to Dr. Henley; teaching assistantship from Botany Department and some tuition waivers from the College of Arts and Sciences and the Graduate College.

Special thanks to my darling wife, Abena for her tender loving care, understanding, encouragement and support. I also thank my parents and parents-in-law for their love and support.

Finally I would also like to thank the many people I cannot mention whom the Almighty Lord used to provide physical, emotional and spiritual support during my stay here at Oklahoma State University.

TABLE OF CONTENTS

LIST OF TABLES

LIST OF FIGURES

Figure Page

CHAPTER I

INTRODUCTION

Origin, Characteristics and Classification of *Picochlorum oklahomensis*

Picochlorum oklahomensis, a unicellular halotolerant green alga, was isolated from shallow evaporitic pools at the Salt Plains National Wildlife Refuge (SPNWR) in northwestern Oklahoma, USA. *Picochlorum* sp is classified as belonging to the Domain Eukarya, Kingdom Protista, Division Chlorophyta and Class Trebouxiophyceae (Graham and Wilcox, 2000; Henley et al. 2002; 2004).

Picochlorum is a spherical green alga of approximately 2 μm in diameter. It has a nucleus, one lateral chloroplast and one mitochondrion. Members of the Trebouxiophyceae generally contain chlorophylls *a* and *b*, lutein, neoxanthin and ß-carotene. Plasmalemma and cell walls are present but it lacks flagella and it is known to reproduce by autosporulation (Henley et al. 2002; 2004).

The SPNWR is characterized as being a hypersaline environment which has a warm-temperate, semiarid, continental climate (Henley et al. 2002). Hypersaline environments, including the SPNWR usually have high salinity, exhibit fluctuations in their salt concentration over time because they are generally found in areas which are occasionally flooded by rain or seawater and are also subject to evaporation. Some minerals may precipitate as a result of the evaporation and this could lead to changes in the brine

composition (Eugster and Jones 1979; Nissenbaum 1980). Nutrient concentrations and ratios do vary with salinity and anion composition in saline lakes and these changes in salinity can potentially affect algal nutrient requirements (Schobert 1974; Cole et al. 1986). Organisms living in the SPNWR are exposed to these variations in various environmental factors and may have develop ways to cope with these changes.

There is uncertainty about the effects of high and variable salinity on nutrient solubility and bioavailability. It is anticipated that high salinity would make nutrient less bioavailable to the organism because of precipitation and therefore organisms found in such environments may become adapted to low nutrient levels. There has been various interest in looking at the effect of salinity on algal and plant growth as well as separate studies investigating the effect of low nutrients on algae and plants. However, there has been very few studies looking at the effects of both salinity and low nutrients concurrently in algae or plants. Recent effort has been looking at either salinity and temperature, temperature and light or salinity and light, but no previous study has examined the effect of salinity and nutrients limitation relating to plants and algae particularly those from the SPNWR.

Objective

The main hypothesis for this study based on the issues raised about multiple stress factors in the previous paragraph is that the effect of salinity stress on growth and photosynthesis in *Picochlorum* will be different under high nutrient compared to limited nutrient levels. In order to test this hypothesis and understand how the nutrient level may affect the effect of salinity, I investigated the effects of three salinity levels under high

and low bicarbonate, phosphate and iron on the growth and photosynthesis of *Picochlorum* as a means to understanding part of its physiology. The specific objectives for this research were to:

- determine the effect of salinity stress on growth rate and yield in *Picochlorum* at high nutrient and nutrient limitation levels, and also
- examine the effects of salinity stress and nutrient limitation on photosynthesis and the photosynthetic apparatus in *Picochlorum*.

I expected that increasing salinity will decrease growth rate, the rate of photosynthesis and yield under high nutrient. Low nutrients should also decrease growth rates, photosynthesis and finally yield. I expected different response to increasing salinity from 10 to 50 to 100 ppt under high nutrient level from that under nutrient limitation. Since different nutrients are needed in different quantities in plants and algae as well as having specific functions they perform, I expected different responses to their limitations in *Picochlorum oklahomensis* (Geider et al. 1993). I decided to study the effects of carbon, phosphorus and iron limitations because these are essential nutrients to algae and plant growth and that phosphorus and iron may be limiting in the natural environment.

Carbon

Carbon is one of the most important elements necessary for plants and algal growth and development. Carbon forms the skeleton of all the biomolecules and structures found in living organisms. It may be taken in as either carbon dioxide commonly in terrestrial habitats and to some extent in aquatic environment or as

bicarbonate (HCO_3^-) mostly in aquatic habitats. There is always less amount of dissolved CO_2 but more of HCO_3^- available at alkaline pH which is the usual pH in marine and hypersaline environment. For example at a pH of about 8.2 when seawater is in equilibrium with air, there is only about 10 μM CO_2 present and CO_2 diffusion is known to be very slow in water (Round 1981).

The problem of not having CO_2 readily available and also the precipitation of HCO_3^- may restrict the supply of inorganic carbon to marine photosynthetic organisms including microalgae. In order to overcome the challenge of carbon availability for photosynthesis, most microalgae have developed various mechanisms to efficiently take up dissolved inorganic carbon and making it available in the cells for use. The mechanisms include the active uptake of CO_2 and HCO_3^- from the growing medium, production of carbonic anhydrase and also an inorganic carbon concentrating mechanism (Falkowski and Raven 1997; Kaplan and Reinhold 1999; Giordano et al. 2005; Spalding 2008).

Apart from the normal diffusion of CO_2 into cells which is slow (Riebesell et al. 1993), some organisms have CO_2 and HCO_3^- protein transporters which help in active uptake of these inorganic carbon forms into the cells from their growing medium which require the use on energy (Rees 1984; Rotatore et al. 1995; Merrett et al. 1996; Sukenik et al. 1997; Huertas et al. 2000). Some marine microalgae have Cah genes which codes for the production of carbonic anhydrase (CA). There are different forms of these enzymes which operate under different inorganic carbon concentration levels. Depending on where they operate, there are external and internal carbonic anhydrases. The external CA catalyzes the conversion between HCO_3^- and CO_2, according to the formula: CO_2 +

$H_2O \leftrightarrow H_2CO_3 \leftrightarrow H^+ + HCO_3^-$ outside the cell but closer to the cell membrane which ensures there is enough CO_2 at the site of the CO_2 transporter (Williams and Turpin 1987; Nimer et al. 1997, Roberts et al. 1997). There are also internal carbonic anhydrases which function within the cells. Some organisms also have pyrenoids which serve as a component of the carbon dioxide concentrating mechanism (CCM) within which CO_2 is generated from HCO_3^- or in the nearby thylakoid. The main purpose of CCM is to make CO_2 more available and thus increase the CO_2 / O_2 ratio at the active site of ribulose-1,5-bisphosphate carboxylase-oxygenase (Rubisco). This favours carbon fixation and prevent Rubisco from carrying out its oxygenase activity and therefore reducing photorespiration associated with C_3 photosynthesis. Rubisco is an important component of pyrenoids in the chloroplast (Raven 1997; Raven and Beardal 2003).

During photorespiration which also uses ATP and NADPH, oxygen instead of carbon dioxide is added to ribulose-1,5-bisphosphate producing one molecule of 3-Phosphoglycerate and a molecule of 2-Phosphoglycolate. Within the chloroplast, phosphoglycolate is converted to glycolate releasing the inorganic phosphate. The glycolate is then sent to the peroxisome where oxygen is used and the glycolate is finally converted to glycine which is then sent to the mitochondria. In the mitochondria, serine is formed from glycine with the release of ammonia and CO_2. The serine is then sent to the peroxisome where NADPH is used and finally glycerate is formed which is then sent back to the chloroplast. Within the chloroplast ATP is used and the phosphoglycerate formed enters into the Calvin cycle (Siedow and Day 2000). Limitation in the supply of carbon dioxide restrict photosynthesis since CO_2 is the substrate for ribulose-1,5-bisphosphate carboxylase-oxygenase, and thereby leading to decreases in growth.

Phosphorus

Phosphorus is an essential nutrient needed for plant and algal growth (Davies 1988; Wykoff et al. 1998). It is required for the formation of biomolecules such as nucleic acids (DNA and RNA), phospholipids, sugar phosphates and catalytic cofactors. It is also associated with energy transfer (ATP) and metabolic regulation. Formation of ATP from ADP and inorganic phosphate requires a lot of energy and so the bonds between two phosphorus atoms are at a higher energy level and when these are broken down energy is released and used by the cell. Phosphorus is usually taken up actively by algae as inorganic oxyanion phosphate (PO_4^{3-}) from their growing medium. In marine environments P is mostly found dissolved organic phosphomonoesters as a result of phosphorus being esterified to organic compounds. In this form it is very difficult for algae to take them in and use.

Some algae are able to produce extracellular phosphatases which are secreted to make phosphorus available under such P limited conditions from organic phosphomonoesters, (Weich and Graneli 1989; Hernández et al. 1993; Lee 2000). Some of these phosphatases are already in the cells while others are only produced under P limited conditions to increase their activities. Since algae are able to store phosphorus as inorganic phosphorus or polyphosphate when P is readily available (Lundberg et al. 1989), they are able to use the stored phosphorus under P limited conditions thereby delaying or slowing the effects of the P limitation for a while. Low phosphorus is likely to affect the formation of nucleic acids and protein synthesis and subsequently affect cell division. Due to its involvement in the formation of ATP and the proper functioning of proton-ATPase, low P may affect active uptake and metabolism of nutrients such as

inorganic carbon and nitrogen and may also affect signal transduction. This could lead to decreases in photosynthesis and respiration, a decline in growth, and possibly result in the death of the cells if the limitation or starvation continues for a long time (Davies 1988; Plesnicar et al. 1994; Wykoff et al. 1998).

Iron

Iron is considered to be a micronutrient however it is very important for all organisms. It is commonly found in plants and algae as metalloproteins which are necessary for photosynthesis, respiration and nitrogen assimilation (Crosa 1997; Bulter 1998). Cytochromes, iron-sulphur proteins and ferredoxin all contain iron (Guikema and Sherman 1983). Raven (1990) estimated that 80% of the iron in phytoplankton forms part of the photosynthetic electron transport chain. Iron is also needed in the biosynthesis of chlorophyll and is also required for nitrate and nitrite reductases activity. In saline water iron occurs as ferric hydroxides and it normally precipitate because it forms complexes with organic ligands which then affect its solubility and availability to algae (Motekaitis and Martell 1987, Millero et al. 1995, Sunda and Huntsman 1995).

Some phytoplanktons have iron transporters to help with the uptake of iron from the environment. However a limitation encountered is that these are found to be responsive to only dissolved inorganic iron (Anderson and Morel 1982; Hudson and Morel 1990; 1993). Another mechanism for efficient iron uptake used by eukaryotic phytoplanktons is the production of siderophores which help to release the iron bound to organic ligands. The siderophores are usually produced under low iron and are thought to be low molecular weight chelators which form stable complexes with Fe (III) (Trick 1989; Wilhelm and Trick 1994).

It has been observed that in order to easily release the iron bound to the siderophores, microorganisms and plants make use of ligand exchange at the cell surface, hydrolysis, and acidification and reduction of Fe (III) (Neilands 1974; Guerinot and Yi 1994). Since iron is part of almost all the components of the photosynthetic electron transport chain, implies that photosynthesis would be greatly affected by iron deficiency. Doucette and Harrison (1991) have report of decrease in the size and structure of chloroplast in iron limited grown cells.

Salinity

Salinity refers to the salt content of water or the soil. It is considered to be a very important environmental factor because of its role in reducing crop yield in most part of the world (Komori et al. 2003). Apart from challenges experienced by organisms in the natural habitats such as marine and hypersaline environment, increases in salinity is also encountered as a result of inappropriate irrigation techniques employed by farmers in soils considered to be arid or semiarid. Salinity stress may affect plants and algae through osmotic and ionic stress. Water deficit bring about osmotic stress while as a result of excess Na^+ and Cl^- and reduction in the uptake of other mineral nutrients can bring about ionic imbalances or stress (Ashraf and Harris 2004). Plants which are sensitive to salinity stress are called glycophytes and those which are able to tolerate salt stress are referred to as being halotolerant or halophytes.

Plants and algae may differ in the way they respond to salt stress. Some are able to tolerate the salt stress within certain limits without any problem. Others are able to exclude the salts through their leaves or salt glands. Still others produce compounds

making their tissues tolerant to the salt concentration. One of such common ways is the production of osmoprotectants or compatible solutes to lower the internal water potential of the cell and thus being able to take up water from the environment. The compatible solutes include mannitol and proline. Proline is produced in the cell from glutamate and the synthesis requires ATP and NADPH. Trying to maintain proper osmotic conditions nay therefore be at a high energy cost which may be manifested in reduced growth rates and decrease in photosynthetic electron transport activities (Gimmler et al. 1981; Kirst 1989; Ashraf and Harris 2004). Lawlor (2002) suggested that these osmoprotectant may also play other roles in organisms such as being nitrogen sources during periods of reduced growth and photosynthesis.

Salt stress also affects protein synthesis, the functioning of some enzymes and also the membrane integrity. Salinity may also cause disorganization of PSII. When salinity negatively affects membrane lipids, it leads to problems with membrane permeability, transporters and enzymes (Kerkeb et al. 2001).

CHAPTER II

MATERIALS AND METHODS

Organism

The organism used in this study is *Picochlorum oklahomensis,* a unicellular green alga, which was isolated from the Salt Plains National Wildlife Refuge, Oklahoma, USA in 1998.

Growth media

The cultures were maintained in artificial seawater medium, AS100 (Starr and Zeikus, 1993) but with some modification. The sodium chloride (NaCl) content was changed to give a concentration of 10, 50 and 100 ppt. The salinity was checked using a hand-held refractometer (A366ATC). In preparing the AS100 medium, $MgSO_4$, KCl, $NaNO_3$, $CaCl_2$, NH_4Cl and Tris buffer (pH of 8.08) were added to the sodium chloride solution and then after autoclaving, the vitamins, sodium thiosulfate, chelated iron, sodium bicarbonate, and potassium dihydrogen phosphate solutions were added, using a syringe and Acrodisc 0.2-μm sterile syringe filters.

Iron limitation was induced by not adding iron to the medium (though minute quantities of impurities may be present in the chemicals used). For low bicarbonate and low phosphate, the concentrations were 500 μM and 1.8 μM respectively. The control medium had 2 mM HCO_3^-, 37 μM PO_4^{3-} and 11.7 μM chelated iron. 50 ml of each

treatment was poured into a 125-ml Erlenmeyer flask made from optically clear polycarbonate and plugged with cotton wool surrounded with aluminium foil. There were three flasks maintained for each treatment giving three replicate cultures of *Picochlorum* for each treatment. The preparation of the medium and the inoculation procedures were carried out in a laminar flow hood under sterile conditions.

Growth conditions

The experimental cultures were kept in a growth room at a day/night temperature regime of about 27° to 35° C and a photon fluence rate (PFD) of about 200 μmol photons·m^{-2}· s^{-1}. The source of light was a 1000-watt metal halide lamp at a 14:10-h light:dark (L:D) cycle. For the experiments, the inoculum from the stock culture in Salt Plain medium (prepared from salt brine from the salt plains) was preacclimated in a 50 ppt AS 100 medium for seven days before inoculating for the beginning of the two-stage experiment. Samples from the first culture were used to inoculate the second set of cultures in triplicate after ten days of growth. The first stage of culture enabled the *Picochlorum* cells to acclimate to the nutrient treatments and to ensure that most of the stored nutrients had been completely used. Each treatment had three replicates.

Determination of cell numbers and initial growth rate

Samples were taken daily from each of the cultures throughout the experiment and actual cell counts performed. Total cell densities were determined by transferring 10 μl of each sample unto a hemacytometer and performing total cell count. The initial growth rate (μ, d^{-1}) was determined by fitting Jassby and Platt (1976) function of a

nonlinear curve to the graph of ln (cell density) versus time for each replicate culture using Sigma Plot 2000 software. The mathematical function by Jassby and Platt (1976) is given below:

$$F = CDm \times \tanh \{(\mu \times T)/CDm\} + CDo$$

where CDm is increase in In cell density, CDo is Initial In cell density, μ is growth rate (in d^{-1}, which is the initial slope) and T is time in days.

This equation was used because there was no prolonged exponential phase giving a linear line for the determination of initial growth rate. The cell densities at the end of day 10 were used as the final cell yield.

In order to further analysis the curvature of the graphs as a way of getting more information from my growth data, I used Bannister's function (1979) to obtain the convexity values.

$$F= CDm \times (\mu \times d/\{CDm^c + (\mu \times d)^c)^{(1/c)}\} + CDo$$

where CDm is Final In cell density, CDo is initial ln cell density, μ is growth rate (in d^{-1}, which is the initial slope), T is time in days, and c is convexity.

Photosynthetic Measurement

Six days old second stage cultures were used for this experiment. Some of the cells were concentrated in order to obtain cell densities almost equal to all treatments and spiked with 8 mM $NaHCO_3$. Photosynthetic light-response (P-I) curves were measured as whole cell oxygen exchange at 27^0C in a Hansatech DW water-jacketed, 9-mL electrode chamber with continuous stirring and connected to a computer. Samples were exposed to a series of 12 increments of photon flux densities (PFD) from darkness to > 1500 μmol

photons m^{-2} s^{-1} using a slide projector as source of light fitted with neutral density filters. Exposure to each PFD was 4 min after a 30-second equilibration period.

Photosynthetic rates (μmol O_2 hr^{-1}) were automatically calculated in real time by linear regression after each PFD. The calculated photosynthetic rates were also checked manually from the data generated and normalized to cell density. Light saturated photosynthesis (P_{max}), initial slope (α) and dark respiration (R_d) were determined by fitting individual curves to a Jassby and Platt (1976) function using Sigma Plot 2000 software.

$$F = Pm \times \tanh \{(\alpha \times I)/Pm\} - R_d$$

where Pm is light-saturated photosynthetic rate, R_d is rate of respiration in darkness, α is the initial ascending slope and I is light intensity.

Pigment Content

In order to understand the effect of low nutrient and salinity stress on the pigments in *Picochlorum*, cultures in the second stage were harvested on day 6 and the chlorophyll content determined by filtering 3 mL of each culture suspension and transferring the cells together with filter paper into 3.5 mL dimethyl-formamide (DMF) and keeping them in the dark for 24 hours. I used DMF because it has been identified as being able to chemically stabilize chlorophyll and as well as preventing its oxidation. DMF is also able to extract a lot of chlorophyll from samples compared to other solvents commonly used (Porra et al. 1989). Extracts were centrifuged to remove cellular debris and the absorption spectra measured from 400 to 750 nm using a spectrophotometer with

2-nm band pass. The concentrations of chlorophylls a and b were determined using the equations by Porra et al. (1989):

$$\text{Chlorophyll a} = 12.00\ A_{664} - 3.11\ A_{647}$$

$$\text{Chlorophyll b} = 20.78\ A_{647} - 4.88\ A_{664}$$

where A is the absorbance at the specified wavelength, corrected for scattering by subtracting A_{750}.

Total carotenoids were calculated using Wellburn's equation (1994).

$$\text{Total carotenoids} = (1000\ A_{480} - 0.89\ C_a - 52.02\ C_b)/245$$

where A_{480} is the absorbance at 480 nm, and C_a and C_b are concentrations of chlorophyll a and b respectively.

Chlorophyll fluorescence

Six days old second stage cultures were used for this experiment. Chlorophyll fluorescence quenching analysis was carried out at room temperature using a Dual–Modulation Kinetic fluorometer (PhotoSystems Instruments, Czech Republic). The fluorometer was connected to a computer with data acquisition software, Fluowin. Two mL of culture was put into a cuvette and the cuvette placed into the sample compartment for the measurement to proceed. Each sample was dark-adapted for 10 min before starting with the measurement. The minimal fluorescence level in the dark-adapted state (F_o) was measured by activating the modulated light (ML) which was very low in order to prevent the induction of significant variable fluorescence.

A 0.8 s flash of saturating white light (>1000 μmol photons·m^{-2}· s^{-1}) was then applied to determine the maximal fluorescence in the dark-adapted state, (F_m). After a lag

phase of 20 seconds, the actinic light, AL (about 400 μmol photons·m^{-2}· s^{-1}) from light-emitting diode was turned on to provide continuous white illumination for 30 seconds. In order to determine the light-adapted maximal chlorophyll fluorescence (F_m'), saturating pulses were applied to the sample at different intervals during the period of actinic light driving photosynthesis.

Using both the dark and light fluorescence parameters, I calculated the following for the fluorescence analysis: the maximum efficiency also known as optimal quantum yield of PS II photochemistry in the dark-adapted state, (F_v / F_m); the actual quantum yield of PSII electron transport in the light-adapted state, Φ_{PSII} = (F_m' - F') / F_m'; the photochemical quenching coefficient, qP = (F_m' - F') / (F_m'- F_o'), which gives a measure of the proportion of open PSII reaction centers and the non-photochemical quenching, NPQ = (F_m – F_m') / F_m' (Genty et al. 1989; Bilger and Björkman 1990). The fluorescence nomenclature used in this section follows van Kooten and Snel (1990).

Experimental design & Statistical analysis

A factorial design was used for the experiments with salinity as one factor at three levels (10 ppt, 50 ppt and 100 ppt) and nutrient as the other factor at two levels (high and low). Data of the initial growth rates, cell densities, photosynthetic parameters, pigment content and the fluorescence parameters were analyzed by using two-way analysis of variance (ANOVA) with replication at p = 0.05. The significance of the pairwise differences between treatments analyzed using Tukey HSD multiple comparison. I used SYSTAT 10 software for all the statistical analysis.

CHAPTER III

RESULTS

Growth Rates and Cell growth

There were marked differences observed in the growth curves of *Picochlorum* due to nutrient limitation and salinity stress (Fig. 1, 5 & 8). The semilog growth curve of *Picochlorum* did not follow the usual hyperbolic growth curve. The initial linear part was too brief (2 to 3 data points) for the determination of the initial growth rate using linear regression. Jassby and Platt (1976) non-linear function was therefore used in fitting it to each replicate in order to determining initial growth rates of *Picochlorum* in this experiment (Fig. 2). The function is given as:

$$F = CDm \times \tanh \{(\mu \times T)/CDm\} + CDo$$

where CDm is Final In cell density, CDo is Initial In cell density, μ is growth rate (in d^{-1}, which is the initial slope) and T is time in days.

The curve fittings for the replicates for each treatment in determining the initial growth rates using the Jassby and Platt's function are in appendix A and the Bannister's function (1979) used in determining the convexity of the growth graphs are also in appendix B.

Salinity, low bicarbonate and Growth

Picochlorum growth is largely unaffected by salinity below 50 ppt, but is reduced by about one-third at 100 ppt in high bicarbonate (HC) (Figs. 3, 5 & 8). Low bicarbonate

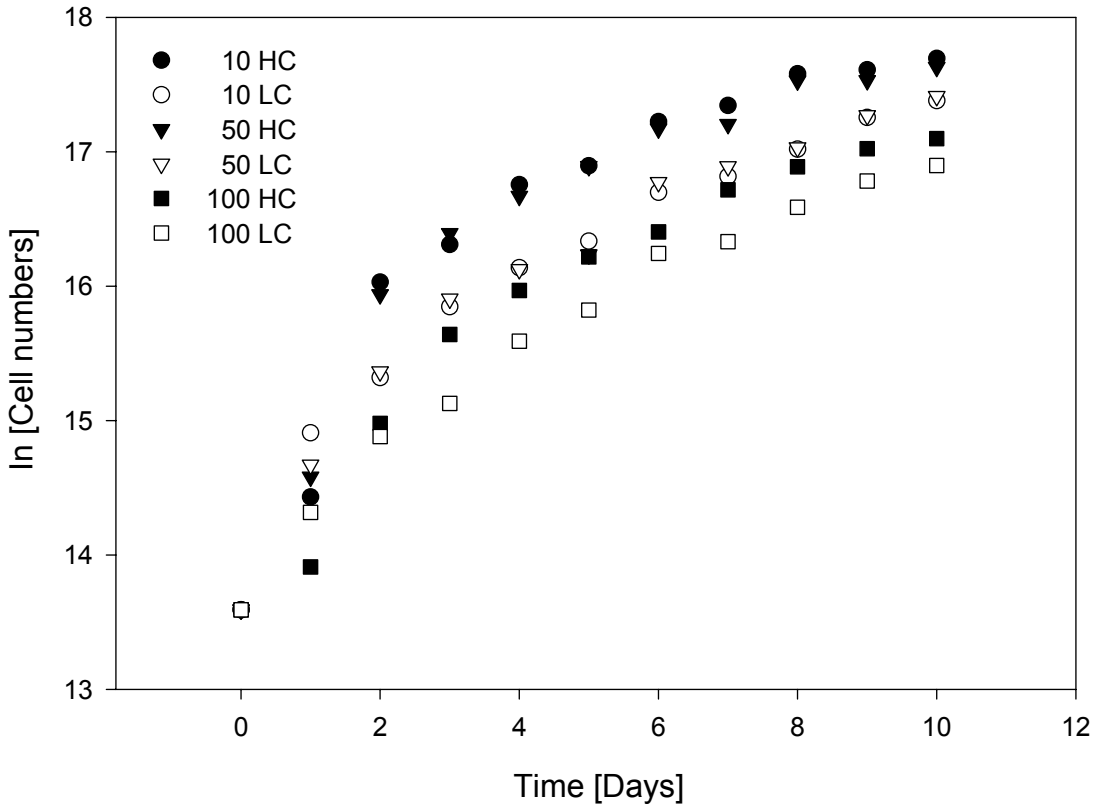

Figure 1. Mean growth response of *Picochlorum* sp. to high bicarbonate (shaded symbols, HC) and low bicarbonate (open symbols, LC) at different salinities of 10, 50 and 100 ppt (numbers after symbols). n = 3 for all treatments

A)

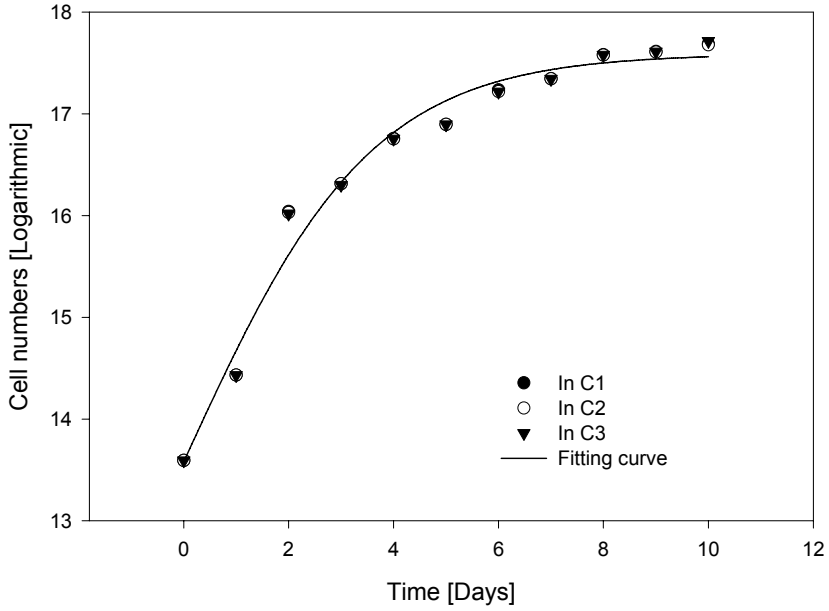

B)

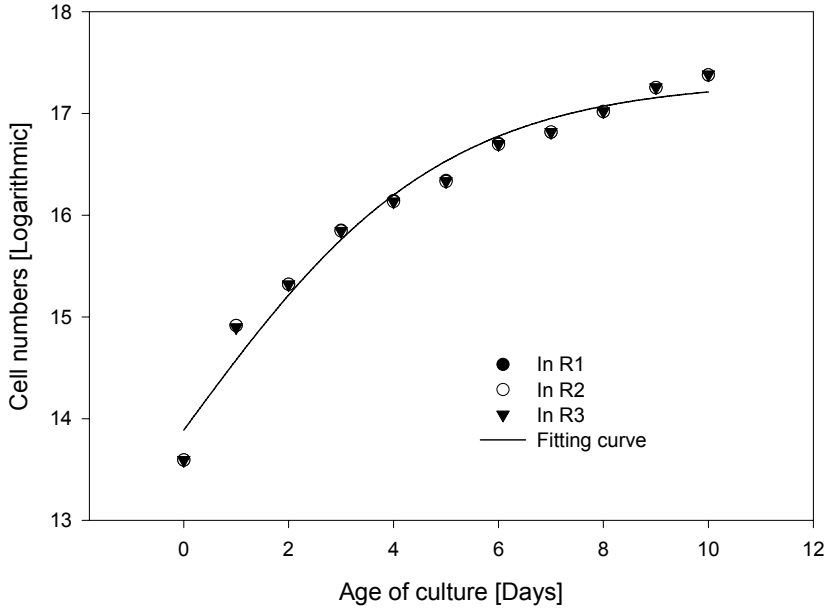

Figure 2. Growth curves of triplicate cultures of *Picochlorum* sp. in a) high bicarbonate and b) low bicarbonate at 10 ppt showing the curve fitting of Jassby and Platt's function to the logarithm of the cell densities as examples from which the initial growth rates, μ was obtained.

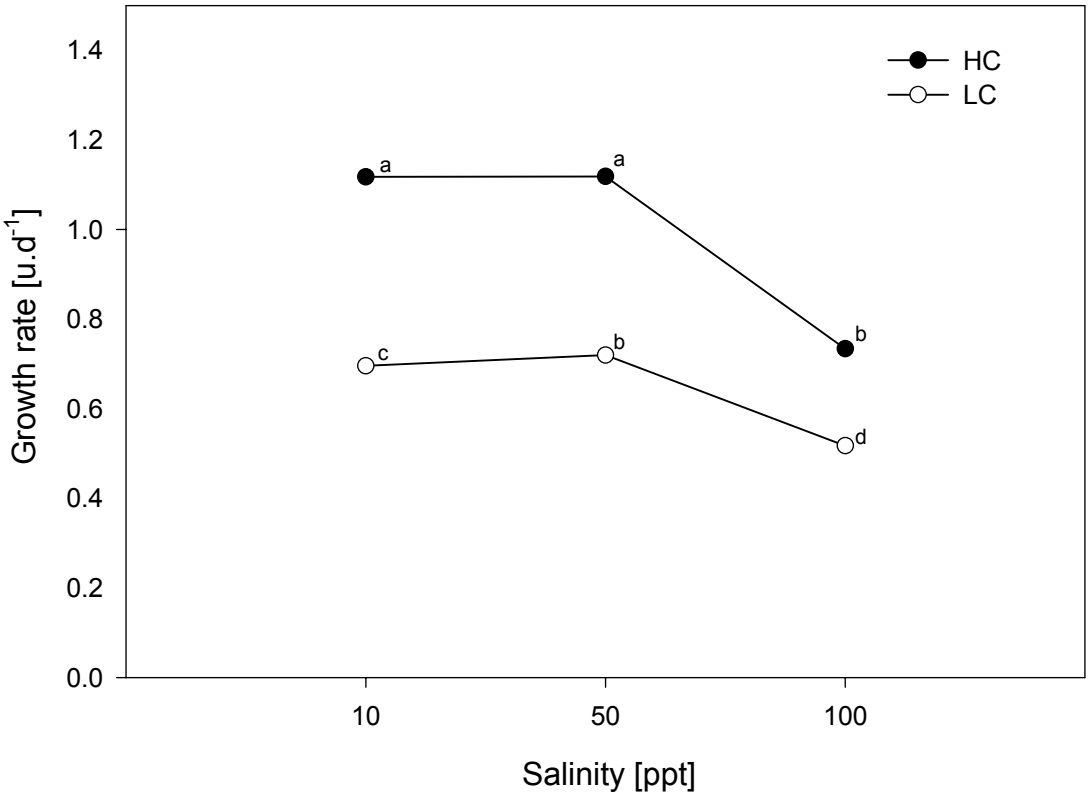

Figure 3. Initial growth rate of *Picochlorum* sp. to high bicarbonate (shaded symbols, HC) and low bicarbonate (open circles, LB) at different salinities of 10, 50 and 100 ppt. Mean values ± Standard deviation, n = 3 for all treatments (Error bars smaller than symbols). Different letters indicate significance

(LC) cultures exhibit the same pattern as HC but are shifted to lower growth rates. Primary effects of both salinity and bicarbonate were highly significant in two-way ANOVA ($p<0.01$). All individual treatments were significantly different except high bicarbonate at 10 and 50 ppt (Tukey, $p>0.05$). In addition, bicarbonate-salinity interaction was significant, because initial growth rates in high bicarbonate were the same at 10 ppt and 50 ppt but were reduced in the low bicarbonate treatment at 10 ppt. The effect of low bicarbonate was proportionately the same at 10 and 50 ppt (LC/HC = 0.6), but greater at 100 ppt. The absolute reduction of 0.2 d^{-1} at 100 ppt was the lowest compared to twice that value at 10 and 50 ppt.

Cell yields at day 10 exhibited much the same patterns as initial growth rate, with the exception that high bicarbonate yields at 10 and 50 ppt differed, whereas low bicarbonate yields 10 and 50 ppt did not (Fig. 4). Both primary effects of salinity and low bicarbonate and interaction were significant for cell yields (2-way ANOVA, $p< 0.01$). The effect of low bicarbonate was greater on initial growth rate than on cell yields at day 10.

Phosphorus limitation, salinity and Growth

Low phosphate cultures exhibit the same pattern as high phosphate but are shifted to higher initial growth rates (Fig. 6). Primary effects of both salinity and phosphate were highly significant in two-way ANOVA ($p<0.01$). All individual treatments were significantly different except high phosphate at 10 and 50 ppt and low phosphate at 10 and 50 ppt (Tukey, $p<0.05$). The effect of low phosphate was proportionately the same at

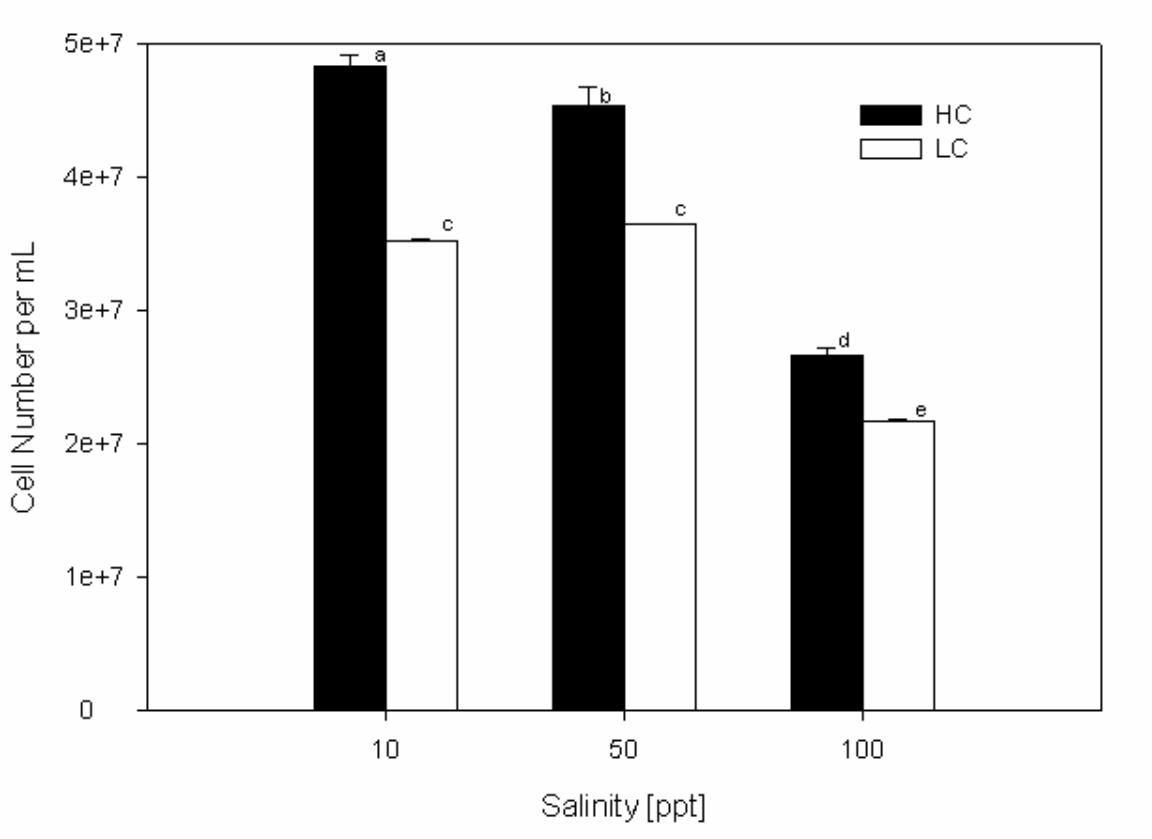

Figure 4. Cell yield of *Picochlorum* sp. at day 10 in low bicarbonate (LC) compared with high bicarbonate (HC) at different salinities. Mean values ± Standard deviation, n = 3 for all treatments. Different letters indicate significance

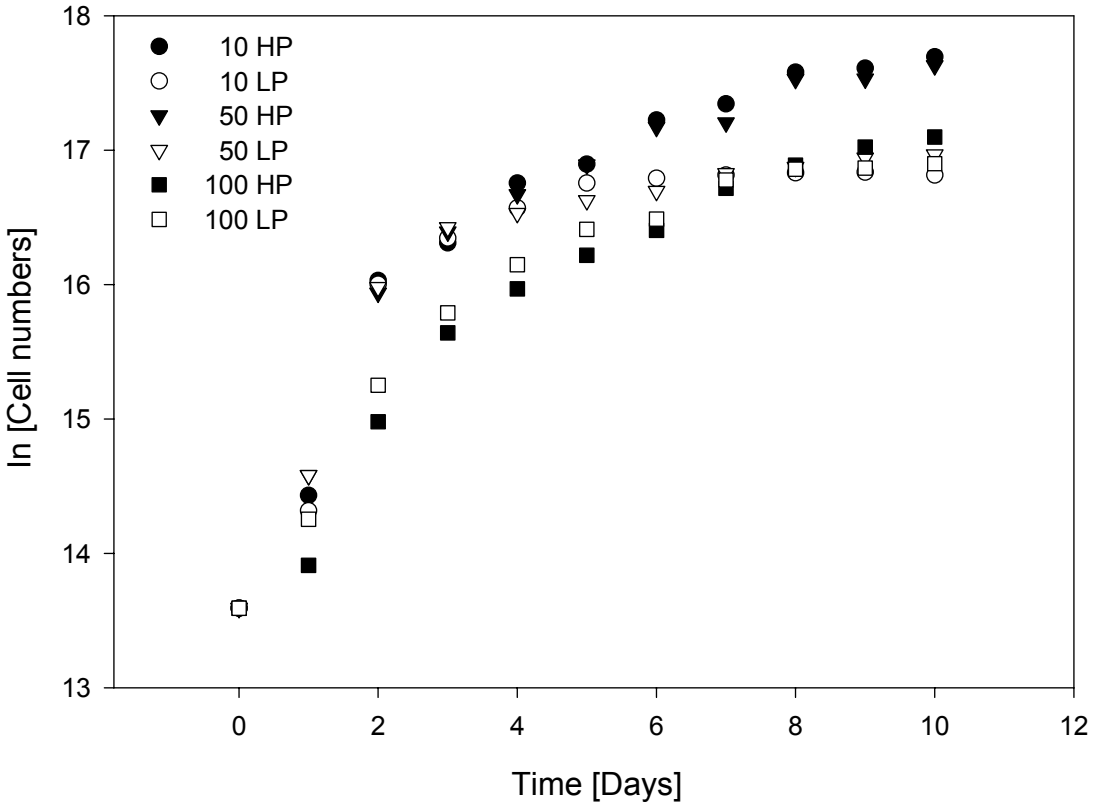

Figure 5. Mean growth response of *Picochlorum* sp. to high phosphate (shaded symbols, HP) and low phosphate (open symbols, LP) at different salinities of 10, 50 and 100 ppt (numbers after symbols). n = 3 for all treatments

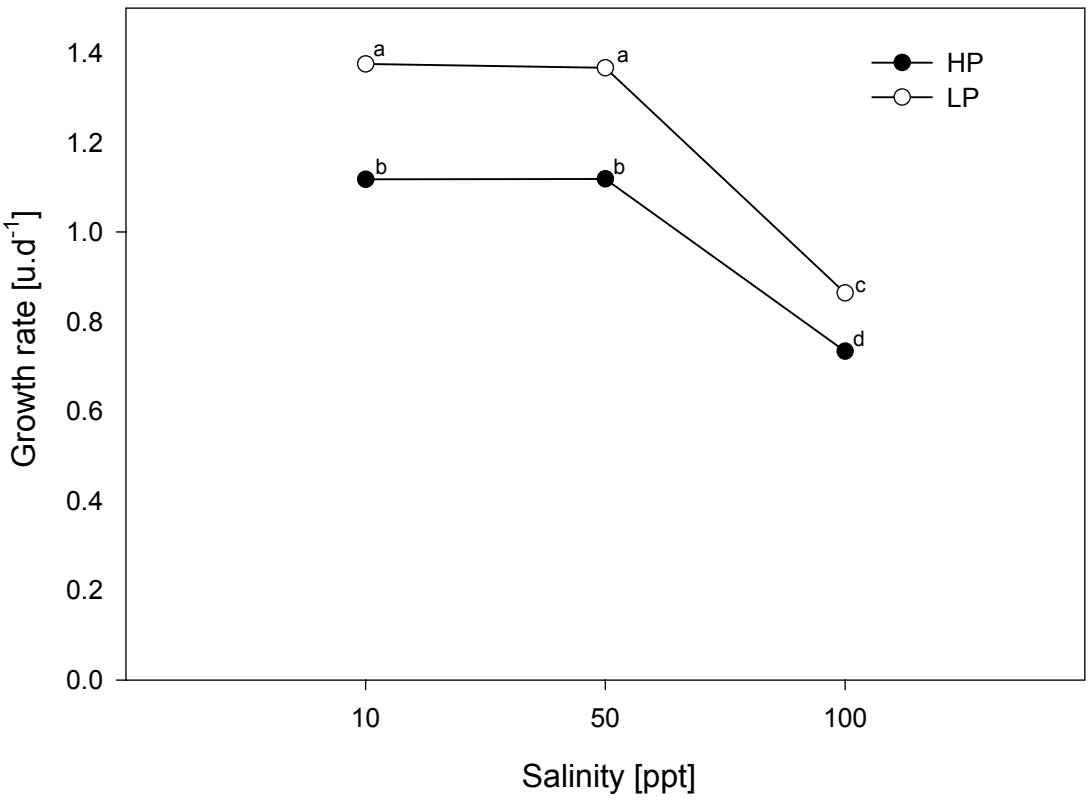

Figure 6 Initial growth rates of *Picochlorum* sp. to high phosphate (shaded symbols, HP) and low phosphate (open circles, LP) at different salinities of 10, 50 and 100 ppt. Mean values ± Standard deviation, n = 3 for all treatments (Error bars smaller than symbols) Different letters indicate significance

all salinities (LP/control = 1.2). The absolute reduction of 0.1 at 100 ppt was the lowest compared to twice that value at 10 and 50 ppt. Thus, although the significant nutrient-salinity interaction is consistent with my hypothesis, the effect is very small.

Even though initial growth rates were significantly higher in low phosphate cultures compared to control, cell yields were significantly reduced in low phosphate. Cell yields at day 10 exhibited much the same response to salinity as initial growth rate, with the exception that high phosphate yields at 10 and 50 ppt differed (Fig. 7). The reduction in yield at day 10 was about 60% at 10 ppt, 50% at 50 ppt and 20% at 100 ppt. In low phosphate, cell yield at 50 and 100 ppt were not significantly different. Both primary effects of salinity and low phosphate and interaction were significant for cell yields (2-way ANOVA, $p < 0.01$).

Iron limitation, salinity and Growth

Low iron cultures exhibit the same pattern as cultures grown in added iron (+Fe) medium but were shifted to lower initial growth rates (Fig. 8 and 9). Primary effects of both salinity and iron were highly significant in two-way ANOVA ($p<0.001$). All individual treatments were significantly different except +Fe at 10 and 50 ppt (Tukey, $p<0.05$). In addition, iron-salinity interaction was significant, because initial growth rate was reduced at 10 ppt relative to 50 ppt in the -Fe treatment, but not in the +Fe grown cells. The effect of low iron was proportionately the same at all salinities (LFe/control = 0.3). The absolute reduction of 0.6 d^{-1} at 100 ppt was the lowest compared to 0.8 d^{-1} at 10 and 50 ppt. Cell yields at day 10 exhibited different patterns from the initial growth rate.

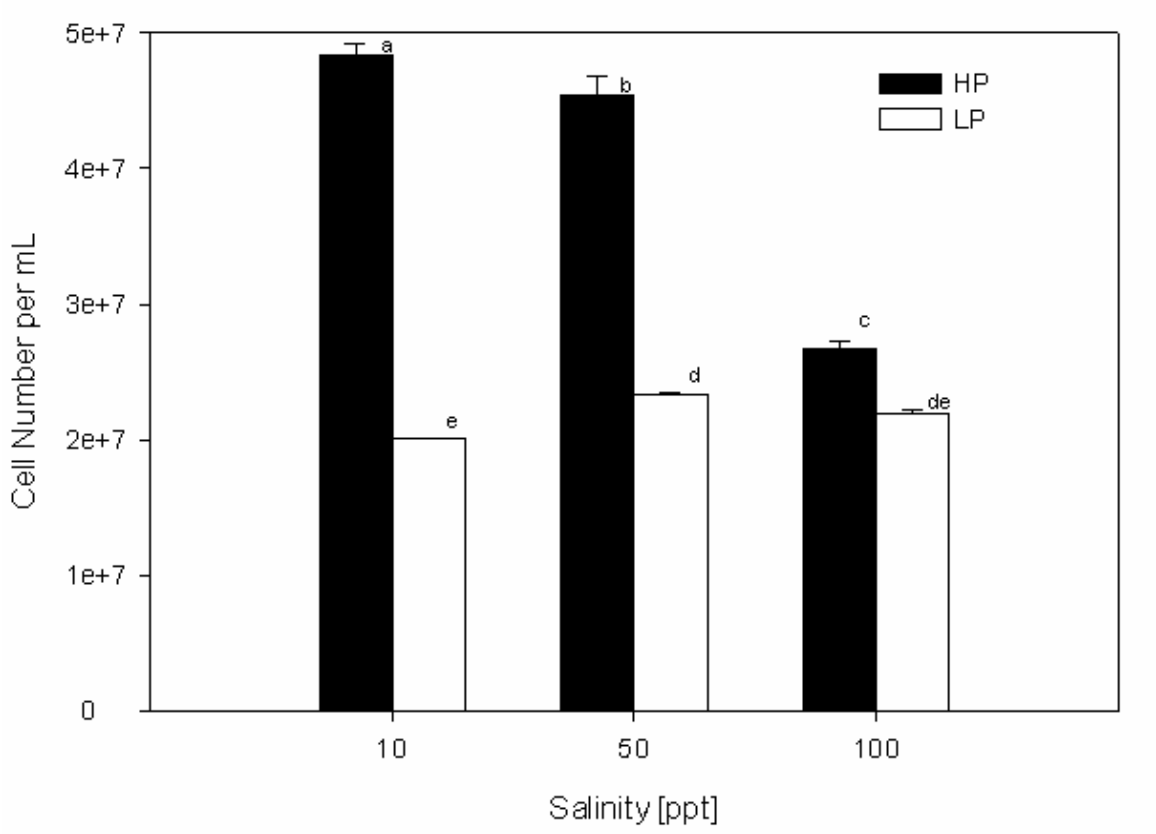

Figure 7. Cell yield of *Picochlorum* sp. at day 10 in low phosphate (LP) compared with high phosphorus (HP) at different salinities. Mean values ± Standard deviation, n = 3 Different letters indicate significance.

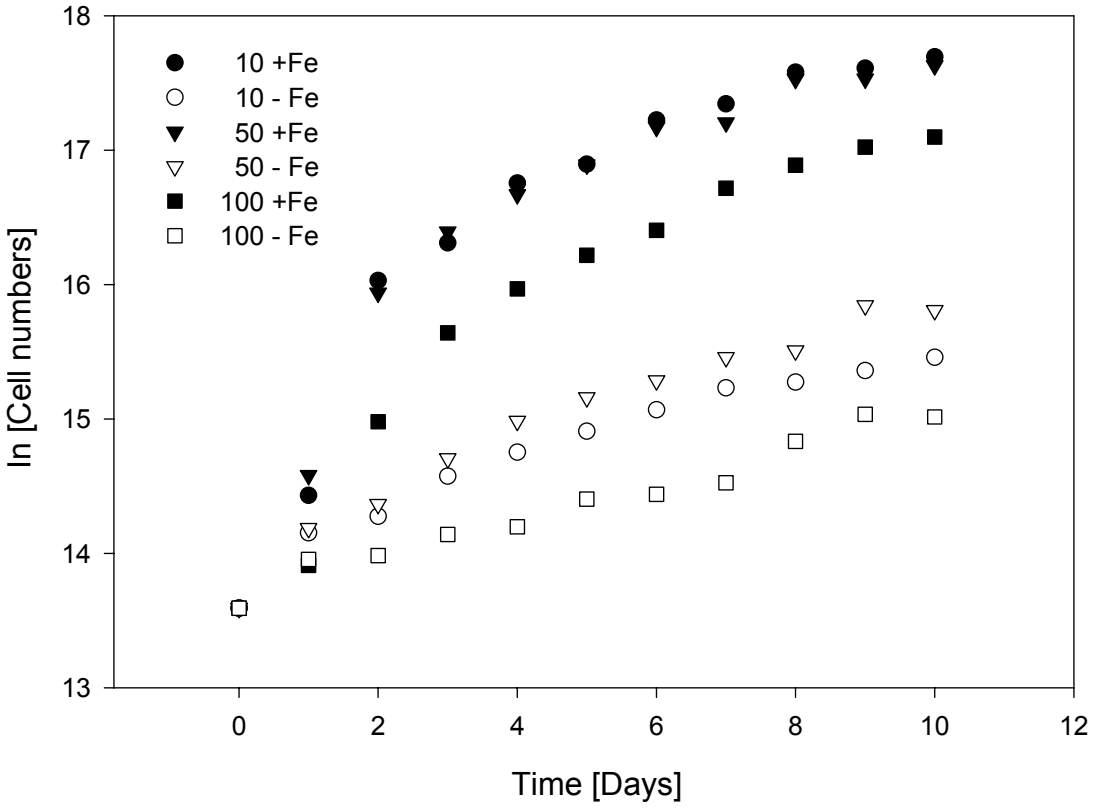

Figure 8 Mean growth response of *Picochlorum* sp. to high iron (shaded symbols, +Fe) and no added iron (open symbols, -Fe) at different salinities of 10, 50 and 100 ppt (numbers after symbols). n = 3 for all treatments

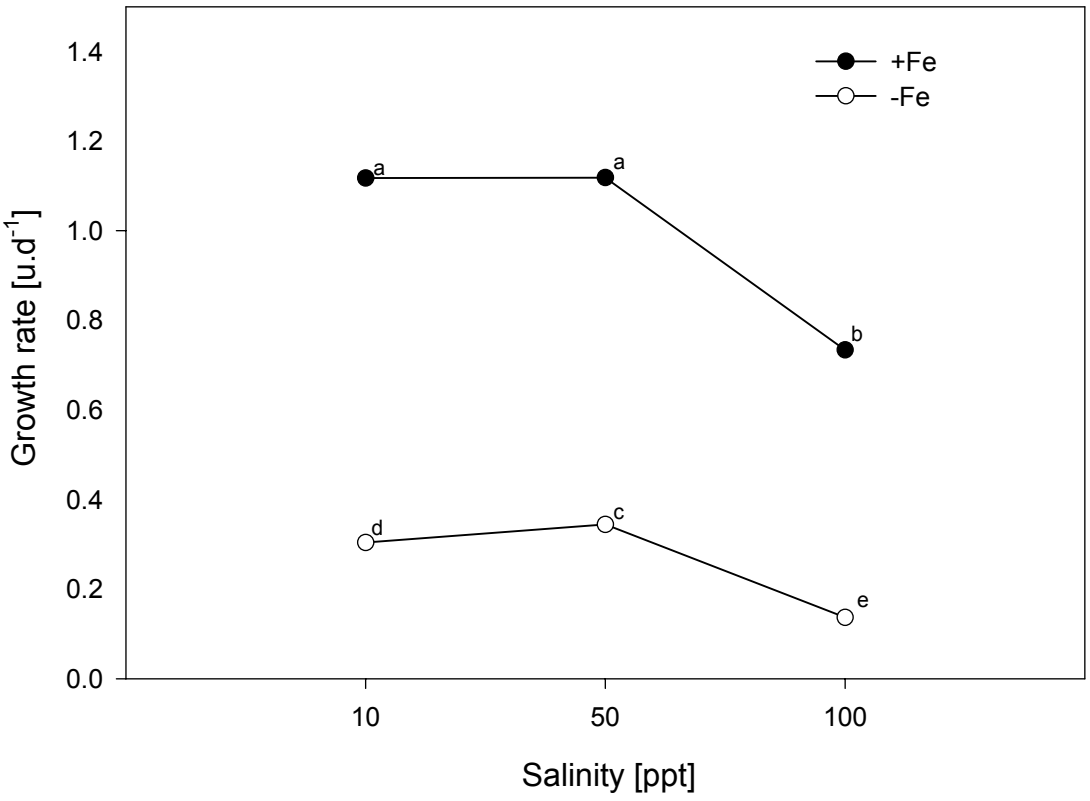

Figure 9 Initial growth rates of *Picochlorum* sp. to high iron (shaded symbols, +Fe) and low iron (open circles, -Fe) at different salinities of 10, 50 and 100 ppt. Mean values ± Standard deviation, n = 3 for all treatments (Error bars smaller than symbols). Different letters indicate significance

Increasing salinity significantly decreased cell yield in the +Fe medium however in –Fe grown cells, an increase in salinity from 10 and 50 ppt rather increased cell yield at day 10 (Fig. 10). Both primary effects of salinity and low iron as well as the interaction between these two factors were significant for cell yields (2-way ANOVA, $p< 0.01$).

Photosynthetic Measurements

In order to investigate the effect of nutrient limitation and salinity on photosynthesis in *Picochlorum*, oxygen evolution was measured and the following three fundamental parameters were calculated: The rate of respiration in darkness (R_d), the slope at limiting PFDs, α, (which comprises both light-harvesting efficiency and photosynthetic energy conversion efficiency), and the light-saturated photosynthetic rate (P_{max}). P_{max} is normally limited by the rate of carbon fixation, either by enzymatic reactions of the Calvin cycle or by diffusion and transport processes (Sukenik et al. 1987, Henley, 1993). Photosynthetic rates (μmol O_2 hr^{-1}) were automatically calculated in real time by linear regression after 270 sec exposures to PFD (Figure 11). Photosynthetic light-response (P-I) curves are shown in figures 12 – 14. These parameters were obtained for each replicate of a particular treatment (3 per treatment) and then were analyzed using ANOVA.

Neither salinity nor low bicarbonate significantly affected dark respiration, since variability was large relative to rate values (Table 1). Salinity, but not low bicarbonate, significantly affected α, (2-way ANOVA, $p<0.05$). However, none of the individual treatments differed in multiple pairwise comparisons (Tukey, $P>0.05$), probably due to inadequate statistical power with n=3. Both salinity and bicarbonate treatments

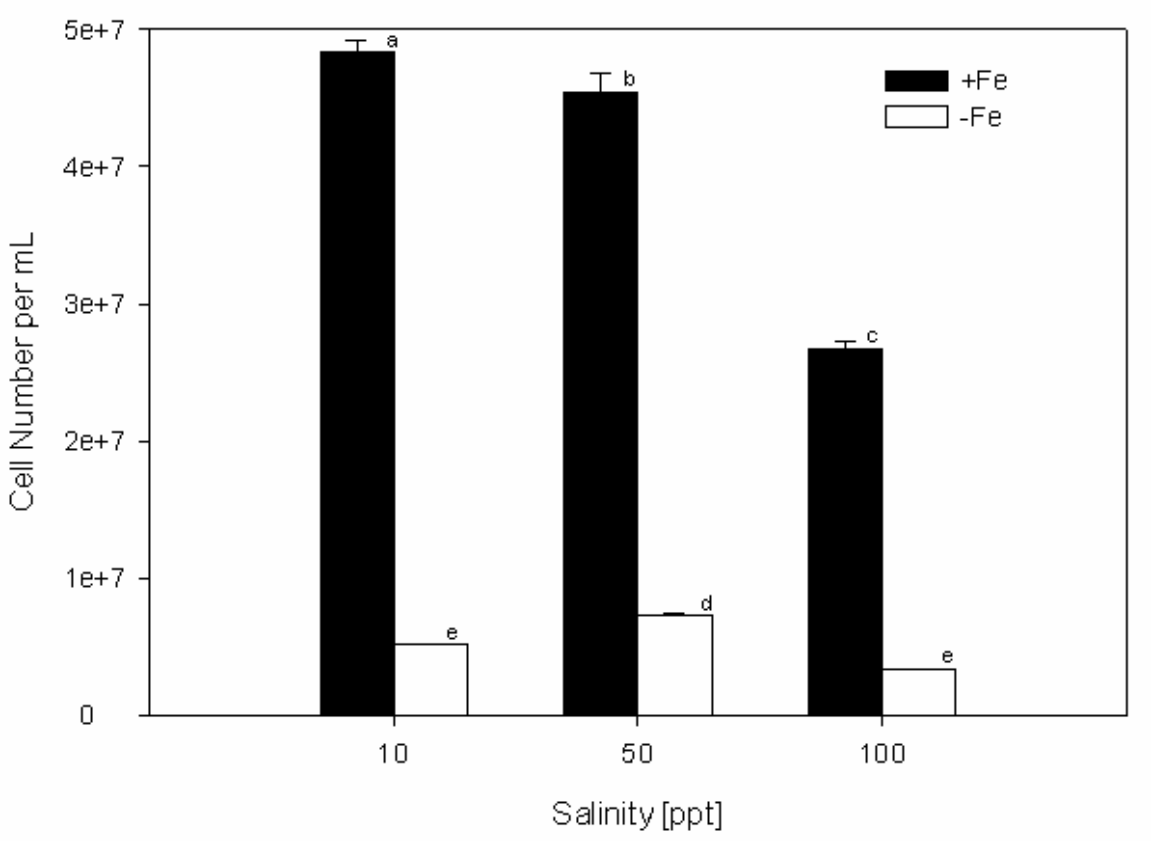

Figure 10. Cell yield of *Picochlorum* sp. at day 10 in low iron (-Fe) compared with the on added iron (-Fe) at different salinities. Mean values ± Standard deviation, n = 3. Different letters indicate significance.

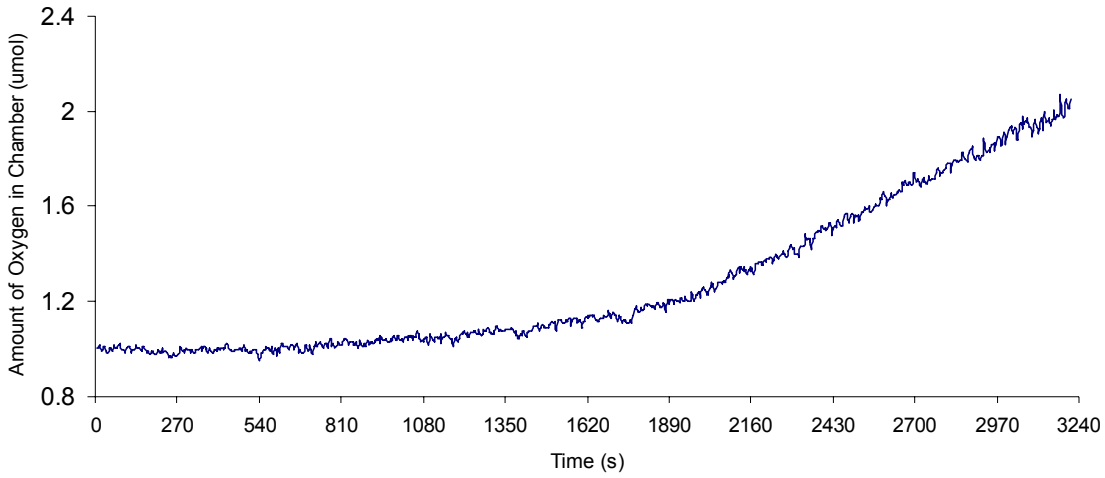

Figure 11. An example of a raw dissolved O_2 trace during photosynthesis by *Picochlorum oklahomensis* from which the rates of photosynthesis were calculated. Each 270 seconds represents photosynthesis under different photo flux density with the first 30 seconds used for the equilibration of the electrode and sample. Photosynthetic rates were calculated by linear regression slope over the next 240 seconds.

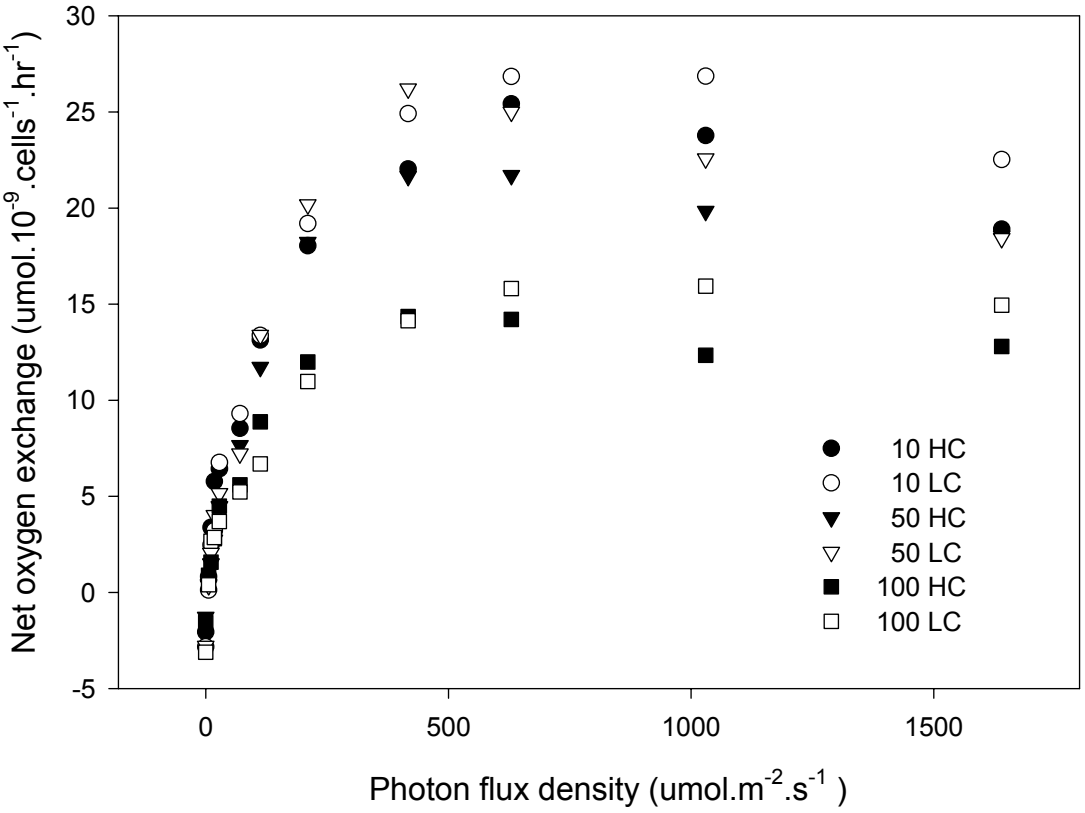

Figure 12. Photosynthetic light-response curves of *Picochlorum* sp. cultured in high bicarbonate (HC, shaded symbols) and in low bicarbonate (LC, open symbols) at different salinities (indicated by the numbers next to symbols). Mean values, n = 3 for all treatments (Error bars not shown for clarity).

Table 1. P-I parameters P_{max} (fmol O_2.cell^{-1}.hr^{-1}), α and R_d (fmol O_2.cell^{-1}.hr^{-1}) measured for *Picochlorum* sp. in high and low bicarbonate at different salinities. Mean ± Standard deviation, n = 3. Different letters indicate significance

P_{max} (fmol O_2.cell^{-1}.hr^{-1})

	High Bicarbonate	Low Bicarbonate
10 ppt	21.51 ± 0.32 a	25.29 ± 3.87 a
50 ppt	20.96 ± 1.17 a	23.50 ± 0.50 a
100 ppt	13.31 ± 1.37 b	15.15 ± 0.58 b

α fmol O_2.cell^{-1} (μmol photons m^{-2} s^{-1}) $^{-1}$ hr $^{-1}$

	High Bicarbonate	Low Bicarbonate
10 ppt	0.12 ± 0.03	0.14 ± 0.03
50 ppt	0.14 ± 0.05	0.15 ± 0.02
100 ppt	0.11 ± 0.06	0.07 ± 0.02

Dark Respiration (R_d)[fmol O_2.cell^{-1}.hr^{-1}]

	High Bicarbonate	Low Bicarbonate
10 ppt	-0.30 ± 0.93	-0.03 ± 0.87
50 ppt	-0.40 ± 0.49	-0.43 ± 0.76
100 ppt	-0.27 ± 0.28	-0.15 ± 0.22

significantly affected P_{max} (2-way ANOVA $p<0.01$). In both high and low bicarbonate treatments, P_{max} was lower at 100 ppt than at lower salinities. P_{max} was not significantly affected by low bicarbonate and the salinity-bicarbonate interaction was also not significant for any of these parameters.

Neither salinity nor phosphate significantly affected dark respiration and light-limited photosynthetic efficiency, α, (Table 2). Both salinity and phosphate significantly affected P_{max} (2-way ANOVA $p<0.01$). In both high and low phosphate, P_{max} was lower at 100 ppt than at 10 and 50 ppt. However, P_{max} for high phosphate grown cells was not significantly different from the low phosphate cultures at salinities.

Only salinity affected light-limited photosynthetic efficiency, α, (Table 3). Both salinity and iron treatment significantly affected P_{max} (2-way ANOVA $p<0.01$). In both +Fe and –Fe treatments, P_{max} was significantly lower at 100 ppt than at lower salinities (Tukey, $P<0.01$). P_{max} was significantly lower at each salinities in –Fe grown cells than those cultured in +Fe medium (Tukey, $P<0.05$). There was also a significant interaction between salinity and low iron interaction for this parameter (2-way ANOVA $p<0.01$).

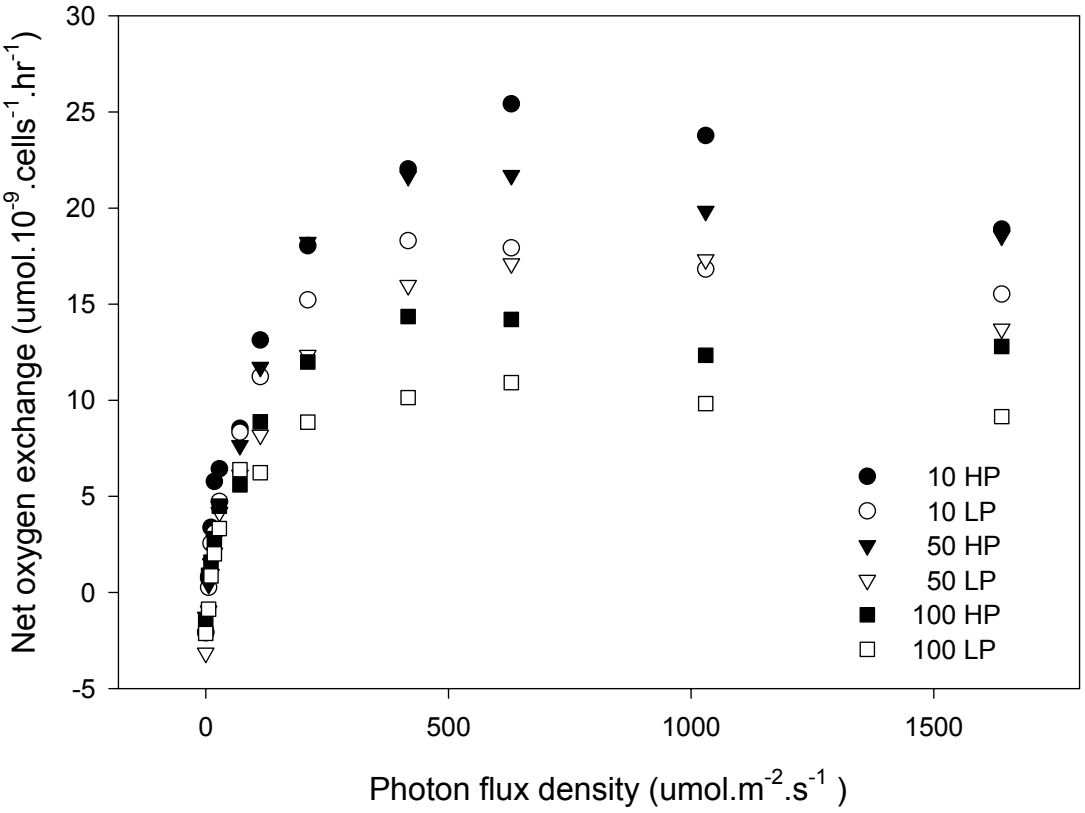

Figure 13. Photosynthetic light-response curves of *Picochlorum* sp. cultured in high phosphate (HC, shaded symbols) and in low phosphate (LP, open symbols) at different salinities (indicated by the numbers next to symbols). Mean values ± Standard deviation, n = 3 for all treatments (Error bars not shown for clarity).

Table 2. P-I parameters P_{max} (fmol O_2.cell^{-1}.hr^{-1}), α and R_d (fmol O_2.cell^{-1}.hr^{-1}) measured for *Picochlorum* sp. in high and low phosphate at different salinities. Mean ± Standard deviation, n = 3. Different letters indicate significance

P_{max} (fmol O_2.cell^{-1}.hr^{-1})

	High Phosphate	Low Phosphate
10 ppt	21.51 ± 0.32 a	17.13 ± 1.69 a
50 ppt	20.96 ± 1.17 a	16.91 ± 3.35 a
100 ppt	13.31 ± 1.37 b	11.25 ± 1.71 b

α fmol O_2.cell^{-1} (μmol photons m^{-2} s^{-1})$^{-1}$ hr^{-1}

	High Phosphate	Low Phosphate
10 ppt	0.12 ± 0.03	0.13 ± 0.01
50 ppt	0.14 ± 0.05	0.11 ± 0.06
100 ppt	0.11 ± 0.06	0.21 ± 0.20

Dark Respiration (R_d)[fmol O_2.cell^{-1}.hr^{-1}]

	High Phosphate	Low Phosphate
10 ppt	-0.30 ± 0.93	-0.12 ± 0.32
50 ppt	-0.40 ± 0.49	-0.95 ± 0.97
100 ppt	-0.27 ± 0.28	-0.30 ± 0.13

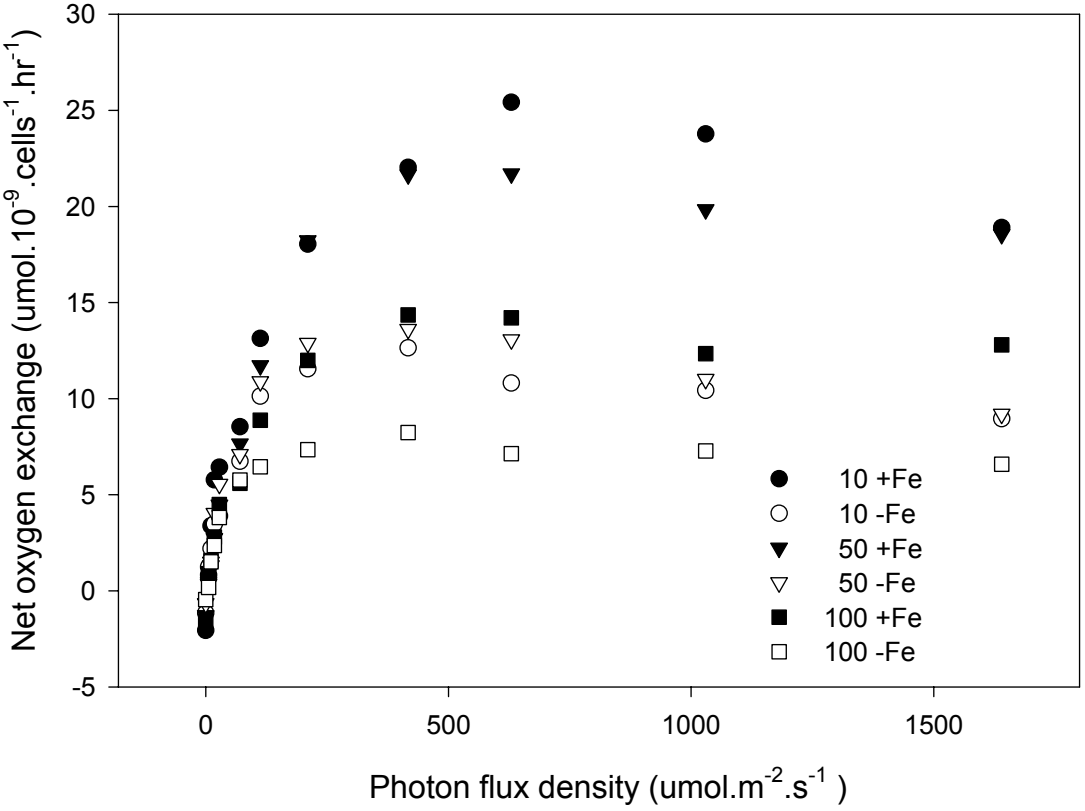

Figure 14. Photosynthetic light-response curves of *Picochlorum* sp. cultured in added iron medium (+Fe, shaded symbols) and in no added iron (-Fe, open symbols) at different salinities (indicated by the numbers next to symbols). Mean values, n = 3 for all treatments (Error bars not shown for clarity).

Table 3. P-I parameters P_{max} (fmol O_2.cell^{-1}.hr^{-1}), α and R_d (fmol O_2.cell^{-1}.hr^{-1}) measured for *Picochlorum* sp. in high and low iron at different salinities. Mean ± Standard deviation, n = 3. Different letters indicate significance

P_{max} (fmol O_2.cell^{-1}.hr^{-1})

	High Iron	Low Iron
10 ppt	21.51 ± 0.32 a	12.24 ± 0.49 b
50 ppt	20.96 ± 1.17 a	11.26 ± 0.95 b
100 ppt	13.31 ± 1.37 b	7.51 ± 0.58 c

α fmol O_2.cell^{-1} (μmol photons m^{-2} s^{-1}) $^{-1}$ hr $^{-1}$

	High Iron	Low Iron
10 ppt	0.12 ± 0.03	0.17 ± 0.11
50 ppt	0.14 ± 0.05	0.19 ± 0.08
100 ppt	0.11 ± 0.06	0.15 ± 0.02

Dark Respiration (R_d)[fmol O_2.cell^{-1}.hr^{-1}]

	High Iron	Low Iron
10 ppt	-0.30 ± 0.93	-0.18 ± 1.26
50 ppt	-0.40 ± 0.49	-0.36 ± 0.86
100 ppt	-0.27 ± 0.28	-0.33 ± 0.15

Pigment content

In order to understand how nutrient limitation and salinity stress affect the photosynthetic pigments in *Picochlorum*, these were extracted with DMF and analysed using a spectrophotometer.

Salinity, carbon limitation and pigments

Chlorophyll (*a* + *b*) per cell was significantly affected by salinity but not bicarbonate treatment. The interaction between salinity and bicarbonate was also significant (Fig. 15a; 2-way ANOVA, $p<0.01$). Chlorophyll decreased with increasing salinity, with most of the decrease occurring at 100 ppt. Chlorophyll levels were reduced by about 28% and 46% at 100 ppt in high and low bicarbonate cells, respectively, relative to 10 and 50 ppt. Chlorophyll a/chlorophyll b ratio was not significantly affected by salinity or bicarbonate (Fig. 15b). Total carotenoids per cell were significantly affected by salinity, bicarbonate treatment and the interaction between these factors (Fig. 16a; 2-way ANOVA, $p<0.05$). Carotenoids decreased with increasing salinity, with most of the decrease occurring at 100 ppt in both high and low bicarbonate treatment. Differences among 10 and 50 ppt cultures were small (<14%). At 100 ppt, carotenoids decreased by about 21-38% relative to 10 and 50 ppt. Chlorophyll/carotenoids ratio was significantly affected by salinity and the salinity-bicarbonate interaction (Fig. 16b; 2-way ANOVA, $p<0.01$), but not by bicarbonate alone (Fig. 16b; 2-way ANOVA, $p>0.05$). Low bicarbonate effect was inconsistent among salinities, and salinity effect differed between bicarbonate treatments. However, none of the differences exceeded 17%.

(a)

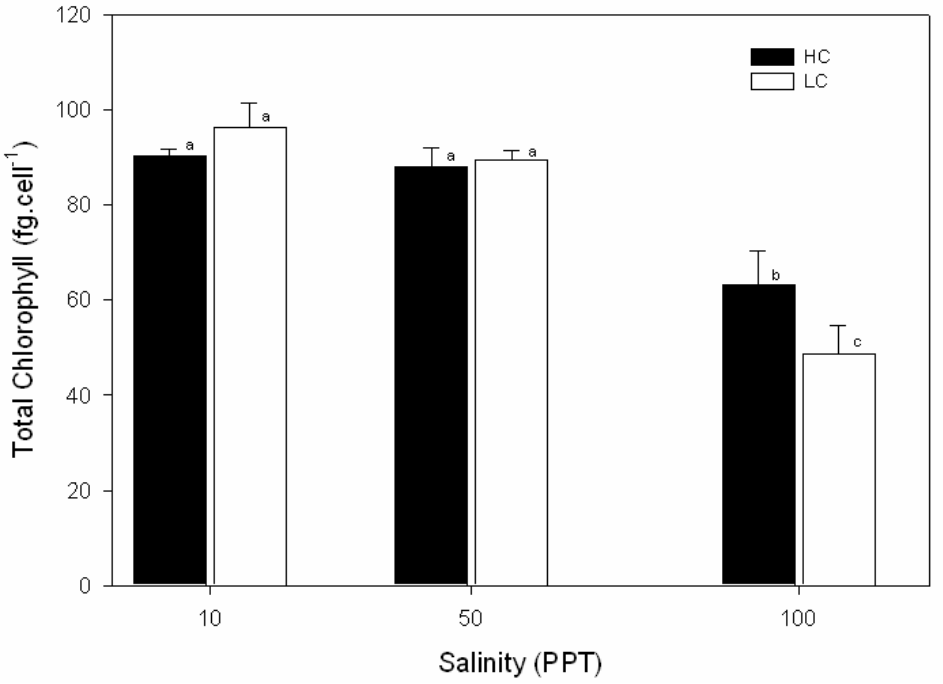

(b)

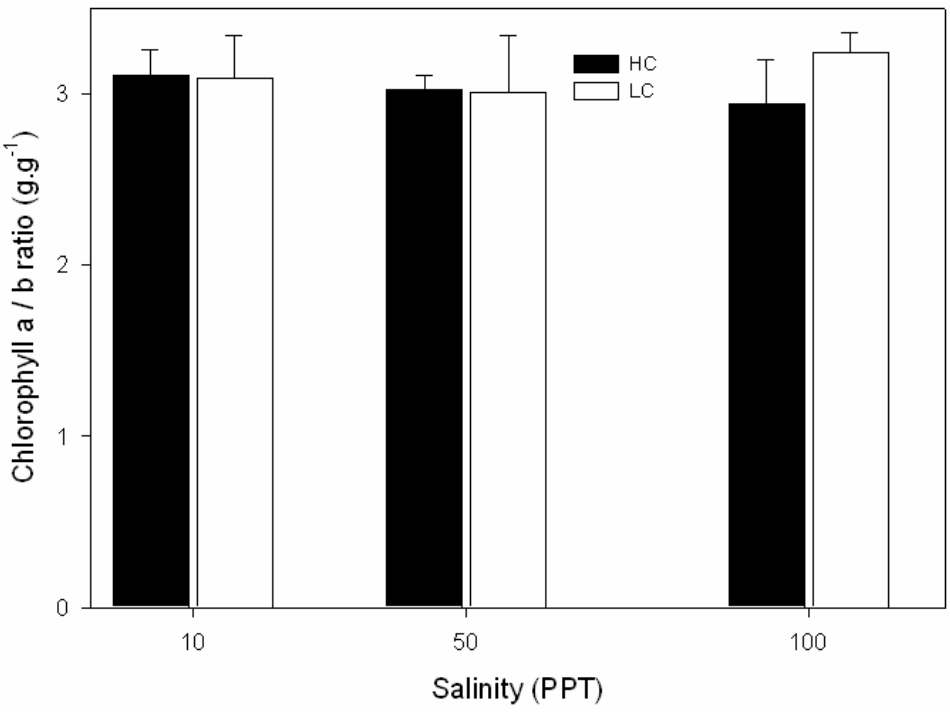

Figure 15. Average total chlorophyll (a) and chlorophyll a/b ratio (b) of *Picochlorum* sp. grown in high (HC) and low bicarbonate (LC) and at different salinities. Mean values ± Standard deviation, n = 3 for all treatments. Different letters indicate significance.

(a)

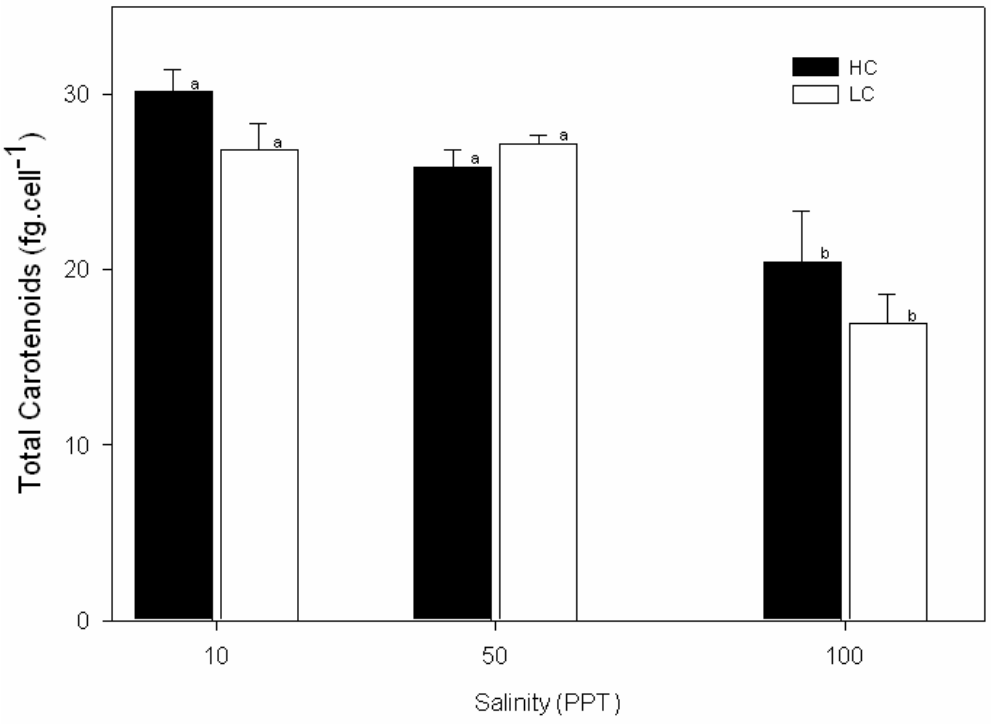

(b)

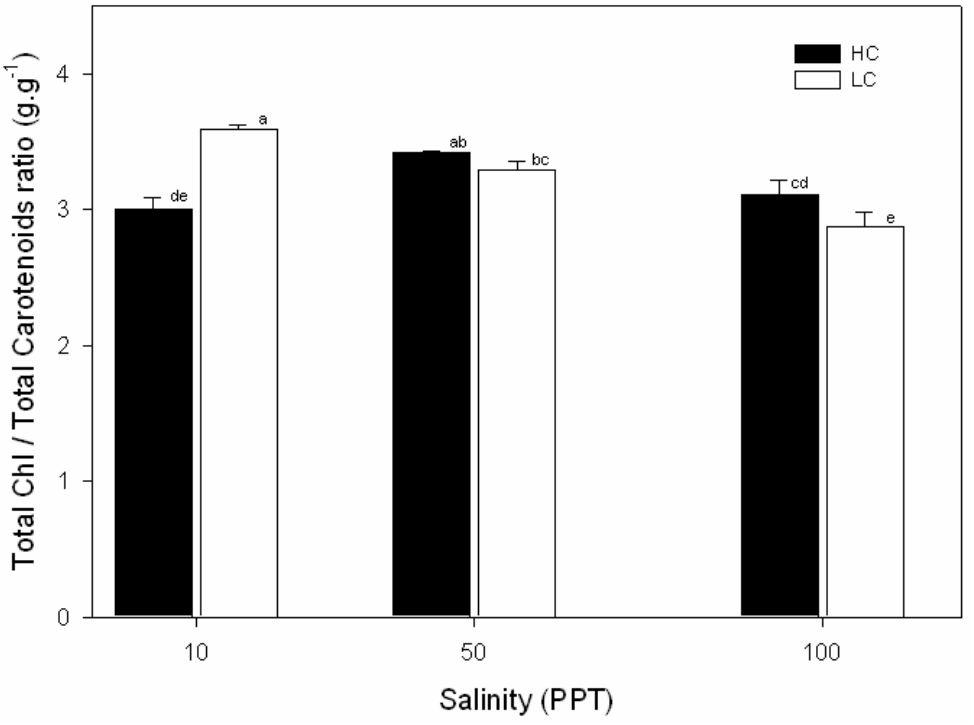

Figure 16. Average total carotenoids (a) and total chlorophyll / total carotenoids ratio (b) of *Picochlorum* sp. grown in high (HC) and low bicarbonate (LC) and at different salinities. Mean values ± Standard deviation, n = 3 for all treatments. Different letters indicate significance.

Salinity, phosphorus limitation and pigments

Chlorophyll (*a* + *b*) per cell was significantly affected by salinity, phosphate treatment and the interaction between these factors (Fig. 17a; 2-way ANOVA, $p<0.01$). Chlorophyll decreased by about 25% and 14% at 100 ppt in high and low phosphate treatment respectively, relative to 10 and 50 ppt. Differences among 10 and 50 ppt cultures were small (<5%). Chlorophyll a/ b ratio was not significantly affected by salinity or phosphate (Fig. 17b; 2-way ANOVA, $p > 0.05$) .

Total carotenoids per cell were significantly affected by salinity, phosphate treatment and the interaction between these factors (Fig. 18a; 2-way ANOVA, $p<0.01$). Total carotenoids decreased with increasing salinity in high phosphate cultures (about 30% reduction at 100 ppt compared to 10 ppt). However within the low phosphate cultures increasing salinity did not affect total carotenoids. Low phosphate resulted in significant reductions of carotenoids at 10 and 50 ppt (25% and 14%, respectively), but not 100 ppt compared to high phosphate treatments. Chlorophyll / carotenoids ratio was significantly affected by salinity, phosphate treatment and the interaction between these factors (Fig. 18b; 2-way ANOVA, $p<0.05$). The chlorophyll/carotenoids ratio was significantly increased at 50 ppt relative to 10 and 100 ppt for both high and low phosphate treatments. Low phosphate significantly increased chlorophyll/carotenoids ratio at 10 ppt (Tukey test, $p<0.05$) compared to high phosphate, though the difference did not exceed 8%.

(a)

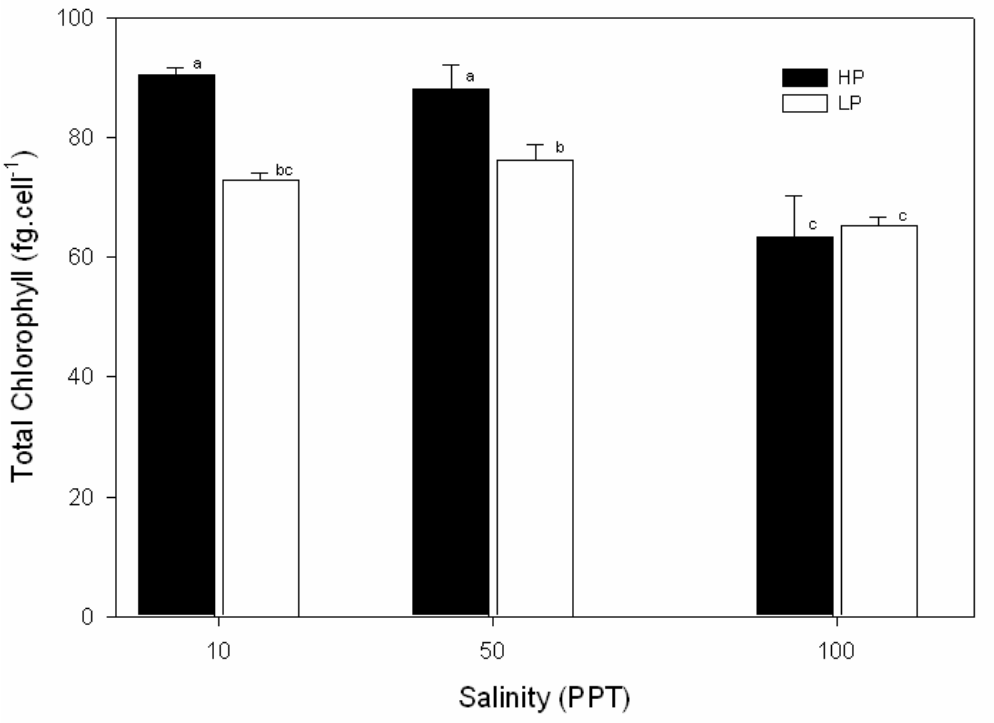

(b)

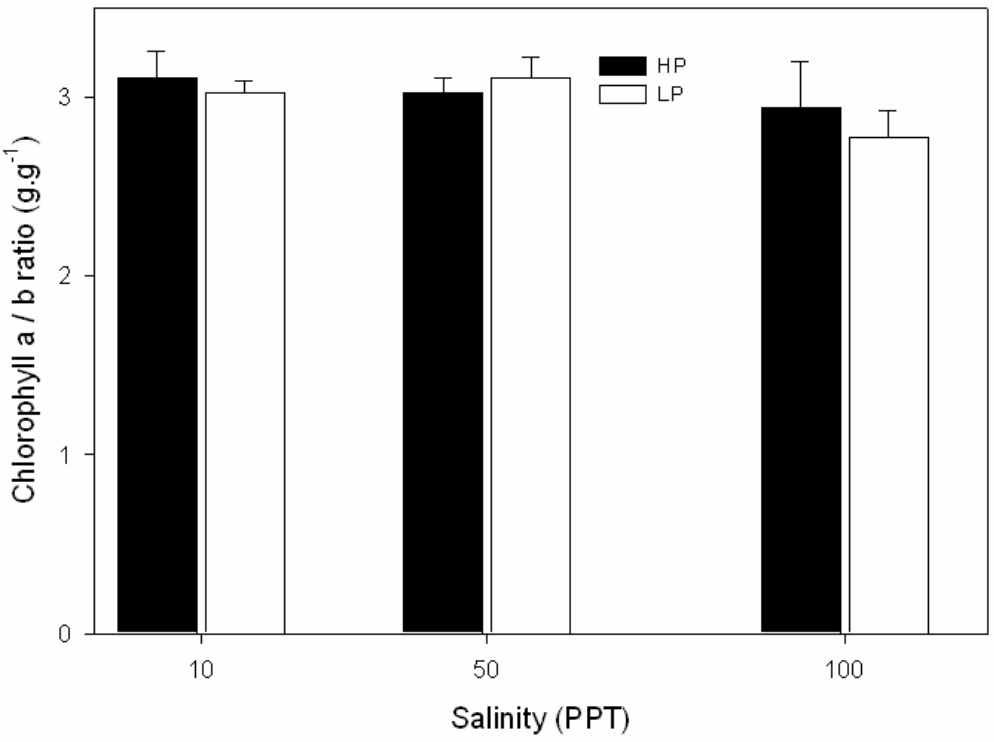

Figure 17. Average total chlorophyll (a) and chlorophyll a/b ratio (b) of *Picochlorum* sp. grown in high (HP) and low phosphate (LP) and at different salinities. Mean values ± Standard deviation, n = 3 for all treatments. Different letters indicate significance.

(a)

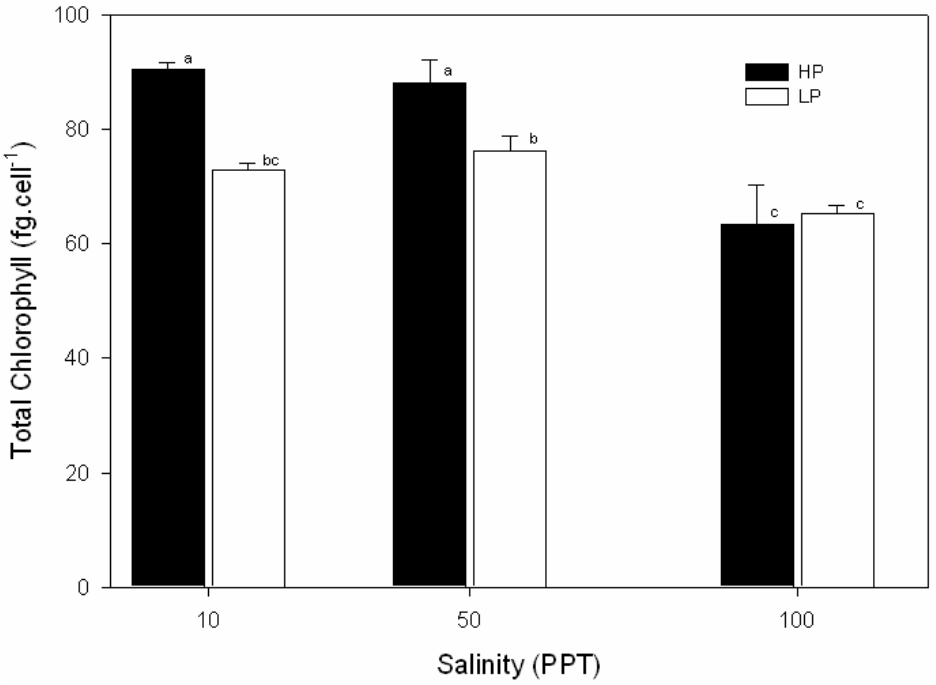

(b)

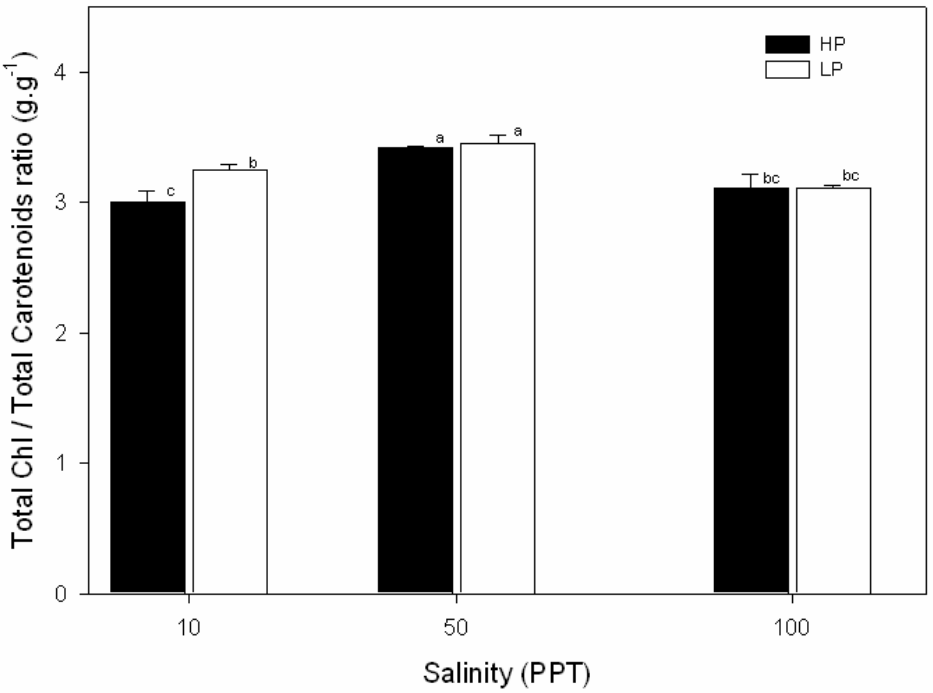

Figure 18. Average total carotenoids (a) and total chlorophyll / total carotenoids ratio (b) of *Picochlorum* sp. grown in high (HP) and low phosphate (LP) and at different salinities. Mean values ± Standard deviation, n = 3 for all treatments Different letters indicate significance.

Salinity, iron limitation and pigments

Total chlorophylls per cell were significantly affected by salinity, iron treatment and the interaction between these factors (Fig. 19a; 2-way ANOVA, $p<0.05$). Chlorophyll decreased with increasing salinity in added iron cultures (+Fe), with most of the decrease (28%) occurring at 100 ppt. Iron limitation significantly decreased total chlorophyll per cell by 18% at 10 ppt and 41% at 50 ppt, but significantly increased by 25% at 100 ppt (Tukey test, $p<0.01$) compared to +Fe grown cells. Chlorophyll a/ b ratio was significantly reduced by low iron (Fig. 19b; 2-way ANOVA, $p<0.01$), but not salinity or the interaction between these factors. The reduction by low iron was about 43% at 10 and 100 ppt and 61% at 50 ppt.

Total carotenoids per cell were significantly affected by salinity and iron treatments as well as the salinity-iron interaction (Fig. 20a; 2-way ANOVA, $p<0.01$). In +Fe cultures, total carotenoids decreased with increasing salinity but this was different in –Fe grown cells. At 100 ppt, carotenoids decreased by about 30% relative to 50 ppt in +Fe cultures. Low iron significantly reduced carotenoids at 10 and 50 ppt (22% and 42%, respectively), but not at 100 ppt which had a significant increase of 22%. The total chlorophylls / total carotenoids ratio was not significantly affected by salinity or iron treatment (Fig. 20b; 2-way ANOVA, $p>0.05$).

(a)

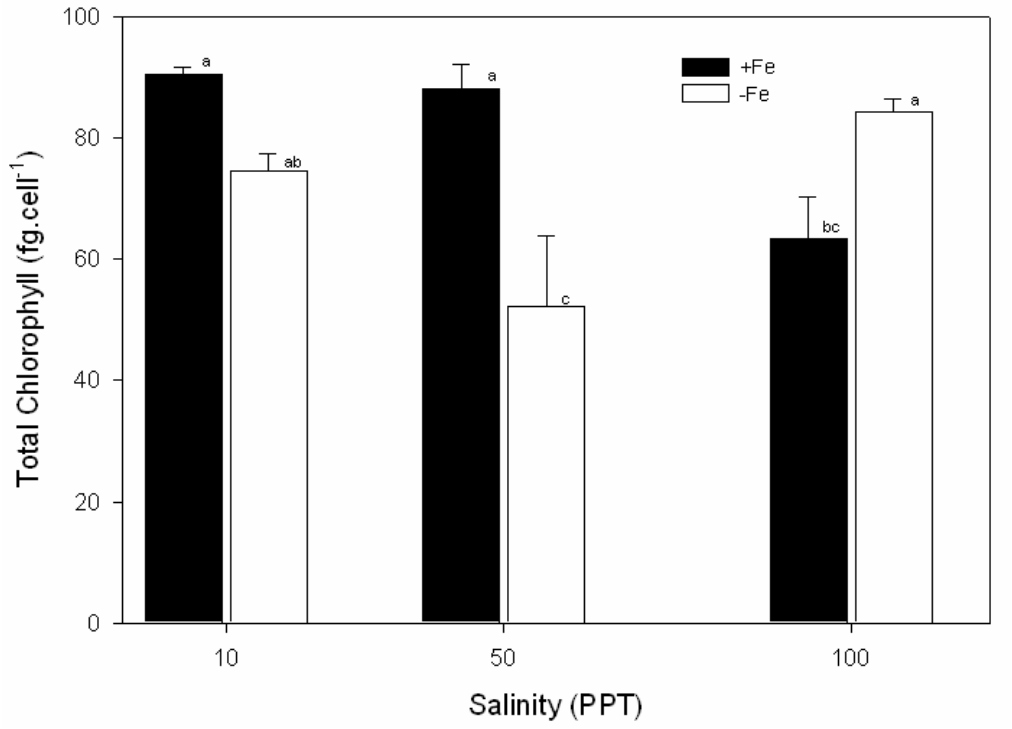

(b)

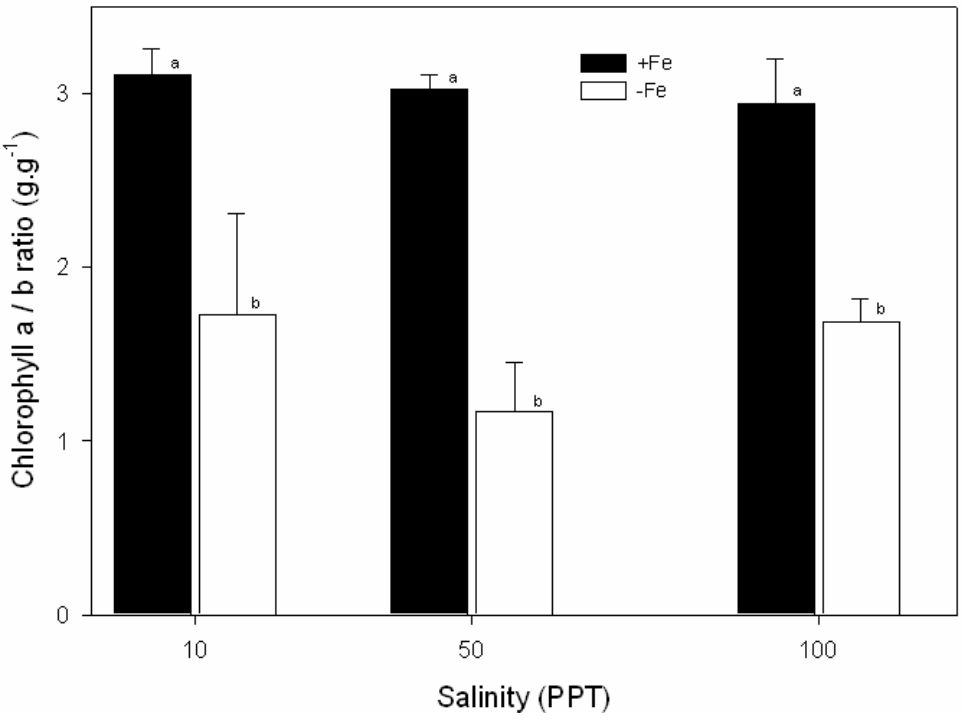

Figure 19. Average total chlorophyll (a) and chlorophyll a/b ratio (b) of *Picochlorum* sp. grown in added iron (+Fe) and no added iron (-Fe) and at different salinities. Mean values ± Standard deviation, n = 3 for all treatments Different letters indicate significance

(a)

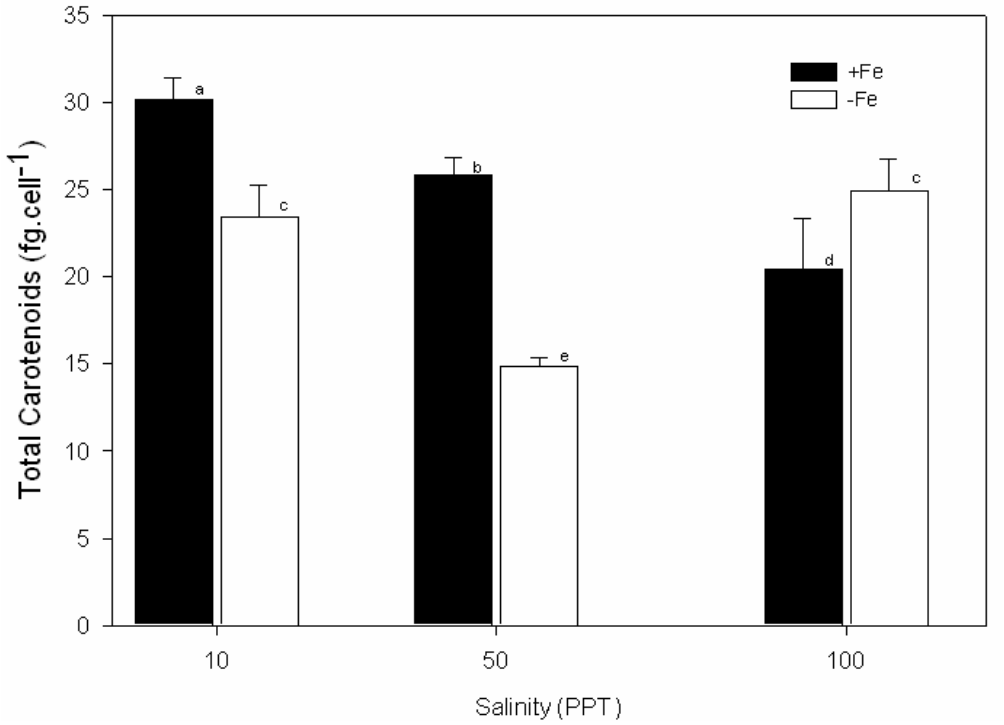

(b)

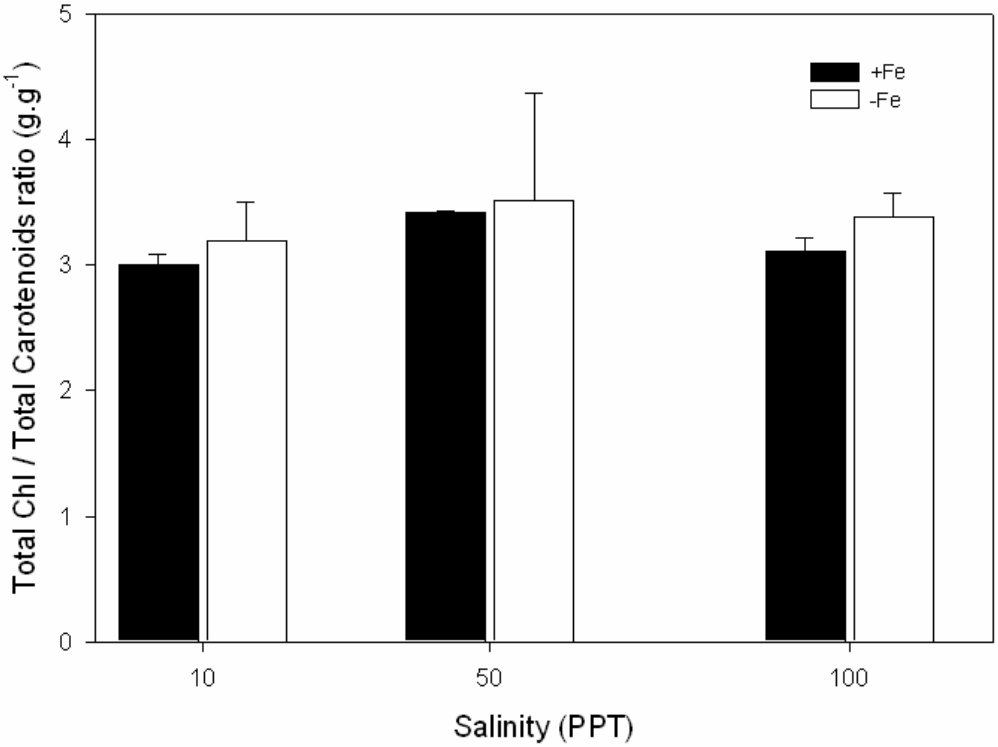

Figure 20. Average total carotenoids (a) and total chlorophyll / total carotenoids ratio (b) of *Picochlorum* sp. grown in added iron (+Fe) and no added iron (-Fe) and at different salinities. Mean values ± Standard deviation, n = 3 for all treatments. Different letters indicate significance.

Determination of Fluorescence Parameters

The determination of the chlorophyll a fluorescence parameters in *Picochlorum* by the saturation pulse method were calculated from the fluorescence measurements as demonstrated by those cultured in control medium (Fig. 21).

Salinity, bicarbonate and fluorescence

The maximum quantum yield of PS II photochemistry in the dark-adapted state, (F_v / F_m) was significantly affected by only salinity but not low bicarbonate or the interaction between salinity and bicarbonate treatment (Fig. 22; 2-way ANOVA, $p>0.05$). Within the high bicarbonate cultures, there was a decrease of approximately 5% in F_v / F_m at 50 ppt relative to 10 ppt. Low bicarbonate slightly increased F_v / F_m at 10 and 50 ppt. The effective quantum yield of PSII electron transport in the light-adapted state, Φ_{PSII} given by (F_m' – F') / F_m', was significantly affected by salinity and bicarbonate treatment (Fig. 22a; 2-way ANOVA, $p<0.01$) but not the interaction between these factors. Increasing salinity resulted in a decrease in Φ_{PSII}. In high bicarbonate, the reduction was 26% and 21% respectively at 50 and 100 ppt compared to 10 ppt. Low bicarbonate significantly increased Φ_{PSII} by 35% at 50 ppt (Tukey test, $p<0.05$) and an insignificant increase of about 23% at 10 ppt and 100 ppt.

The photochemical quenching coefficient, qP which is calculated as (F_m' - F') / (F_m' – F_o'), was significantly affected by salinity and bicarbonate treatment (Fig. 22b; 2-way ANOVA, $p<0.01$) but not the interaction between these factors. In the high bicarbonate treatment, increasing salinity decreased photochemical quenching by 25% and 31% at 50 and 100 ppt respectively compared to 10 ppt (Tukey test, $p<0.05$). Low

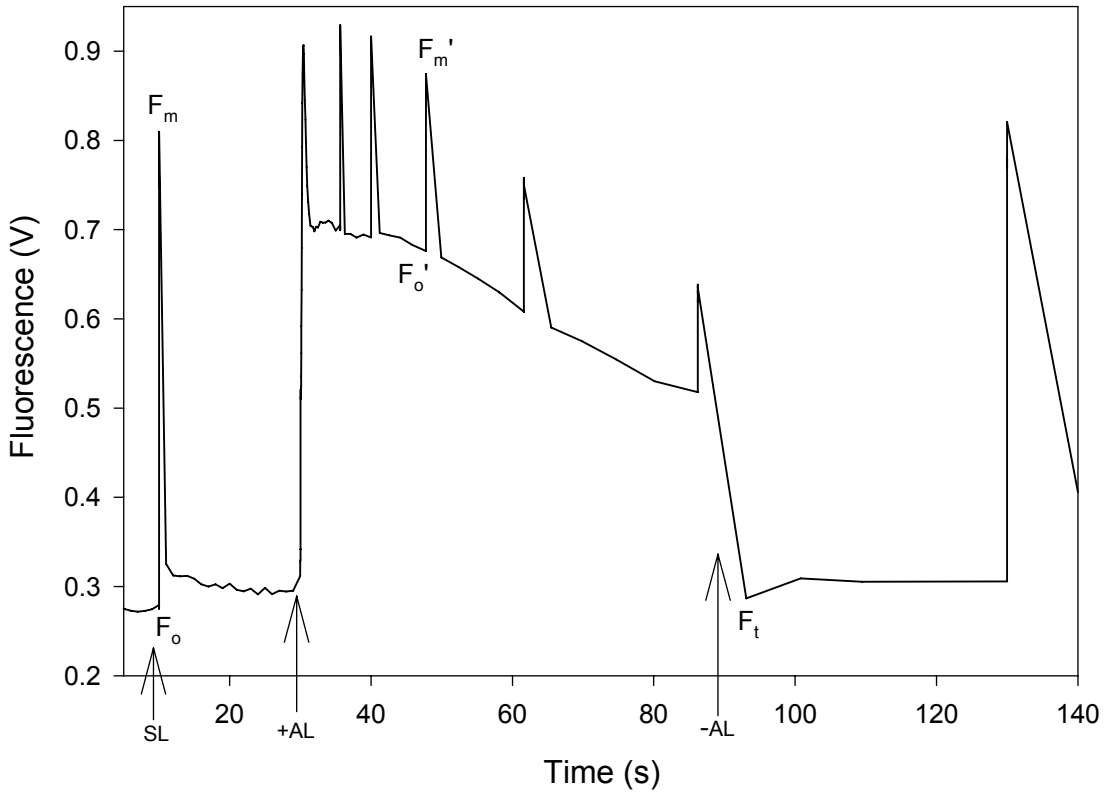

Figure 21. Chlorophyll fluorescence of *Picochlorum sp.* grown in control media at 10 ppt by the saturation pulse method. SL is saturating flash of light to determine maximum fluorescence, F_m from initial fluorescence, F_o. Actinic light, +AL, was switched on to drive photosynthesis, -AL indicate when actinic light was switched off.

(a)

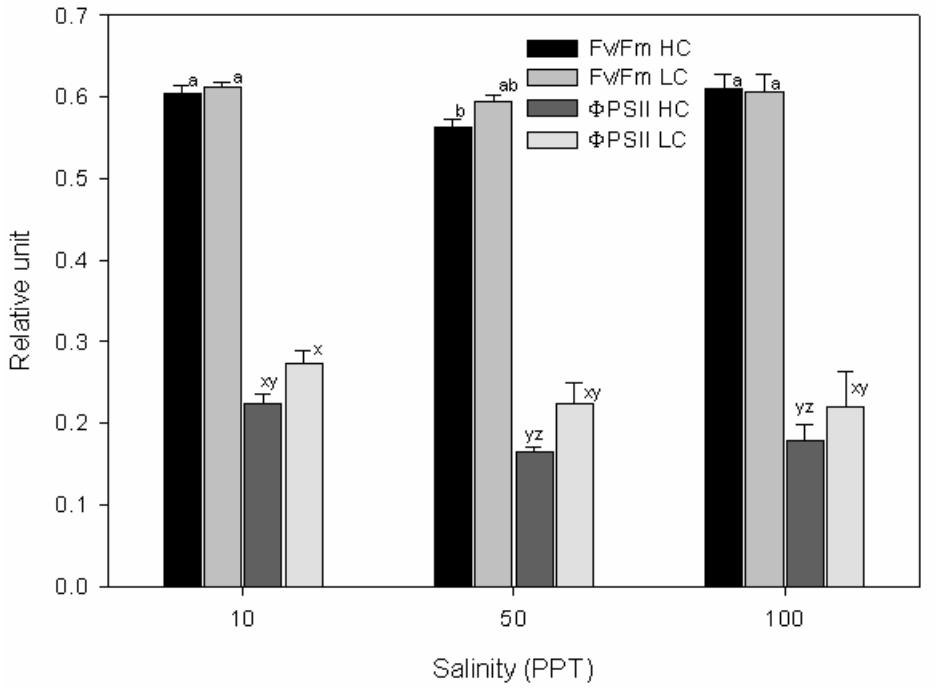

(b)

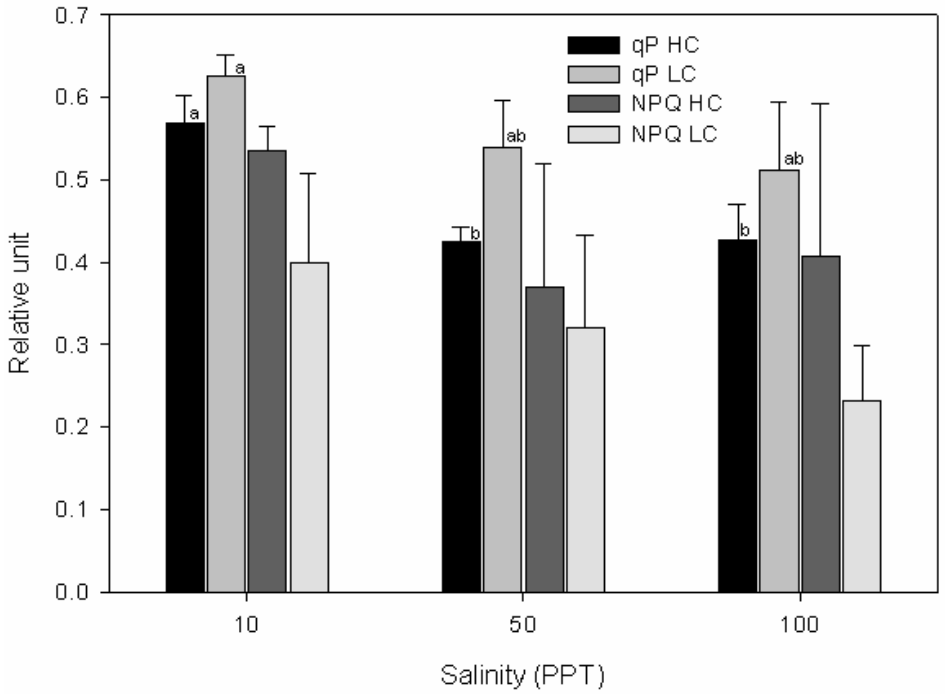

Figure 22. Changes in fluorescence parameters in *Picochlorum* sp. due to growth in low bicarbonate (LC) compared with high bicarbonate (HC) at different salinities. F_v/F_m is PSII maximum quantum efficiency, ΦPSII is Quantum yield electron transport of PSII, qP, Photochemical quenching and NPQ, Non-photochemical quenching. Mean values ± Standard deviation, n = 3 for all treatments. Different letters indicate significance.

bicarbonate increased photochemical quenching by 10%, 27% and 20% at 10, 50 and 100 ppt respectively. Neither salinity nor bicarbonate treatment significantly affected non-photochemical quenching, NPQ, which is given as $(F_m - F_m') / F_m'$, although low bicarbonate reduced non-photochemical quenching at all salinities (Fig. 22b). Large variability in NPQ values resulted in low statistical power.

Salinity, phosphate and fluorescence

The maximum quantum yield of PS II photochemistry in the dark-adapted state, (F_v / F_m) was significantly affected by salinity and phosphate treatment (Fig. 23a; 2-way ANOVA, $p<0.01$). The interaction between salinity and phosphate treatment was also significant. Within the high phosphate samples, there was a significant decrease of approximately 5% in F_v / F_m at 50 ppt relative to 10 ppt. Low phosphate treatment significantly decreased F_v / F_m by 14% at 10 ppt, but had no effect at 50 and 100 ppt compared to the high phosphate treatments. Within the phosphate treatments, F_v / F_m increased by 12% from 10 to 100 ppt. The effective quantum yield of PSII electron transport in the light-adapted state, Φ_{PSII} given by $(F_m' - F') / F_m'$, was significantly affected by salinity and phosphate treatment as well as the interaction between these factors (Fig. 23a; 2-way ANOVA, $p<0.05$). In high phosphate cultures, Φ_{PSII} decreased by 26% and 21% at 50 and 100 ppt, respectively, compared to 10 ppt. Low phosphate significantly decreased Φ_{PSII} by 51%, 23% and 18% at 10 ppt, 50 ppt and 100 ppt respectively (Tukey test, $p<0.05$). Within the phosphate treatments, Φ_{PSII} increased by 24% from 10 to 100 ppt.

(a)

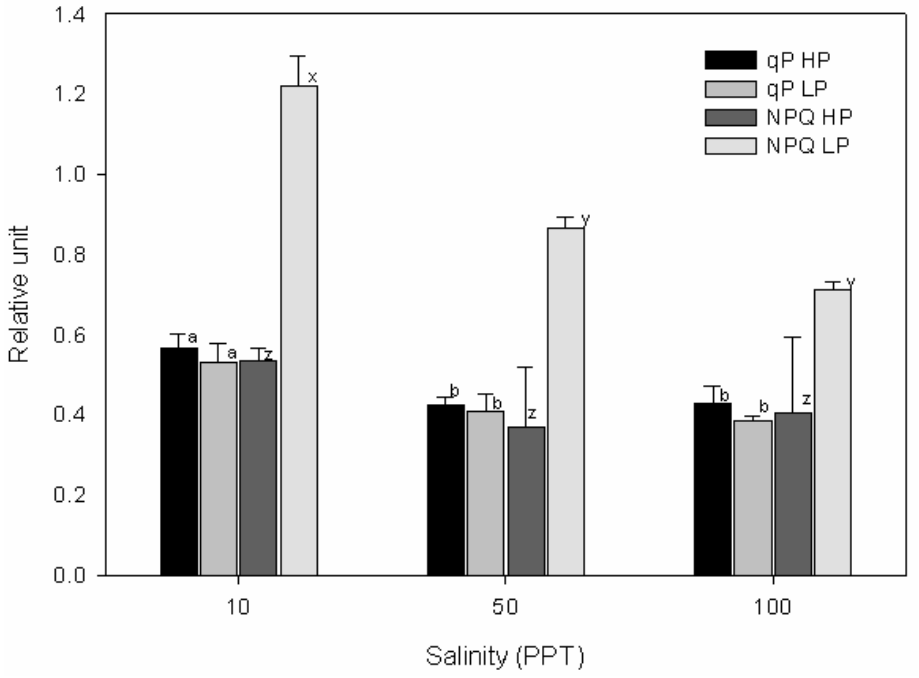

(b)

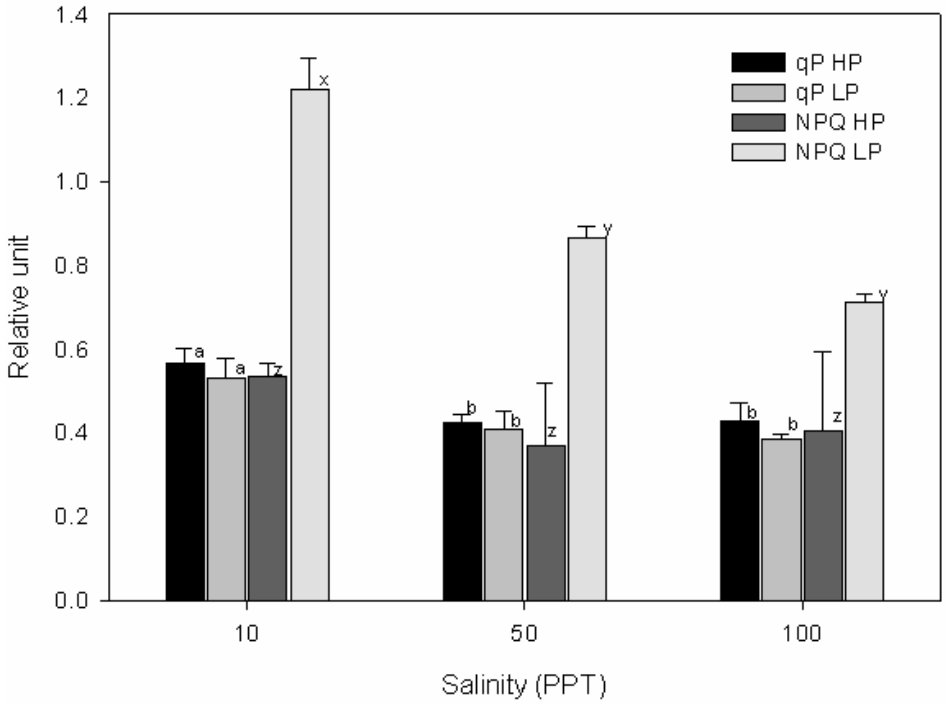

Figure 23. Changes in fluorescence parameters in *Picochlorum* sp. due to growth in low phosphate (LP) compared with high phosphate (HP) at different salinities. F_v/F_m is PSII maximum quantum efficiency, ΦPSII is Quantum yield electron transport of PSII, qP, Photochemical quenching and NPQ, Non-photochemical quenching. Mean values ± Standard deviation, n = 3 for all treatments. Different letters indicate significance.

The photochemical quenching coefficient, qP which is calculated as (F_m' - F') / (F_m' – F_o'), was significantly affected by salinity (Fig. 23b; 2-way ANOVA, $p<0.01$) but not phosphate treatment nor the interaction between salinity and phosphate treatment. In high phosphate cultures, increasing salinity decreased photochemical quenching by 25% and 31% at 50 and 100 ppt respectively, compared to 10 ppt (Tukey test, $p<0.05$). Within the low phosphate treatments, qP was reduced by 27% from 10 ppt to 100 ppt. The non-photochemical quenching, NPQ, was significantly affected by salinity, phosphate treatment and the interaction between these two factors (Fig. 23b; 2-way ANOVA, $p<0.01$). In low phosphate cultures, increasing salinity significantly decreased NPQ by 29% and 42% at 50 and 100 ppt relative to 10 ppt (Tukey test, $p<0.05$), whereas salinity did not significantly affect NPQ in high phosphate cultures. Low phosphate significantly increased non-photochemical quenching by 125%, 135% and 75% at 10 ppt, 50 ppt and 100 ppt respectively compared to the controls (Tukey test, $p<0.01$).

Salinity, low iron and fluorescence

The maximum quantum yield of PS II photochemistry in the dark-adapted state (F_v / F_m) was significantly affected by salinity, iron treatments as well as the interaction between salinity and iron treatment (Fig. 24a; 2-way ANOVA, $p<0.05$). Iron limitation treatment significantly decreased F_v / F_m by 80% at 10 ppt, 77% at 50 ppt and 48% at 100 ppt compared to the +Fe medium. Within the -Fe treatments, increasing salinity from 10 and 50 ppt to 100 ppt increased F_v / F_m by about 150%. The effective quantum yield of PSII electron transport in the light-adapted state, Φ_{PSII}, was significantly affected by low iron treatment (Fig. 24a; 2-way ANOVA, $p<0.01$) but not salinity or the interaction

(a)

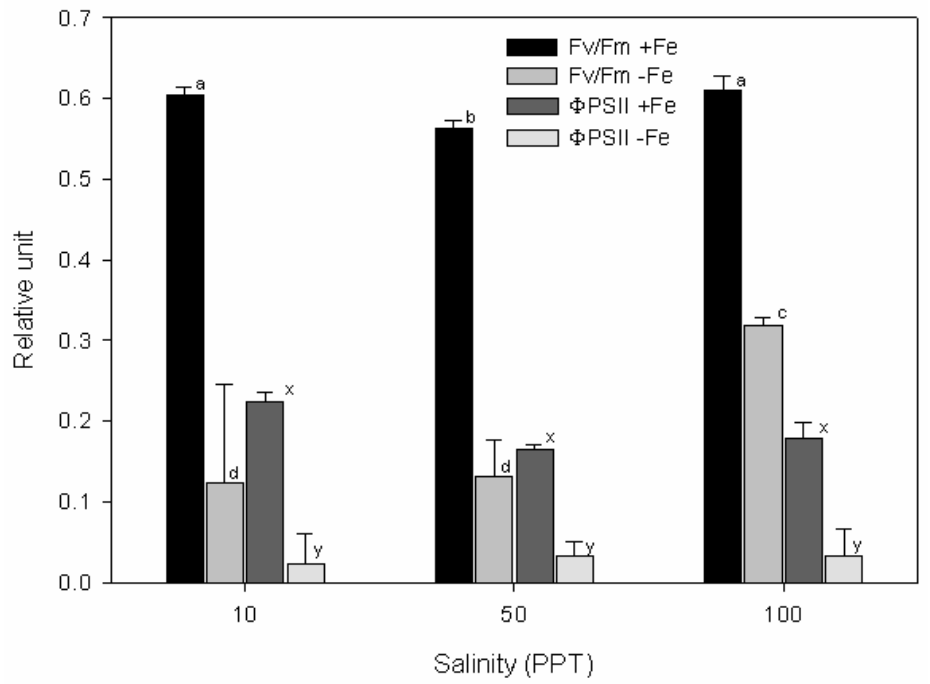

(b)

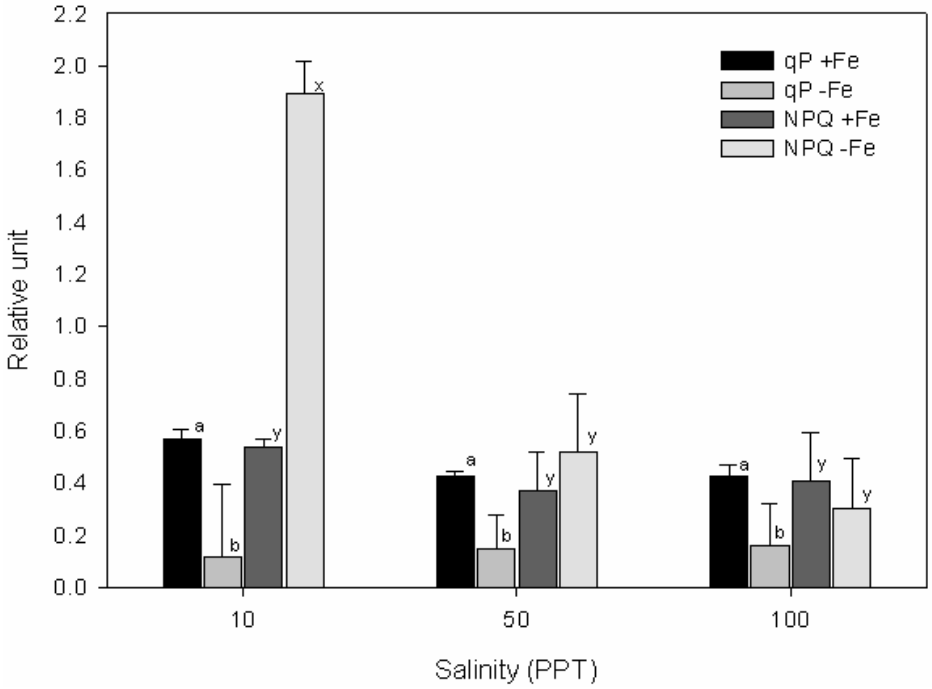

Figure 24. Changes in fluorescence parameters in *Picochlorum* sp. due to growth in no added iron (-Fe) compared with added iron (+Fe) at different salinities. F_v/F_m is PSII maximum quantum efficiency, ΦPSII is Quantum yield electron transport of PSII, qP, Photochemical quenching and NPQ, Non-photochemical quenching. Mean values ± Standard deviation, n = 3 for all treatments. Different letters indicate significance.

between these factors. Low iron significantly decreased Φ_{PSII} by 89% at 10 ppt and about 80% at 50 ppt and 100 ppt (Tukey test, $p<0.05$) compared to the controls.

The photochemical quenching coefficient, qP, was significantly affected by low iron treatment (Fig. 24b; 2-way ANOVA, $p<0.01$) but not salinity nor the interaction between salinity and low iron treatments. Low iron reduced qP by 80% at 10 ppt and 63% at 50 and 100 ppt compared to the controls. The non-photochemical quenching, NPQ, was significantly affected by iron treatment (Fig. 24b; 2-way ANOVA, $p<0.01$) as well as salinity and the interaction between these factors. Increasing salinity significantly decreased NPQ by 29% and 24% at 50 ppt and 100 ppt respectively, relative to 10 ppt (Tukey test, $p<0.01$). Low iron treatment significantly increased non-photochemical quenching by 250% at 10 ppt (Tukey test, $p<0.01$) but caused a non-significant decrease of 41% and 25% at 50 ppt and 100 ppt respectively, compared to the controls.

CHAPTER IV

DISCUSSION

The hypothesis for this study is that the effect of salinity stress on growth and photosynthesis in *Picochlorum* will be different under high nutrient compared to limited nutrient levels. In other words the pattern of response by *Picochlorum* to the three different salinities of 10, 50 and 100 ppt will not follow the same pattern at the two nutrient levels. This may be due to the influence of the amount of the nutrient present. If there is a change in the response pattern from 10 ppt through 50 ppt to 100 ppt for the two nutrient levels, then there is a salinity-nutrient interaction. Examining the two factors together may result in the intensification of the stress in organisms or possibly the effect of one may reduce the effect of the other factor. The response of *Picochlorum* to the three salinities was investigated under low and high bicarbonate, low and high phosphate and under iron and no added iron conditions. The responses differed depending on the type of nutrient.

Effect of Salinity and Bicarbonate

Salinity did not affect initial growth rate, μ, (Fig. 3) and P_{max} (Table 1) at 10 and 50 ppt but significantly reduced these parameters at 100 ppt at both bicarbonate levels. However, increasing salinity from 10 ppt to 50 ppt to 100 ppt also decreased cell yield on day 10 under HC (Fig. 4). The decreases caused by salinity are expected considering the

problems posed by high salinity in algae and plants. In order to overcome salinity stress and the problems they face such as osmotic and ionic stresses, these organisms may channel their efforts into producing compatible solutes for their survival. For example *Picochlorum* produces proline as an osmoticum (Hironanka 2000) and the biosynthesis of this compound from glutamate requires ATP and NADPH. Glutamate used in this synthesis will also not be available for growth. This may be produced at the expense of growth. Maximum quantum yield of PSII, Fv/Fm, was only reduced slightly at 50 ppt and effective quantum yield of PSII electron transport in light adapted state, Φ_{PSII}, was not affected by salinity at either C level?, indicating that photoinhibition of photosynthesis was not influenced by salinity in *Picochlorum*, at least under the growth conditions used (Powles 1984; Adams et al. 1990). Since P_{max} expressed per cell was reduced at higher salinity and α was not affected (Table 1), this suggests that the size of the photosynthetic unit was not changed (Prézelin 1981). This is consistent with negligible changes in alpha and it is also consistent with relatively small changes in Chl a/b ratio (Fig. 15b).

Higher salinity decreased Φ_{PSII} and the photochemical quenching, qP, by about 20-25% compared to 10 ppt under HC (Fig. 22), an indication that actual electron flow was inhibited (Lu and Vonshak 2002). When there is less water due to salt stress, the water oxidation complex and PSII may be affected and subsequently electron transfer. When membrane potential is affected by salinity, ATP synthesis is also inhibited. Salinity affected reduced total chlorophylls and total carotenoids only at 100 ppt (Figs. 15a, 16a). Even though the pigments may not be affected, electron flow is interrupted and this may finally affect the dark reactions. El-Sheekh (2004) has reported that electron transfer from Q_A to Q_B was decreased by salinity stress in the green alga *Chlorella vulgaris*, a relative

of *Picochlorum* (Henley et al. 2004). Salt stress can inhibit protein synthesis such as the D1 protein which will in turn affects the rates at which damaged D1 proteins are replaced and subsequently affect photosynthesis (Allakhverdiev et al. 2002; Mohanty et al. 2007). In affecting protein synthesis, enzymes in the Calvin cycle may also be affected resulting in a decrease in carbon fixation. Membranes and the transport proteins associated with them are also affected by salinity stress and therefore may affect uptake of some nutrients.

Low bicarbonate (LC) significantly decreased initial growth rate and cell yield at day 10 but did not affect P_{max} and α at all salinities. Low bicarbonate reduced initial growth rate by 38%, 36% and 30% at 10, 50 and 100 ppt respectively (Fig. 3), while P_{max} was increased by 18%, 12% and 14% at 10, 50 and 100 ppt respectively (Table 1). In LC, the cell yield at day 10 was decreased by 27%, 20% and 18% at 10, 50 and 100 ppt respectively (Fig. 4).

The decrease in initial growth rate and cell yield at day 10 is expected. Considering that carbon is an important component of all biomolecules found in organisms, if it is limited in supply, then carbon fixation is likely to decline as well as the biosynthesis and build up of compounds which may lead to a reduction in growth. This is consistent with the report by Huertas et al. (2000) that the green alga, *Nannochloris* exhibited growth limitation at lower CO_2 concentration. Marine members of the genus *Nannochloris* have been reassigned as *Picochlorum* (Henley et al. 2004) and therefore this is related to *P. oklahomensis*.

Analysis of the curvatures of the growth curves revealed significantly lower convexity values for cells grown in LC medium compared to those in HC medium. HC

grown cells had convexity between 1.77 and 2.33 while those grown in LC medium ranged from 0.25 to 0.66 (Table 4). The lower values indicate that *Picochlorum* grown in LC were stressed as indicated by the nature of the curvature of the curves although this is not evident in the higher P_{max} values in LC (Table 1). The increase in P_{max} in LC is intuitively unexpected, although it was accompanied by increases by LC in maximum quantum yield of PS II photochemistry in dark-adapted state cells, F_v/F_m (except at 100 ppt), effective quantum yield of PS II electron transport in light-adapted state, Φ_{PSII}, and photochemical quenching, qP (Fig. 22 a and b) compared to HC.

The increase in P_{max} may be attributed to the fact that photosynthesis was measured under high HCO_3^- by adding 8 mM of HCO_3^-. This was added to all the treatment samples in the photosynthetic set up chamber to ensure that there was enough carbon for photosynthesis. Therefore it appears that *Picochlorum* grown in LC environment may have become efficient in HCO_3^- uptake, but not necessarily absolute photosynthesis at the growth CO_2 concentration compared to the high bicarbonate (HC). However, during the fluorescence measurements no additional HCO_3^- was added, yet Φ_{PSII} and qP were slightly higher in LC grown cells (Fig. 22). The increase in P_{max}, Φ_{PSII} and qP by LC may be a way of getting more energy from the light reactions for active uptake of HCO_3^- rather than being channeled into the dark reactions, as is evident in the lower initial growth rate (Fig. 3) and cell yield at day 10 (Fig. 4).

Some photosynthetic microorganisms have developed mechanisms to help them adapt to low HCO_3^-or CO_2 conditions (Kaplan and Reinhold 1999; Giordano et al. 2005; Spalding 2008). One such mechanism is to enhance the acquisition of CO_2 by producing carbonic anhydrase. This enzyme reversibly converts between HCO_3^- and CO_2, according

Table 4. Convexity values obtained by fitting the Bannister's function to the growth curves of *Picochlorum* sp. in high and low nutrients at different salinities. Mean ± standard deviation, n = 3. Different letters indicate significance.

	High Bicarbonate	Low Bicarbonate
10 ppt	1.80 ± 0.02 b	0.25 ± 0.01 f
50 ppt	1.65 ± 0.02 c	0.51 ± 0.00 e
100 ppt	2.30 ± 0.04 a	0.64 ± 0.03 d

	High Phosphate	Low Phosphate
10 ppt	1.80 ± 0.02 e	4.67 ± 0.03 a
50 ppt	1.65 ± 0.02 f	3.16 ± 0.09 b
100 ppt	2.30 ± 0.04 d	2.45 ± 0.02 c

	High Iron	Low Iron
10 ppt	1.80 ± 0.02 b	0.38 ± 0.02 d
50 ppt	1.65 ± 0.02 c	0.36 ± 0.01 d
100 ppt	2.30 ± 0.04 a	0.32 ± 0.06 d

to the formula: $CO_2 + H_2O \leftrightarrow H_2CO_3 \leftrightarrow H^+ + HCO_3^-$. The external carbonic anhydrase is produced by the cell are located on the plasma membrane with direct communication with the immediate surrounding of the cell. Other cells also produce internal carbonic anhydrase which functions in the chloroplast within the cell. A second mechanism that may be used is the active transport of HCO_3^-or CO_2 across the plasma membrane and chloroplast envelope by transporters which require the use of energy (Huertas and Lubian 1998; Moroney and Somanchi 1999; Huertas et al. 2000). The occurrence of an active CO_2 transport system in two marine species of *Nannochloris* (=*Picochlorum*, Henley et al. 2004), *N. atomus* and *N. maculata*, which may explain their higher capacity for using CO_2 than HCO_3^- (Huertas and Lubian 1998; Huertas et al. 2000). Since *Picochlorum* can grow in media with either CO_2 or HCO_3^- as the source of DIC, although it may prefer CO_2, probably both mechanisms are used by this species of *Picochlorum* depending on which of these sources of inorganic carbon is available in the environment.

Some organisms also have pyrenoids which serve as a component of the carbon dioxide concentrating mechanism (CCM) within which CO_2 is generated from HCO_3^-. This makes CO_2 more available and thus increases the CO_2 / O_2 ratio at the active site of ribulose-1,5-bisphosphate carboxylase-oxygenase (Rubisco), which favours carbon fixation over oxygenase activity (photorespiration). Rubisco is an important component of pyrenoids in the chloroplast (Raven and Beardall 2003). Although Hironanka (2000) reported the absence of pyrenoid in *Picochlorum*, an examination of the micrographs of *Picochlorum* compared with that of some unicellular organisms which possess pyrenoids, and were surrounded by starch grains suggests *P. oklahomensis* may possess a pyrenoid which may play a role in CCM. Further transmission electron microscopy work on fresh

samples would be necessary to confirm this. Also performing molecular studies to confirm the presence and quantify the amount of carbonic anhydrase (CA) in *Picochlorum* under low and high bicarbonate media will help to resolve whether CA and/or CCM is active in *Picochlorum*.

Under LC, carbon fixation is presumably reduced and this may also affect nitrogen and sulphur metabolism. When biomolecules such as nucleic acids and proteins are not available, cell division and growth rates are slowed down and eventually yield is also reduced. It appears that at LC, *Picochlorum* maintained and/or increased the light reaction process to supply energy (ATP) to meet the high energy requirement of active transport of HCO_3^- and, at higher salinities, Na^+ efflux and synthesis of glycerol. Because of limiting carbon in the environment and consequent diversion of energy, carbon fixation to support growth was reduced. The cells were probably producing only needed molecules to help them survive.

Effect of Salinity and Phosphorus

This study has shown that the effect of salinity stress on growth and photosynthesis may change under different phosphorus concentration. That is, the response to salinity depends on high or low phosphorus present in the growing environment. My results showed different responses to salinity under high and low phosphorus: cell yield at day 10 (Fig. 7), total chlorophyll (Fig. 17a), total carotenoids (Fig. 18a), total chlorophyll/total carotenoids ratio (Fig. 18b), maximum quantum yield of PSII, F_v/F_m (Fig. 23a), effective quantum yield of PS II electron transport in light-adapted state, Φ_{PSII} (Fig. 23a), and non-photochemical quenching, NPQ (Fig. 23b).

In this study, low phosphorus (LP) significantly increased initial growth rate compared to cells grown in high phosphorus (HP) medium (Fig. 6). Even though initial growth rates were higher in LP cultures compared to HP, these increases could not be sustained once phosphate was depleted, as observed in the significantly reduced cell yields at day 10 in *Picochlorum oklahomensis* (Fig. 7). Low phosphorus also decreased P_{max} by about 15 - 20% at all salinities but did not affect α. The analysis of the convexity values of the growth curves using Bannister's function (Table 4,) indicate that growth in LP medium was less stressed compared to HP medium.

The increase in the initial growth rate is unexpected considering that these cells were cultured in low phosphorus. A possible explanation for the increase in the initial growth rates is that growth in low phosphorus medium may have induced an efficient mechanism of acquiring P from the environment such as producing extracellular phosphatases to ensure maximum uptake of phosphate from the LP medium and store it for use. The cells are therefore able to undergo rapid cell divisions despite limited availability of phosphorus, as observed in the cell numbers within the first three days. Phosphorus is a component of biomolecules such as sugar phosphates and nucleic acids, which may affect protein synthesis. This may account for the increases in the initial growth rates. However, with the depletion of phosphorus without any replacement in the batch cultures, cell division is slowed, resulting in lower cell numbers and significantly reduced yield at day 10 (Fig. 7). In order to confirm the involvement of phosphatases, an experiment may be performed and the ambient phosphate and also the levels of phosphatase measured over time during batch growth.

In LP, cell yield at 50 ppt was higher compared to 10 ppt though neither differed from yield at 100 ppt (Fig. 7). Even though LP caused decreases in P_{max} compared to HP, the absolute values are not significantly different (Table 2). This agrees with the chlorophyll a fluorescence measurements (Fig. 23). LP caused (1) a decrease in F_v/F_m only at 10 ppt, (2) significant decreases in Φ_{PSII} and increases in NPQ at all salinities, but (4) did not affect photochemical quenching. Also, LP reduced total chlorophylls by about 16% at 10 and 50 ppt but the chlorophyll a/b ratio was not affected. This is not surprising since P is not directly involved in the biosynthesis of chlorophyll.

The decreases in P_{max} by LP suggest that the photosynthetic capacity was negatively affected with respect to electron transport and carbon fixation. The main products of the light reactions of photosynthesis are ATP and NADPH which are used in the Calvin cycle. Low phosphorus in the chloroplast would imply insufficient availability of inorganic P to form ATP through photophosphorylation. This may lead to an increase in the energization of the thylakoid membrane and result in a decline in electron transfer (Heineke et al. 1989). The composition of the membrane may also be affected considering that phosphorus is a component of phospholipids which form part of membranes. As a result of insufficient ATP, the fixation of carbon in the Calvin cycle would also be decreased.

P deficient conditions in the cytoplasm also may inhibit the chloroplast membrane triose phosphate-phosphate translocator, blocking transport of the triose phosphate produced in the Calvin cycle to the cytosol for use by the cell. This translocator moves glyceraldehyde-3-phosphate and dihydroxyacetone phosphate from the chloroplast to the cytosol, while at the same time transferring inorganic P from the cytosol to the

chloroplast (Giersch and Robinson 1987; Flügge 1995; Pieters et al. 2001). The triose phosphates which are not transferred from the chloroplast are converted to starch. The accumulation of starch in the chloroplast serves as a feedback signal which reduces carbon fixation. Slow growth also reduces the demand for biomolecules such as proteins and fatty acids, which leads to a decrease in the demand for photosynthates and finally a decrease in carbon fixation.

LP significantly reduced F_v/F_m by less than 15% at 10 ppt only (Fig. 23a), suggesting minor inhibition of PSII. Even though F_v/F_m was only affected by LP at 10 ppt, LP decreased Φ_{PSII} at all salinities, with the most reduction occurring at 10 ppt. This agrees with the reduction in P_{max} by LP observed in *Picochlorum* (Table 2). The reduction in Φ_{PSII} agrees with the increases in non-photochemical quenching (NPQ) observed in LP grown cells (Fig. 23b). The increase in the protective mechanism NPQ suggests that cells grown in LP medium at this stage were somehow under stress and that the stress was more severe at 10 ppt. The increase in NPQ by LP indicates that LP caused excess excitation pressure (Maxwell et al. 1995) in *Picochlorum*, though the cells were able to dissipate this excess energy, possibly through the xanthophyll cycle.

Photochemical quenching, qP, was not affected by LP suggesting that there were no changes in the proportion of opened PSII centers. This unexpected lack of effect of LP on qP is consistent with the absence of an effect of low phosphorus on α (Table 2) and F_v/F_m (Fig. 23a). It is possible that the effect of LP was insufficient to substantially impair PSII. Alternatively, *Picochlorum* may be adapted to low phosphate conditions considering the hypersaline nature and the expected low phosphate in its natural environment (Major et al. 2005).

Considering the response to salinity under high and low phosphate, it is noted that the effect of salinity on initial growth rate and P_{max} in HP was the same as in LP, however the response was different for yield at day 10, total chlorophyll, total carotenoids, F_v/F_m, Φ_{PSII} and NPQ.

Effect of Salinity and Iron

This study has shown that response to growth and photosynthesis is influenced by the interaction between salinity and iron concentration. The response to salinity is different under high and low iron, as evident in my data for initial growth rates (Fig. 9), cell yield at day 10 (Fig. 10), total chlorophyll (Fig. 19a), total carotenoids (Fig. 20a) maximum quantum yield of PSII, F_v/F_m (Fig. 24a) and non-photochemical quenching, NPQ (Fig. 24b).

Low iron significantly reduced initial growth rate, cell yield at day 10 and photosynthetic capacity in *Picochlorum oklahomensis*. Increasing salinity did not affect initial growth rates and P_{max} at lower salinities in the +Fe medium but significantly decreased these parameters at 100 ppt in the +Fe medium (Fig. 9) which led to a decrease in the cell yields.

This concept has been applied to P-I curves, but never before to batch grown cultures. However, I used this unusual analysis because of the shape of the μ curves. When an alga or a plant is stressed, the curvature of P-I curves is very low relative to unstressed organisms (Bannister 1979; Henley 1993). It is unclear whether this would also apply to the semi-log time course of cell densities. In my analysis, the growth curves of *Picochlorum* in +Fe had much higher convexity values than that of –Fe grown cells (Table 4), indicating that they were much stressed growing in -Fe medium. The effect on

initial growth rate by and cell yield salinity were both different under +Fe and –Fe grown cultures.

The reduction in initial growth rate of *Picochlorum* at 100 ppt salinity in +Fe medium is expected. Salinity stress affects algae and plants through osmotic stress, ion toxicity and ionic imbalance. Organisms adapted to high salinity try to overcome these effects by producing compatible osmolytes which require high energy cost leading to reduced growth rates and decline in photosynthetic electron transport (Gimmler et al. 1981; Kirst 1989; Gilbert et al. 1998). This is also consistent with the P_{max} values in +Fe medium. As mentioned earlier, *Picochlorum* produces and accumulates proline (Hironanka, 2000), a compound which has been reported to play a major role in salt tolerance in some organisms, and its production from glutamate requires much extra energy and carbon. Salt may also affect the repair of D1 proteins, which ultimately will increase excitation pressure and result in a decrease in electron transport.

In -Fe medium, however, initial growth rate and day 10 cell yields were highest at 50 ppt; day 10 yields were similarly reduced at 10 and 100 ppt but initial growth rate was significantly more reduced at 100 ppt than 10 ppt (Figs. 9, 10). This shows that the response of *Picochlorum* to salinity may be influenced by the level of iron present in the culture medium. This is consistent with my primary hypothesis that the response to growth and yield response of *Picochlorum* at the different salinities will show different patterns under high and low iron. Even though P_{max} and initial growth rates were different at 10 ppt and 100 ppt in -Fe media, the cell yields at day 10 were the same. These differences may be due to changing physiology with time in the batch cultures as nutrient is depleted. Iron stress in *Picochlorum* may affect the acquisition of other nutrients such

as nitrate, as well as the assimilation of nitrogen in the chloroplast and therefore ultimately affecting growth and yield. Rueter and Ades (1987) reported decreased uptake of nitrate in the chlorophyte, *Scenedesmus quadricauda*, grown in iron-limited medium compared to those in iron sufficient cultured cells. Further experiments may be performed to study the uptake of nitrate by *Picochlorum* in low iron medium.

The reduction in P_{max} in -Fe medium suggests that the photosynthetic capacity was affected with respect to electron transport and/or carbon fixation. Iron is an essential cofactor of some components of the electron transport chain such as ferredoxin, cytochromes and the iron-sulphur proteins. Iron deficiency is likely to affect the amount of electron carriers available in the electron transport chain and the function they perform. If inadequate ATP and reductants are produced in the light reactions of photosynthesis, then assimilation of carbon in the Calvin cycle would be reduced.

Low iron reduced P_{max} in *Picochlorum* by about 45% at all salinities, but decreased initial growth rate by about 70% at lower salinities and 80% at 100 ppt, and decreased yield by more than 84% at all salinities. This indicates that photosynthesis may not be the only factor contributing to the reduced growth in *Picochlorum.* Iron is required for the functioning of nitrite reductase and nitrate reductase and therefore when iron is limiting, nitrogen assimilation is affected as well as protein synthesis. Cell division may be slowed down as a result of insufficient nitrogen for the formation of proteins and nucleic acids.

As evidenced in my fluorescence results (Fig. 24a), low iron massively decreased the maximum quantum yield of PS II photochemistry in dark-adapted state cells (F_v/F_m), which indicates that there is photodamage to some portions of PS II. The LHCII may

have been decoupled from PSII due to iron deficiency (Morales et al. 2001) and may have contributed to the decrease. F_v/F_m was affected differently by salinity in *Picochlorum* grown in +Fe and -Fe media. Whereas there was little effect of salinity in +Fe medium, F_v/F_m increased at 100 ppt in -Fe medium, an indication of a salinity-nutrient interaction. The likely explanation is that high salinity reduces iron stress, for example by reduced demand (lower growth rate at high salinity). Another interpretation for this decrease is that *Picochlorum* is adapted to coping with higher salinity at iron deficient conditions. This is consistent with my result that within the –Fe treatments, increasing salinity from 10 ppt to 100 ppt significantly decreased non-photochemical quenching (NPQ).

Effective quantum yield of PS II electron transport in light-adapted state (Φ_{PSII}) and photochemical quenching (qP), which is an indication of actual open reaction centers as well as indicating the redox state of plastoquinone (Q_A), were reduced in *Picochlorum* by low iron as expected (Fig. 24). The fewer open PSII reaction centers as indicated by qP, may be due to a reduced rate of replacement of damaged D1 proteins compared to the rate at which they were being destroyed (Allakhverdiev et al. 2002; Mohanty et al. 2007). As a result of iron deficiency, a reduction in electron carriers to accept and transfer electrons may cause excess excitation pressure with a concomitant decrease in qP. A reduction in the F_v/F_m may also indicate enhanced photoprotection to dissipate excess excitation pressure, for example through the xanthophyll cycle (Demmig-Adams and Adams 1992; Gilmore 1997; Lu et al. 2003). This is supported by the significant increase in non-photochemical quenching caused by low iron at 10 ppt which was not evident in +Fe medium. Interestingly, this elevated NPQ was not evident at 50 and 100 ppt. The

F_v/F_m data indicate that there was more photodamage to portions in PSII at 10 ppt than at 100 ppt. This may explain the higher NPQ values at 10 ppt compared to 100 ppt under –Fe medium. That most of the absorbed energy was not used for photochemical process.

As expected, total chlorophyll and carotenoids per cell were decreased by low iron at 10 and 50 ppt (Figs. 19a and 20a), since iron is required for the synthesis of chlorophyll in algae and plants. However, at 100 ppt, low iron increased total chlorophyll and total carotenoids per cell. This is unexpected considering that iron is required in the biosynthesis of chlorophyll and carotenoids. A deficiency in iron should result in a decrease in the total chlorophyll and carotenoids concentrations in the cells. It is possible that under –Fe at higher salinity, the low growth rate slows the "dilution" of chlorophyll even in the absence of chlorophyll synthesis. Although total chlorophyll per cell was not affected by salinity at 10 and 50 ppt in +Fe medium, chlorophyll content decreased at 50 ppt in -Fe treatment (Fig. 19a), indicating salinity-Fe interaction. The mean cell density at day 6 (when pigments and P-I were measured) for –Fe treatment was 4.4×10^6 at 50 ppt compared to 3.5×10^6 and 1.9×10^6 for 10 and 100 ppt respectively. The higher number of cells at 50 ppt may explain the decrease in the total chlorophyll per cell in the –Fe grown cells: a similar total amount of Chl in the culture may be spread over a larger population of cells.

Salinity did not affect chlorophyll *a*/*b* ratio in +Fe or –Fe grown cells, but -Fe massively decreased chlorophyll *a*/*b* ratio (Fig. 19b). The ratios of about 1.2 to 1.7 in –Fe are extremely low. It is possible that this may be due to insensitivity of the spectrophotometer used because of the very low absorption values (<0.01) of pigment extracts of –Fe cultures. However, assuming the data to be accurate, a possible biological

explanation for the very low chlorophyll *a*/*b* ratios may in part be attributed to the decreases in chlorophyll a per cell caused by -Fe which indicates selective loss of reaction centers. The decrease may also be due to an increase in chlorophyll b per cell at all salinities in –Fe grown medium. This suggests -Fe cultured cells had a larger light-harvesting antenna for absorbing at a high rate, though it appears they were not able to effectively convert the absorbed light into chemical energy as indicated by decreases in F_v/F_m, Φ_{PSII} and qP. The decoupling of the LHCII from PSII may account for this inability to transfer the absorbed energy (Morales et al. 2001). The green alga *Chlamydomonas reinhardtii* grown in iron deficient medium had increased functional antenna size of PS II (Naumann et al. 2007). Similarly, some cyanobacteria form iron deficiency-induced protein A (idiA) and iron stress-induced protein A (isiA), which tend to surround the photosystems under iron limitation (Burnap et al. 1993; Boekema et al 2001).

The relatively high carotenoids at 100 ppt salinity in -Fe medium may be of importance to *Picochlorum* in protecting itself against the detrimental effects of high light. Pigments such as ß-carotene help in the quenching of reactive species and violaxanthin, antheraxanthin and zeaxanthin are involved in the xanthophyll cycle in dissipating excess heat (Demmig-Adams and Adams 1992; Gilmore 1997; Lu et al. 2003). A further study measuring the amount of these pigments may indicate their involvement or otherwise, because I measured only crudely the total carotenoids but not the individual pigments. Also the relatively high total carotenoids at higher salinity may but rather a lack of decrease as a result of the low growth rate as explained earlier for chlorophyll and not an increase in itself considering that in –Fe media the total

carotenoids are the same at 10 ppt and 100 ppt (Fig. 20a), The mean cell density at day 6 was 4.4 x 10^6 at 50 ppt compared to 3.5 x 10^6 and 1.9 x 10^6 for 10 and 100 ppt respectively (Fig. 8), and the pigment content and cell densities vary inversely and proportionately therefore having more cells explains the decrease in the total carotenoids per cell in –Fe grown cells. In order to test the explanation for the relative increase, further studies may be performed by measuring the carotenoids and chlorophyll contents daily through the growth curve. If total pigments in the culture do not change, then the amount per cell must decrease with successive cell divisions.

In summary, some of the results in this study supported my hypothesis that response to the effect of salinity stress on growth and photosynthesis will differ under high iron and under no added iron. The response pattern was different in initial growth rate, cell yield at day 10, total chlorophyll, total carotenoids, F_v/F_m and NPQ. The different response in pigments and F_v/F_m seems to be due mainly to differences at 100 ppt, which may be explained by the extremely low growth rate (slow depletion of Fe) at 100 ppt, a likely survival mechanism. Since *Picochlorum* occurs in a hypersaline environment characterized by fluctuations in salinity and possibly nutrients, it makes sense that at higher salinities and during deficient nutrient periods, it tends to exhibit low growth rates pending more favourable conditions. This way it is able to survive and reproduce to continue its existence.

Summary Perspective

Photosynthetic organisms rarely experience optimal growth conditions in their natural habitat, and at any given time, two or more physical and chemical variables are

likely to be suboptimal. It has been established that the extreme environment of the Great Salt Plains (GSP) results in low algal biomass (Major et al. 2005; Kirkwood et al. 2006; Henley et al. 2007), such that natural selection is likely driven by survival of multiple abiotic stresses rather than rapid growth and biotic interactions (grazing and intra/interspecific competition for resources). This study is an initial effort to determine the effect of combined abiotic stress factors on an alga isolated from the GSP habitat, specifically salinity and the inorganic nutrients P, Fe and C. These three nutrients were selected because of our *a priori* expectation that chemical interactions between PO_4^{3-}, Fe^{3+} and HCO_3^- with ions at high salinity may affect their bioavailability, whereas NH_4^+ and NO_3^- are less likely to complex with other salts. Moreover, the ratio of $(NH_4^+ + NO_3^-)/PO_4^{3-}$ in the groundwater at the GSP is much higher than the Redfield N:P ratio of 16:1 (Major et al. 2005), which is the approximate "typical" composition of microalgae. Thus, P rather than N may limit algal biomass at the GSP.

Various mineral nutrients such as nitrogen and phosphorus generally follow Liebig's law of the minimum, such that only one is limiting at a time. This concept may or may not apply to concurrent physical and nutrient stresses. It remains largely unknown whether interacting stress factors have synergistic or antagonistic effects. It was previously shown in the GSP chlorophyte algae *P. oklahomensis* and *Dunaliella* sp. that at 100 ppt, a salinity high enough to significantly reduce growth, cells are more tolerant of acute high temperature stress (Henley et al. 2002). Similarly, in this study with *P. oklahomensis*, the chlorophyll fluorescence parameters F_v/F_m, Φ_{PSII} and NPQ all exhibit smaller responses to limitation by phosphorus or iron when grown at 100 ppt compared to 10 ppt (Table 5); the response to limiting P and Fe at 50 ppt is

Table 5. Ratio (%) of variables under low nutrient/high nutrient treatments. SD_R is standard deviation for the ratio calculated from the means and corresponding standard deviations according to the formula $SD_R = R_{LC/HC} \cdot \sqrt{\{(SD_{LC}/mean_{LC})^2 + (SD_{HC}/mean_{HC})^2\}}$
For any variable eg. yield, in which the ratio R, between means values under two treatments at 10 ppt, $mean_{LC}$, is the mean yield at day 10 under low carbon at 10 ppt with SD_{LC} as its standard deviation, $mean_{HC}$, is the mean yield at day 10 under high carbon at 10 ppt with SD_{HC} as its standard deviation.

LC/HC

	Whole cell level properties						Thylakoid level properties									
Salinity	μ	SD	Yield	SD	P_{max}	SD	Chl a+b	SD	Fv/Fm	SD	ΦPSII	SD	qP	SD	NPQ	SD
10	62	1	73	1	118	18	106	6	101	2	122	9	110	8	75	21
50	64	0	80	3	112	7	102	5	106	2	135	16	127	14	87	47
100	70	1	82	2	114	13	77	13	99	4	123	29	120	23	57	31

LP/HP

	Whole cell level properties						Thylakoid level properties									
Salinity	μ	SD	Yield	SD	P_{max}	SD	Chl a+b	SD	Fv/Fm	SD	ΦPSII	SD	qP	SD	NPQ	SD
10	123	1	42	1	80	8	81	2	86	2	49	7	93	10	228	19
50	122	1	51	2	81	17	86	5	100	2	77	4	96	11	235	96
100	118	1	82	2	85	16	103	12	96	3	82	10	90	10	175	80

-Fe/
+Fe

	Whole cell level properties						Thylakoid level properties									
Salinity	μ	SD	Yield	SD	P_{max}	SD	Chl a+b	SD	Fv/Fm	SD	ΦPSII	SD	qP	SD	NPQ	SD
10	27	1	11	0	57	2	82	3	20	20	11	16	21	48	354	31
50	31	0	16	1	54	5	59	14	23	8	19	12	34	31	141	83
100	19	0	12	0	56	7	133	15	52	2	19	18	37	38	75	58

nutrient- and parameter-specific. In part, this may be explained by slower growth rate at 100 ppt regardless of nutrient supply, which would slow the depletion of external and internal nutrient reserves due to dilution among more cells. In other words, at the time of characterization, slower growing cells at high salinity may exhibit less nutrient stress than at low salinity. However, in some cases the reduced nutrient-dependent fluorescence effect occurs between 10 and 50 ppt salinity, despite no salinity-induced growth rate difference. Examples include NPQ in low Fe and Φ_{PSII} in both low P and low Fe (Figs. 23 and 24). This indicates that the effect of nutrient dilution by cell division cannot be the only explanation for this phenomenon.

Similarly, with respect to pigment content and most fluorescence parameters, *P. oklahomensis* cultured in low P or Fe exhibit smaller inhibition by 100 ppt salinity relative to 10 ppt (Table 6). That is, high salinity stress appears to be reduced under low nutrient conditions. Both this effect and the previously discussed reduction of low nutrient (P, Fe) stress by high salinity represent interaction between salinity and nutrients. However, it is unclear whether they represent distinct mechanisms or if they are different manifestations of the same phenomenon, and if so which is the primary cause. It is difficult to envision nutrient limitation inducing a general protective response to physical stress factors such as salinity; in fact the opposite might be expected because nutrient stress reduces a cell's ability to make certain essential cellular components. Similarly, although low nutrients alone reduce growth rate, salinity is not a depletable resource, thus a dilution effect cannot be invoked as a simple explanation as it could in the case of the reverse effect of salinity on nutrient response. Intuitively, it seems more likely that

Table 6. Ratio (%) of 100ppt/10ppt for various parameters in high and low P, Fe and C. SD_R is standard deviation for the ratio calculated from the means and corresponding standard deviations according to the formula $SD_R = R_{100/10} \cdot \sqrt{\{(SD_{100}/mean_{100})^2 + (SD_{10}/mean_{10})^2\}}$For any variable eg. yield, in which the ratio R between means values under 100 ppt and 10 ppt for a specific treatment eg. low carbon (LC).

	Whole cell level properties						Thylakoid level properties									
	μ	SD	yield	SD	P_{max}	SD	Chl a+b	SD	F_v/F_m	SD	Φ_{PSII}	SD	qP	SD	NPQ	SD
HC	66	1	55	2	62	6	70	8	101	3	79	10	75	9	76	35
LC	74	1	62	0	60	9	51	7	99	4	80	17	82	13	58	23

	Whole cell level properties						Thylakoid level properties									
	μ	SD	yield	SD	P_{max}	SD	Chl a+b	SD	F_v/F_m	SD	Φ_{PSII}	SD	qP	SD	NPQ	SD
HP	66	1	55	2	62	6	70	8	101	3	79	10	75	9	76	35
LP	63	0	109	2	66	12	90	2	113	3	132	18	73	7	58	4

	Whole cell level properties						Thylakoid level properties									
	μ	SD	yield	SD	P_{max}	SD	Chl a+b	SD	F_v/F_m	SD	Φ_{PSII}	SD	qP	SD	NPQ	SD
+Fe	66	1	55	2	62	6	70	8	101	3	79	10	75	9	76	35
-Fe	45	1	64	1	61	5	113	5	257	255	141	257	134	344	16	10

salinity stress induces a general protective response, as was suggested with respect to acute temperature stress at high salinity (Henley et al. 2002).

How might a general stress response involving heat shock proteins and compatible osmolytes translate into reduced low nutrient stress, beyond what can be explained by lower demand due to slower growth at high salinity? My data cannot indicate which mechanisms are occurring, but the apparent lessening of salinity stress by low P and Fe and/or the lessening of nutrient stress by high salinity are consistent with a general protective response to stress. Similarly, a turfgrass was shown to be more salt tolerant when provided with limiting N compared to replete N (Bowman et al. 2006).

The literature provides limited evidence for at least three types of inducible protective mechanisms: compatible osmolytes, heat shock proteins (Hsp), and protein phosphorylation cascades. High salinity causes accumulation of organic compatible osmolytes which balance internal osmotic pressure with the saline exterior and protect macromolecules and membranes (Chen and Murata 2002; Munns and Tester 2008). It is also likely that high salinity induces heat shock proteins that also protect macromolecules (Sairam and Tyagi 2004). A chloroplast-localized HSP70 is protective with respect to PSII photodamage and repair (Schroda et al. 1999, Yokthongwattana et al. 2001). Those studies only considered high light stress, not interaction among different stresses. However, small Hsp may be induced by a number of stresses (including osmotic) and may have a broad-spectrum protective role for proteins, possibly by acting as molecular chaperones (Hsieh et al. 2002; Sun et al. 2002). Oxidative stress (H_2O_2) induces a mitogen-activated protein kinase cascade in *Arabidopsis*, and a related gene in transgenic tobacco is more tolerant of several stress factors in the absence of apparent signaling

pathways (Kotvun et al. 2000). Thus, it is reasonable to suggest that the broadly halotolerant *P. oklahomensis* may possess similar mechanisms that confer multiple stress resistance in response to any one stress factor. Stressors such as high light/UV, temperature, salinity and oxidation, and low nutrients likely co-occur on hypersaline flats. Evolution of general stress response mechanisms would optimize resources and physiological efficiency, in that the first stress factor would protect against subsequent environmentally inevitable stressors.

From the two-way ANOVA tables, the majority of the measured variables in the carbon experiment did not exhibit significant salinity-carbon interaction and a few did not show a significant primary effect of C. In the P and Fe experiments, most of the variables showed significant primary nutrient effects and salinity-nutrient interaction. This may be attributable to a fundamental difference in the experimental delivery of C compared to P and Fe. The latter nutrients are added in fixed amount at the beginning of batch cultures, thus can be completely depleted within a few days. In contrast, the cultures are an open system with respect to C, which can diffuse through the cotton plug and also enter whenever the plugs are removed for sampling. The equilibration of CO_2 from the headspace into the medium is probably slow in the absence of stirring, however it is likely nonzero so that growth rates but not cell yields are limited by C supply. For this reason, absence of a large effect of low bicarbonate and salinity-C interaction is not surprising. Carbon is also rarely if ever a limiting nutrient *in situ*.

I cannot rigorously compare the P and Fe experiments because, based on magnitudes of responses in most variables, the -Fe cultures appeared more severely stressed than the low P cultures. However, some qualitative differences in the responses

to limitation by P and Fe at the level of fluorescence properties are worth noting. Moderately P-stressed cultures exhibited a slight reduction in P_{max} at all salinities, corresponding to reduced Φ_{PSII} and increased NPQ, but minimal changes in F_v/F_m or qP. Taken together, these results suggest elevated thermal dissipation of energy under P stress, generally interpreted as a reversible photoprotective mechanism. P is not a structural component of photosynthetic macromolecules, thus low P availability is not expected to severely impair the photosynthetic process at the level of electron transport. In contrast, -Fe cultures exhibited a much larger reduction in P_{max} at all salinities, corresponding to greatly reduced F_v/F_m, Φ_{PSII} and qP; in this case NPQ increased only at 10 ppt salinity. This combination of changes is consistent with severe and persistent inhibition of photosystem II by very low Fe. Fe is an essential component of cytochromes, Fe/S complex and ferredoxin in photosynthetic electron transport, and the near absence of added Fe in my experiment consequently had a major effect on the efficiency of photosynthesis. Ferredoxin may be replaced by flavodoxin under low Fe conditions (Vigara et al. 1998), but there is no equivalent for other Fe-containing electron transport components.

I also cannot thoroughly compare corresponding changes in P_{max} and fluorescence parameters, because the apparatus available to me necessitated making the two types of measurements under different conditions. The actinic light level during fluorescence measurements was approximately 400 μmol m^{-2} s^{-1}, which is close to saturation of the P-I curves for most cultures and roughly twice the growth irradiances. It would be useful to repeat selected experiments with fluorescence measured concurrently with the P-I measurements, such that the saturation function of Φ_{PSII} could be determined.

Fluorescence also could in principle be measured directly in the culture flasks for an "*in situ*" estimate of Φ_{PSII}.

One additional series of experiments to resolve mechanisms of salinity-nutrient interaction would involve continuous cultures. Chemostats at varying nutrient compositions but constant dilution (= growth) rate would factor out the dilution effect related to reduced growth rate at high salinity observed in batch cultures. In addition, chemostats would eliminate the progressive physiological deterioration through time observed in batch mode. This is especially problematic when comparing different nutrient treatments, which slow down at different rates and thus may not have the equivalent physiological "age" on a given day. For example, based on low nutrient growth rates in batch cultures, operating chemostats at a dilution rate of 0.3 d^{-1} should allow all nutrient-salinity combinations to grow without washout. If high and low P or Fe chemostat cultures at identical growth rates at all salinities exhibit the same physiological differences (e.g. P_{max}, NPQ, Φ_{PSII}, etc.) as observed in batch cultures, this would indicate that the salinity-induced dilution effect on nutrient demand is unimportant. If on the other hand nutrient-dependent physiological differences seen in batch mode are largely eliminated in identical dilution rate chemostats, this result would imply that the salinity-induced dilution effect is largely responsible for the physiological effects.

REFERENCES

Adams, W. W. III, Demmig-Adams, B., Winter, K. and Schreiber, U. 1990. The ratio of variable to maximum chlorophyll fluorescence from photosystem II, measured in leaves at ambient temperature and at 77K, as an indicator of the photon yield of photosynthesis. *Planta* 180: 166-174.

Allakhverdiev, S., Nishiyama, Y., Miyairi, S., Yamamoto, H., Inagaki, N., Kanesaki, Y., and Murata, N. 2002. Salt Stress Inhibits the Repair of Photodamaged Photosystem II by Suppressing the Transcription and Translation of *psbA* Genes in *Synechocystis*. *Plant Physiol.* 130: 1443-1453.

Ashraf, M. and Harris, P. J. C. 2004 Potential biochemical indicators of salinity tolerance in plants. Plant Science 166: 3-16.

Anderson, M. A. and Morel, F. M. M. 1982. The influence of aqueous iron chemistry on the uptake of iron by the coastal diatom *Thalassiosira weissflogii*. *Limnol. Oceanogr*. 27:789-813.

Bannister, T. T. 1979. Quantitative description of steady state, nutrient-saturated algal growth, including adaptation. *Limnol. Oceanogr.* 24: 76-96.

Bilger, W. and Björkman, O. 1990. Role of the xanthophylls cycle in photoprotection elucidated by measurements of light-induced absorbance changes, fluorescence and photosynthesis in leaves of *Hedera canariensis*. *Photosynth. Res.* 25:173-185.

Boekema, E. J., Hifney, A, Yakushevska, A. E., Piotrowski, M., Keegstra, W., Berry, S., Michel, K.-P., Pistorius, E. K., and Kruip, J. 2001. A giant chlorophyll-protein complex induced by iron deficiency in cyanobacteria. *Nature* 412: 745–748

Bowmann, D. C., Cramer, G. R. and Devitt, D. A. 2006. Effect of nitrogen status on salinity tolerance of tall fescus turf. *Journal of Plant Nutrition* 29: 1491-1497.

Bulter, A. 1998. Acquisition and utilization of transition metal ions by marine organisms. *Science* 281: 207-210.

Burnap, R. L., Troyan, T., and Sherman, L. A. 1993 The highly abundant chlorophyll-protein of iron deficient *Synechococcus* sp. PCC 7942 (CP43') is encoded by the *isiA* gene. *Plant Physiol* 103: 893–902

Chen, T. H. H. and Murata, N. 2002. Enhancement of tolerance of abiotic stress by metabolic engineering of betaines and other compatible solutes. *Current Opinion in Plant Biology*. 5: 250-257.

Cole, J. J., Howarth, R. W., Nolan, S. S. and Marino, R. 1986. Sulfate inhibition of molybdate assimilation by planktonic algae and bacteria: some implications for the aquatic nitrogen cycle. *Biochemistry* 2: 179-196.

Crosa, J.H. 1997. Signal transduction and transcriptional and post-transcriptional control of iron-regulated genes in bacteria. *Microbiol. Mol. Biol. Rev.* 61: 319-339.

Davies, A. G. 1988. Nutrient interactions in the marine environment. *In* D. Rogers and J. Gallon (eds.), Biochemistry of the Algae and Cyanobacteria. Proc. Phytochem. Soc. Europe, vol. 29. Oxford University Press. Oxford, pp. 241-256.

Demmig-Adams, B. and Adams, W. W. III. 1992. Photoprotection and other responses of plants to high light stress. *Annu. Rev.Plant Physiol. Mol. Biol.* 43:599-626.

Doucette, G. J. and Harrison, P. J. 1991. Aspects of iron nutrition in the red tide dinoflagellate *Gymnodinium sanguineum.* I. Effect of iron depletion and nitrogen source on biochemical composition. *Mar. Biol. (Berl.)* 110: 165-173.

EL-Sheekh, M. M. 2004. Inhibition of the water splitting system by sodium chloride stress in the green alga *Chlorella vulgaris*. *Braz. J. Plant Physiol*., 16(1):25-29

Eugster, H. P. and Jones, B. F. 1979. Behavior of major solutes during closed-basin brine evolution. *American Journal of Science* 279: 609-631.

Falkowski, P.G. and Raven, J.A. 1997. Carbon acquisition and assimilation. In: *Aquatic Photosynthesis* pp. 128–162. Blackwell Science, Inc., Malden, Massachusetts.

Flügg, U. I. 1995. Phosphate translocation in the regulation of photosynthesis. J. Exp. Bot. 46:1317 – 1323.

Geider, R. J., Roche, J. L., Greene, R. M. and Olaizola, M. 1993. Response of the photosynthetic apparatus of *Phaeodactylum tricornutum* (Bacillariophyceae) to nitrate, phosphate, or iron starvation. *J. Phycol* 29: 755 – 766.

Genty, B., Britais, J. M. and Baker, N. R. 1989. The relationship between the quantum yield of photosynthetic electron transport and quenching of chlorophyll fluorescence. *Biochem. Biophys. Acta* 990: 87-92.

Giersch, C., and Robinson, S. P. 1987. Regulation of photosynthetic carbon metabolism during phosphate limitation of photosynthesis in isolated spinach chloroplasts. Photosynthesis Research 14: 211 – 227.

Gilbert, G. A., Gadush, M. V., Wilson, C. and Madore, M. 1998. Amino acid accumulation in sink and source tissues of *Coleus blumei* Benth. During salinity stress. *J. Exp. Bot.* 49: 107-114.

Gilmore, A. M. 1997. Mechanistic aspects of xanthophyll cycle-dependent photoprotection in higher plant chloroplasts and leaves. *Physiol.Plant.* 99: 197-209.

Gimmler, H., Wiedemann, C. and Möller, E. M. 1981. The metabolic response of the halotolerant green alga *Dunaliella parva* to hyperosmotic shocks. *Ber. Dtsch. Bot. Gesell.* 94:613–34.

Giordano, M., Beardall, J. and Raven, J. A. 2005. CO_2 concentrating mechanisms in algae: mechanisms, environmental modulation, and evolution. *Annu. Rev. Plant. Biol.* 56: 99 – 131.

Graham, L. E. and Wilcox, L. W. 2000. *Algae*. Prentice Hall. Upper Saddle River, NJ 650pp.

Guerinot, M. L. and Yi, Y. 1994. Iron: nutritious, noxious and not readily available. *Plant Physiol*. 104:815-20.

Guikema, J. A. and Sherman, L. A. 1983. Organization and function of chlorophyll in membranes of cyanobacteria during iron starvation. *Physiol. Plant*. 73:250-256.

Heineke, D., Stitt, M. and Heldt, H. W. 1989. Effects of inorganic phosphate on the light dependent thylakoid energization of intact spinach chloroplasts. Plant Physiol. 91: 221 – 226.

Henley, W. J. 1993. Measurement and interpretation of photosynthetic light-response curves in algae in the context of photoinhibition and diel changes. *J. Phycol.* 29: 729-739.

Henley, W. J., Hironaka, J. L., Buchheim, M. A., Buchheim, J. A., Fawley, M. W. and Fawley, K. P. 2004. Phylogenetic analysis of the "*Nannochloris*-like" algae and diagnoses of *Picochlorum oklahomensis* gen. et sp. nov. (Trebouxiophyceae, Chlorophyta). *Phycologia* 43:641-652.

Henley, W. J., Major, K. M. and Hironaka, J. L. 2002. Response to salinity and heat stress in two halotolerant chlorophyte algae. *Journal of Phycology* 38: 757-766

Henley, W.J., Milner, J., Kvíderová, J., Kirkwood, A.E. and Potter, A. 2007. Life in variable salinity: algae of the Great Salt Plains of Oklahoma, U.S.A. In: J. Sekbach [ed.] *Algae and Cyanobacteria in Extreme Environments*, pp. 683-694. Springer, Berlin.

Hernández, I., Fernández, J. A. and Niell, F. X. 1993. Influence of phosphorus status on the seasonal variation of alkaline phosphatase activity in *Porphyra umbilicalis* (L.) Kutzing. *J. Exp. Mar. Biol. Ecol*. 173:181-196.

Hironaka, J. 2000. *Characterization of a unicellular coccoid green alga collected from the Salt Plains National Wildlife Refuge, Oklahoma*. MS thesis, Oklahoma State University.

Hsieh, T.-H., Lee, J.-t., Charng, Y.-y. and Chan, M.-T. 2002. Tomato plants ectopically expressing Arabidopsis CBF1 show enhanced resistance to water deficit stress. *Plant Physiol.* 130: 618-626.

Hudson, R. J. M. and Morel, F. M. M. 1990. Iron transport in marine phytoplankton: kinetics of cellular and medium coordination reactions. *Limnol. Oceanogr*. 35:1002-20.

Hudson, R. J. M. and Morel, F. M. M. 1993. Trace metal transport by marine microorganisms: implications of metal coordination kinetics. Distinguishing between extra- and intracellular iron in marine phytoplankton. *Deep-Sea Res.* I 40:129-150.

Huertas, I. E., Colman, B., Espie, G. S. and Lubian, L. M. 2000. Active transport of CO_2 by three species of marine microalgae. *Journal of Phycology* 36 (2), 314-320.

Huertas, I. E. and Lubian, L. M. 1998. Comparative study of dissolved inorganic carbon utilization and photosynthetic responses in *Nannochloris* (Chlorophyceae) and *Nannochloropsis* (Eustigmatophyceae) species. *Can. J. Bot*. 76:1104-1108.

Jassby, A. A. and Platt, T. (1976) Mathematical formulation of the relationship between photosynthesis and light for phytoplankton. *Limnol. Oceanogr.* 21: 540-547.

Kaplan, A., and Reinhold, L. 1999. CO_2 concentrating mechanisms in photosynthetic microorganisms. *Annu. Rev. Plant. Physiol. Plant Mol. Biol.* 50: 539 – 570.

Kerkeb, L., Donaire, J. P., Venema, K. and Rodríguez-Rosales, M. P. 2001. Tolerance to NaCl induces exchanges in plasma membrane lipid composition, fluidity and H^+-ATPase activity of tomato calli. *Physiol. Plant.* 113: 217-224.

Kirkwood, A.E. and Henley, W. J. 2006. Algal community structure and halotolerance as related to the extreme conditions of a terrestrial, hypersaline environment. *J. Phycol.* 42:537-547.

Kirst, G. O. 1989. Salinity tolerance of eukaryotic marine algae. *Annu. Rev. Plant Physiol. Plant Mol. Biol.* 40:21-53.

Komori, T., Yamada, S., Myers, P. and Imaseki, H. 2003. Biphasic response to elevated levels of NaCl in *Nicotiana occidentalis* subspecies *oblique* Burbidge. *Plant Sci.* 165: 159 – 165.

Kovtun, Y., Chiu, W.-L., Tena, G. and Sheen, J. 2000. Functional analysis of oxidative stress-activated mitogen-activated protein kinase cascade in plants. *Proc. Nat. Acad. Sci.* 97: 2940-2945.

Lawlor, D. W. 2002. Carbon and Nitrogen assimilation in relation to yield: mechanisms are the key to understanding production systems. *J. Exp. Bot.* 53: 773–787.

Lee, Tse-Min 2000. Phosphate starvation induction of acid phosphatase in *Ulva lactuca* L. (Ulvales, Chlorophyta) *Bot. Bull. Acad. Sin.* 41:19-25.

Lu, C., Qiu, N. and Lu, Q. 2003. Photoinhibition and the xanthophyll cycle are not enhanced in the salt-acclimated halophyte *Artimisia anethifolia*. *Physiol. Plant.* 118:532-537.

Lu, C. and Vonshak, A. 2002. Effects of salinity stress on photosystem II function in cyanobacterial Spirulina platensis cells. *Physiologia Plantarum* 114: 405-413.

Lundberg, P., Weich, R. G., Jensen, P. and Vogel, H. J. 1989. Phosphorus-31 and nitrogen-14 NMR studies of the uptake of phosphorus and nitrogen compounds in the marine macroalgae *Ulva lactuca*. *Plant Physiol.* 89:1380-1387.

Major, K.M., Kirkwood, A.E., Major, C.S., McCreadie, J.W. and Henley, W.J. 2005. *In situ* studies of algal biomass in relation to physicochemical characteristics of the Great Salt Plains, Oklahoma, USA. *Saline Systems* 1:11 (open access online journal).

Maxwell, D. P., Falk, S. and Huner, N. P. A. 1995. Photosystem II Excitation Pressure and Development of Resistance to Photoinhibition. *Plant Physiol*. 107: 687 – 694

Merrett, M. J., Nimer, N. A. and Dong, L. F. 1996. The utilization of bicarbonate ions by the marine microalga *Nannochloropsis oculata* (Droop) Hibberd. *Plant Cell Environ*. 19:478-84.

Millero, F. J., Yao, W. and Aicher, J. 1995. The speciation of Fe (II) and Fe (III) in natural waters. *Mar. Chem.* 50:21-39.

Mohanty, P., Allakhverdiev, S. I. and Murata, N. 2007. Application of low temperatures during photoinhibition allows characterization of individual steps in photodamage and the repair of photosystem II. *Photosynthesis Research* 94: 217-224

Morales, F., Moise, N., Quilez, R., Abadia, A., Adadia, J and Moya, I. 2001. Iron deficiency interrupts energy transfer from a disconnected part of the antenna to the rest of photosystem II. *Photosynthesis Res.* 70: 207 – 220.

Moroney, J. V. and Somanchi, A. 1999. How do Algae concentrate CO_2 to increase the efficiency of photosynthetic carbon fixation? *Plant Physiol.* 119: 9-16.

Motekaitis, R. J. and Martell, A. E. 1987. Speciation of metals in the oceans. I. Inorganic complexes in seawater, and influence of added chelating agents. *Mar. Chem*. 21:101-16.

Munns, R. and Tester, M. 2008. Mechanisms of salinity tolerance. *Annu. Rev. Plant Biol*. 59: 651-681.

Naumann, B., Busch, A. Allmer, J., Ostendorf, E., Zeller, M., Kirchhoff, H. and Hippler, M. 2007. Comparative quantitative proteomics to investigate the remodeling of bioenergetic pathways under iron deficiency in *Chlamydomonas reinhardtii Proteomics* 7: 3964-3979.

Neilands, J. B. 1974. *Microbial Iron Metabolism*. Academic Press, New York, 597 pp.

Nimer, N. A., Iglesias-Rodriguez, M. D., and Merrett, M. J. 1997. Bicarbonate utilization by marine phytoplankton species. *J. Phycol*. 33:625–31.

Nissenbaum, A. [Ed] 1980. *Hypersaline Brines and Evaporitic Environments. Proceedinds of the Bat Sheva Seminar on Saline Lakes and Batural Brines. Developments in Sedimentology.* Vol. 28. Elservier, Amsterdam, 270 pp.

Pieters, A., Paul, M. J. and Lawlor, D. W. 2001. Low sink demand limits photosynthesis under P_i deficiency. J. Exp. Bot. 52:1083 – 1091.

Plesnicar, M. Kastori, R. Petrovic, N. and Pankoviv, D. 1994. Photosynthesis and chlorophyll fluorescence in sunflower (*Helianthus annulus* L) leaves as affected by phosphorus limitation. J. Exp. Bot. 45:919 – 924.

Porra, R. J., Thompson, W. A. and Kriedemann, P. E. 1989. Determination of accurate extinction coefficients and simultaneous-equations for assaying chlorophylls a and b extracted with four different solvents: Verification of the concentration of chlorophyll standards by atomic absorption spectroscopy. *Biochim. Biophys. Acta* 975:384-394.

Powles, S. B. 1984. Photoinhibition of photosynthesis induced by visible light. *Annu. Rev.Plant Physiol.* 35:15-44.

Prézelin, B. B. 1981. Light Reactions in Photosynthesis. In Platt, T. (ed.) *Physiological Bases of Phytoplankton Ecology.* Canandian Bulletin of Fisheries and Aquatic Science 210: 1-43.

Raven, J.A. 1990. Predictions of Mn and Fe use efficiencies of phototrophic growth as a function of light availability for growth and of C assimilation pathway. *New Phytol.* 116: 1-18.

Raven, J.A. 1997. Inorganic carbon acquisition by marine autotrophs. *Adv. Bot. Res.* 27: 85-209.

Raven, J. A. and Beardall, J. 2003. Carbohydrate metabolism and respiration in algae. In: Larkum, A. W. D., Douglas, S. E. and Raven, J. A. (ed.) Advances in photosynthesis and respiration – Photosynthesis in algae. Kluwer Academic Publ. London. pp 205-224.

Rees, T. A. V. 1984. Sodium-dependent photosynthetic oxygen evolution in a marine diatom. *J. Exp. Bot*. 35:332-337.

Riebesell, U., Wolf-Gladrow, D., and Smetacek, V. 1993. Carbon dioxide limitation of phytoplankton growth rates. *Nature* 361:249–51.

Roberts, S. B., Lane, T. W., and Morel, F. M. M. 1997. Carbonic anhydrase in the marine diatom *Thalassiosira weissflogii* (Bacillariophyceae). *J. Phycol*. 33:845-50.

Rotatore, C., Colman, B. and Kuzma, M. 1995. The active uptake of carbon dioxide by *Phaeodactylum tricornutum* and *Cyclotella* sp. *Plant Cell Environ*. 18:913 -918.

Round, F. E., 1981. The physical and chemical characteristics of the environment. In: Round, F.E. (ed.) *The Ecology of Algae* Cambridge University Press, Cambridge, pp. 7–26.

Rueter, J. G. and Ades, D. R. 1987. The role of iron nutrition in photosynthesis and nitrogen assimilation in *Scenedesmus quadricauda* (Chlorophyceae). *J. Phycol.* 23:452-457.

Sairam, R. K. and Tyagi, A. 2004. Physiology and molecular biology of salinity stress tolerance in plants. *Current Science* 86 (3): 407-421

Schobert, B. 1974. The influence of water stress on the metabolism of diatoms. I. Osmotic resistance and proline accumulation in *Cyclotella meneghiniana*. *Zeitscrift für Pflanzenphysiology* 74: 106-120.

Schroda, M., Vallon, O., Wollman, F.-A. and Beck, C. F. 1999. A chloroplast-targeted heat shock protein 70 (hsp70) contributes to the photoprotection and repair of photosystem II during and after photoinhibition. *Plant Cell* 11: 1165-1178.

Siedow, J. N. and Day, D. A. 2000. Respiration and Photorespiration. In Buchanan, B. B., Gruissem, W. and Jones, R. L. (eds) *Biochemistry and Molecular Biology of Plants*, American Society of Plant Physiologists, Rockville, MD, pp 676 – 728.

Spalding, M. H. 2008. Microalgal carbon-dioxide-concentrating mechanisms: *Chlamydomonas* inorganic carbon transporters. *J. Exp. Bot.* 59: 1463-1473

Starr, R. C. and Zeikus, J. A. 1993. UTEX—The culture collection of algae at the University of Texas at Austin. *J. Phycol*. 29 (2 Suppl.): 90-91.

Sukenik, A., Bennett, J. and Falkowski, P. 1987. Light-saturated photosynthesis – limitation by electron transport or carbon fixation? *Biochim. Biophys. Acta* 891: 205-215.

Sukenik, A., Tchernov, D., Kaplan, A., Huertas, I. E., Lubian, L. M., and Livne, A. 1997. Uptake, efflux and photosynthetic utilization of inorganic carbon by the marine eustigmatophyte *Nannochloropsis* sp. *J. Phycol*. 33:969-74.

Sun, W., Montagu, M. V. and Verbruggen, N. 2002. Small heat shock proteins and stress tolerance in plants. *Biochimica et Biophysica Acta* 1577: 1-9.

Sunda, W. G. and Huntsman, S. A. 1995. Iron uptake and growth limitation in oceanic and coastal phytoplankton. *Mar. Chem.* 50:189–206.

Trick, C. G. 1989. Hydroxamate-siderophore production and utilization by marine eubacteria. *Curr. Microbiol*. 18:375-8.

van Kooten, O and Snel J. F. H. 1990. The use of chlorophyll fluorescence nomenclature in plant stress physiology. *Photosynthesis Research* 25**,** 147–150.

Vigara, A. J., Inda, L. A., Vega, J. M., Gómez-Moreno, C., and Peleato, M. L. 1998 Flavodoxin as an electronic donor in photosynthetic inorganic nitrogen assimilation by iron-deficient *Chlorella fusca* cells. *Photochem. Photobiol.* 67:446–449.

Wellburn, A. R. 1994. The spectral determination of chlorophylls a and b, as well as total carotenoids, using various solvents with spectrophotometers of different resolutions. *J. Plant Physiol*. 144:307-313.

Weich, R. G. and Graneli, E. 1989. Extracellular alkaline phosphatase in *Ulva lactuca* L. *J. Exp. Mar. Biol. Ecol.* 129:33-44.

Wilhelm, S. M. and Trick, C. G. 1994. Iron-limited growth of cyanobacteria: multiple siderophore production is a common response. *Limnol. Oceanogr*. 39:1979-84.

Williams, T. G. and Turpin, D. M. 1987. The role of external carbonic anhydrase in inorganic carbon acquisition by *Chlamydomonas reinhardtii*. *Plant Physiol*. 80:92-96.

Wykoff, D. D., Davies, J. P., Melis, A. and Grossman, A. R. 1998. The regulation of photosynthetic electron transport during nutrient deprivation in *Chlamydomonas reinhardtii*. *Plant Physiol.* 117: 129 – 139.

Yokthonwattana, K., Chrost, B., Behrman, S., Caspaer-Lindley, C. and Melis, A. 2001. Photosystem II Damage and Repair cycle in the Green Alga *Dunaliella salina*: Involvement of a Chloroplast-Localized HSP70. *Plant Cell Physiol.* 42(12): 1389-1397.

APPENDICES

Appendix A.1 Table for non-linear regression parameters and graph showing Jassby and Platt's function fit to the growth curve of *Picochlorum* at 10 ppt in high carbon for a replicate. This was used in obtaining the initial growth rates.

$F = CDm \times \tanh \{(\mu \times d)/CDm\} + CDo$

where CDm is increase in In cell density, CDo is Initial In cell density, μ is growth rate (in d^{-1}, which is the initial slope) and d is time in day.

Parameter	Value	StdErr	CV(%)	Dependencies
CDm	4.006e+0	1.931e-1	4.820e+0	0.7382476
CDo	1.358e+1	1.793e-1	1.321e+0	0.8827076
μ	1.120e+0	1.273e-1	1.137e+1	0.7420913

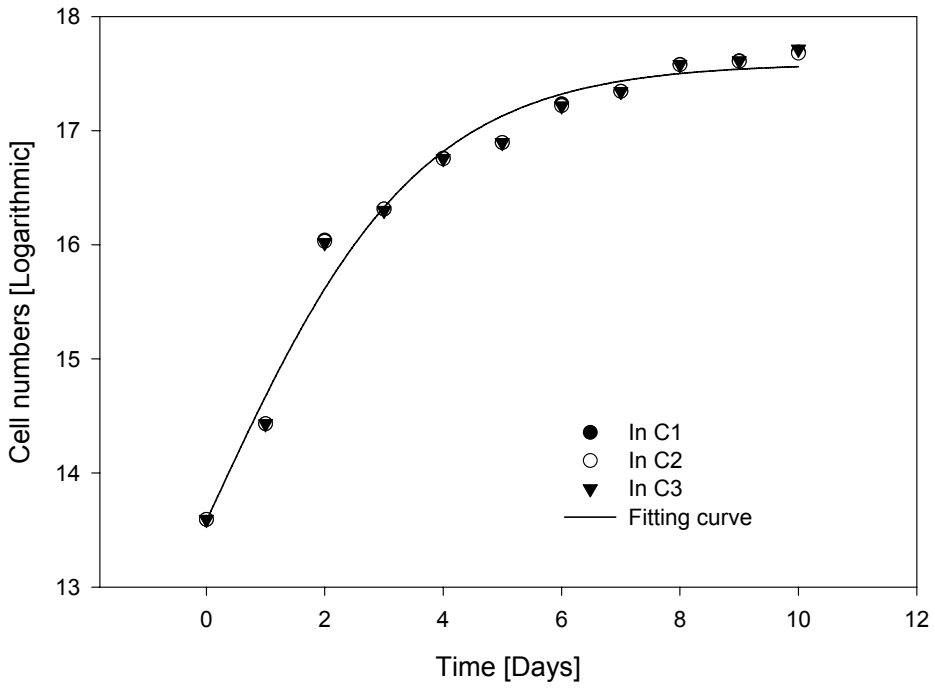

Appendix A.2 Table for non-linear regression parameters and graph showing Jassby and Platt's function fit to the growth curve of *Picochlorum* at 50 ppt in high carbon for a replicate. This was used in obtaining the initial growth rates.

Parameter	Value	StdErr	CV(%)	Dependencies
CDm	3.871e+0	1.640e-1	4.237e+0	0.7515646
CDo	1.362e+1	1.532e-1	1.125e+0	0.8843859
μ	1.123e+0	1.125e-1	1.002e+1	0.7331010

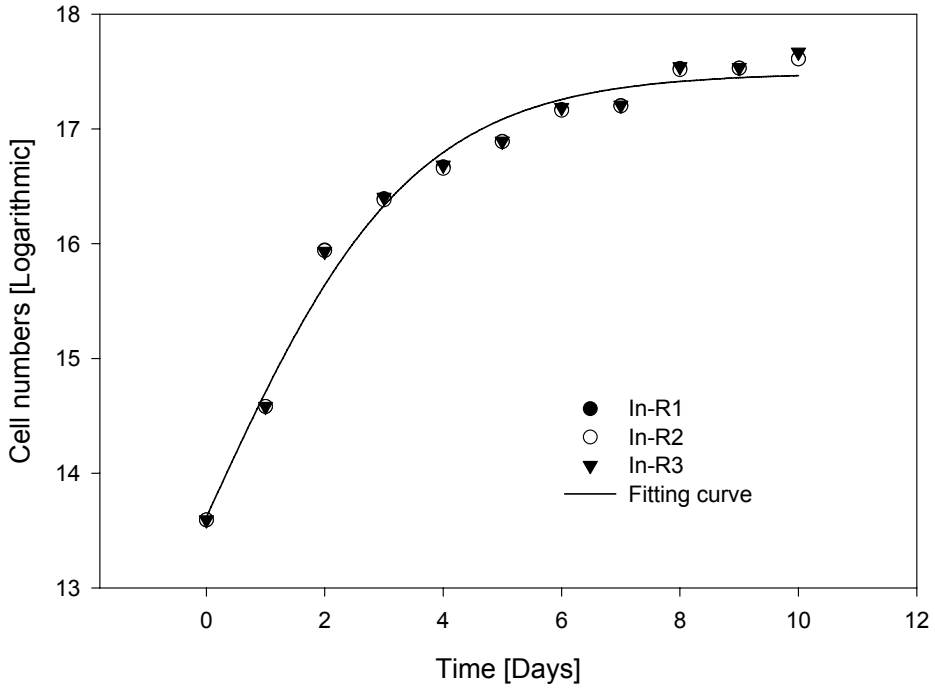

Appendix A.3 Table for non-linear regression parameters and graph showing Jassby and Platt's function fit to the growth curve of *Picochlorum* at 100 ppt in high carbon for a replicate. This was used in obtaining the initial growth rates.

Parameter	Value	StdErr	CV(%)	Dependencies
CDm	3.718e+0	1.546e-1	4.157e+0	0.6000434
CDo	1.348e+1	1.240e-1	9.199e-1	0.8664265
μ	7.308e-1	6.726e-2	9.203e+0	0.8191031

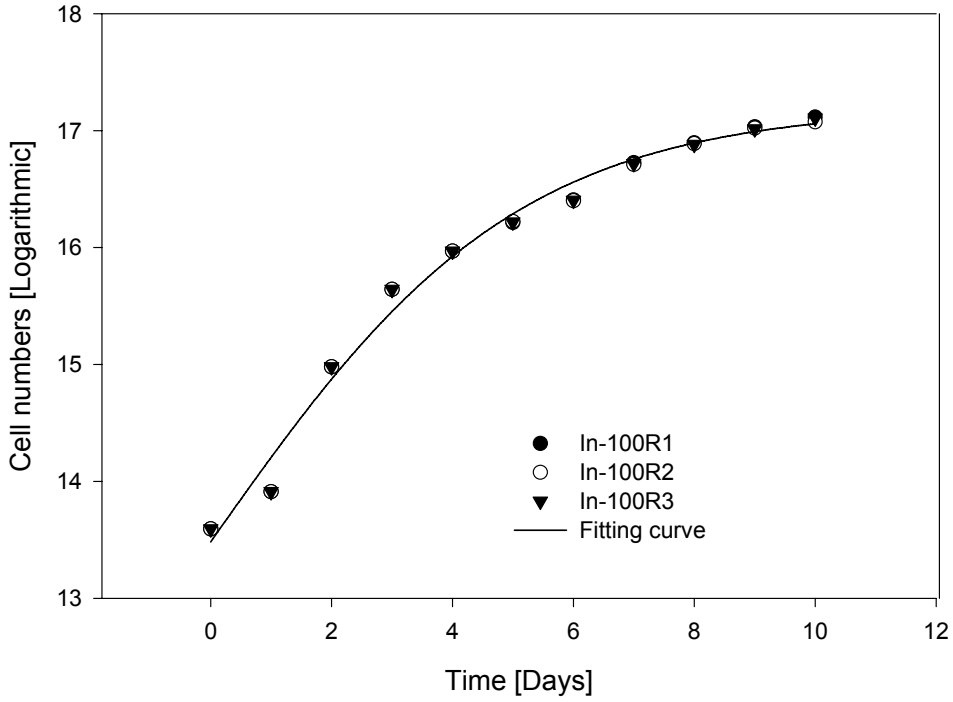

Appendix A.4 Table for non-linear regression parameters and graph showing Jassby and Platt's function fit to the growth curve of *Picochlorum* at 10 ppt in low bicarbonate for a replicate. This was used in obtaining the initial growth rates.

Parameter	Value	StdErr	CV(%)	Dependencies
CDm	3.440e+0	2.020e-1	5.871e+0	0.6128065
CDo	1.389e+1	1.669e-1	1.202e+0	0.8682340
μ	7.001e-1	9.291e-2	1.327e+1	0.8113591

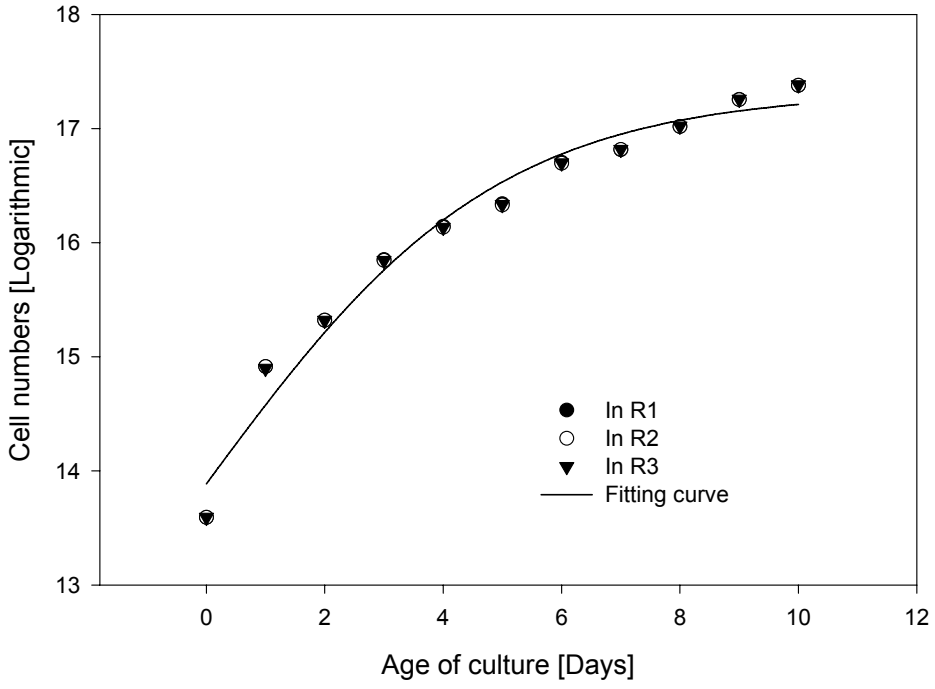

Appendix A.5 Table for non-linear regression parameters and graph showing Jassby and Platt's function fit to the growth curve of *Picochlorum* at 50 ppt in low bicarbonate for a replicate. This was used in obtaining the initial growth rates.

Parameter	Value	StdErr	CV(%)	Dependencies
CDm	3.564e+0	1.834e-1	5.146e+0	0.6125890
CDo	1.380e+1	1.515e-1	1.098e+0	0.8682052
μ	7.254e-1	8.431e-2	1.162e+1	0.8114841

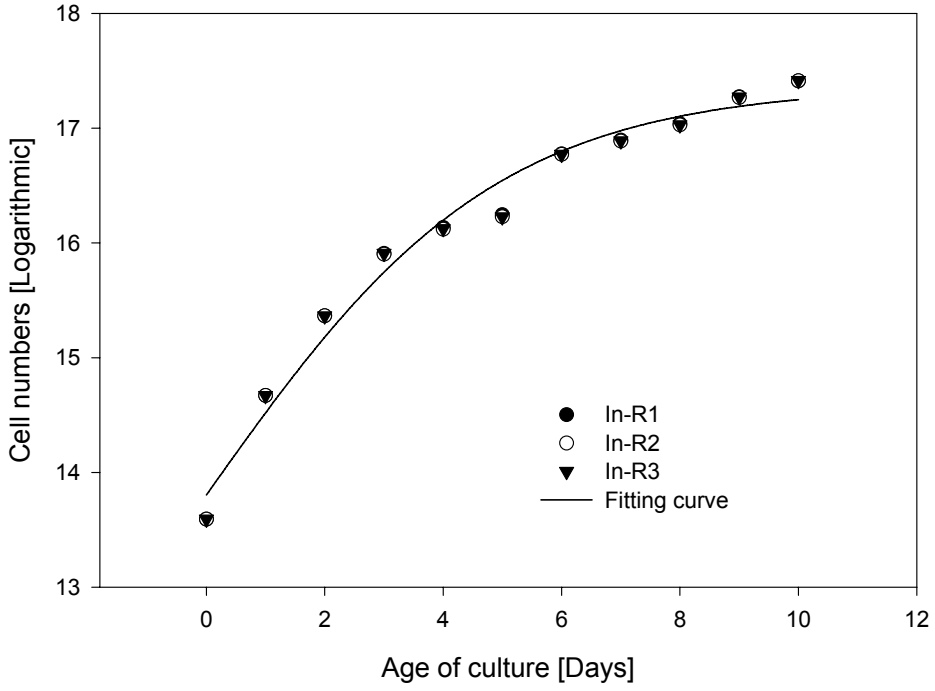

Appendix A.6 Table for non-linear regression parameters and graph showing Jassby and Platt's function fit to the growth curve of *Picochlorum* at 100 ppt in low bicarbonate for a replicate. This was used in obtaining the initial growth rates.

Parameter	Value	StdErr	CV(%)	Dependencies
CDm	3.471e+0	1.424e-1	4.101e+0	0.5966326
CDo	1.372e+1	7.660e-2	5.582e-1	0.8533159
μ	5.144e-1	3.510e-2	6.824e+0	0.8690241

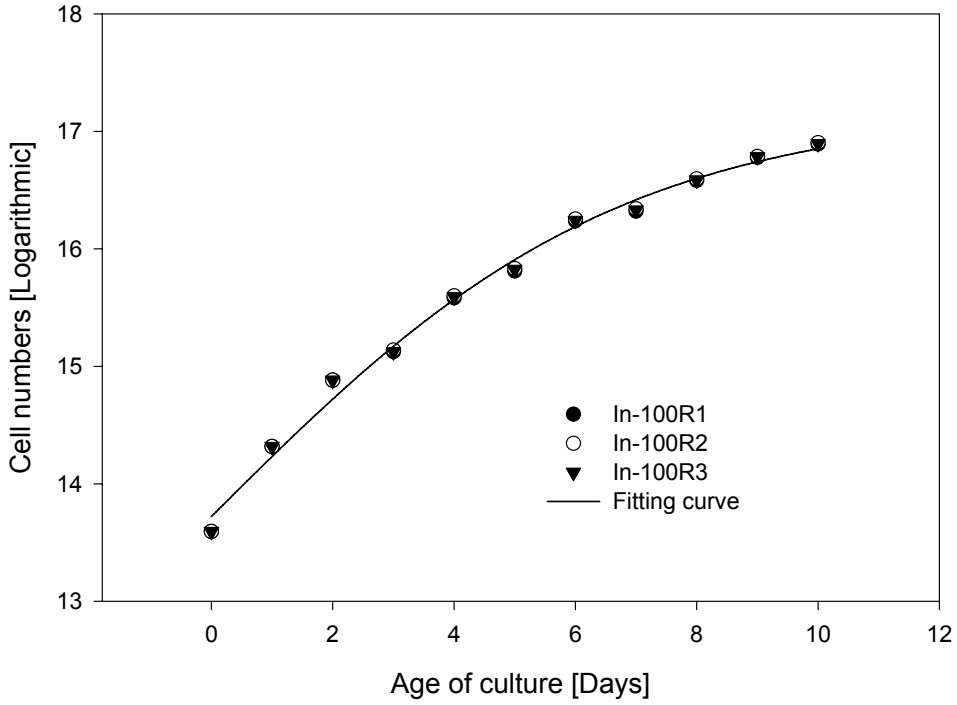

Appendix A.7 Table for non-linear regression parameters and graph showing Jassby and Platt's function fit to the growth curve of *Picochlorum* at 10 ppt in low phosphate for a replicate. This was used in obtaining the initial growth rates.

Parameter	Value	StdErr	CV(%)	Dependencies
CDm	3.416e+0	1.888e-1	5.528e+0	0.8305890
CDo	1.343e+1	1.796e-1	1.337e+0	0.8965843
μ	1.374e+0	1.793e-1	1.305e+1	0.6551805

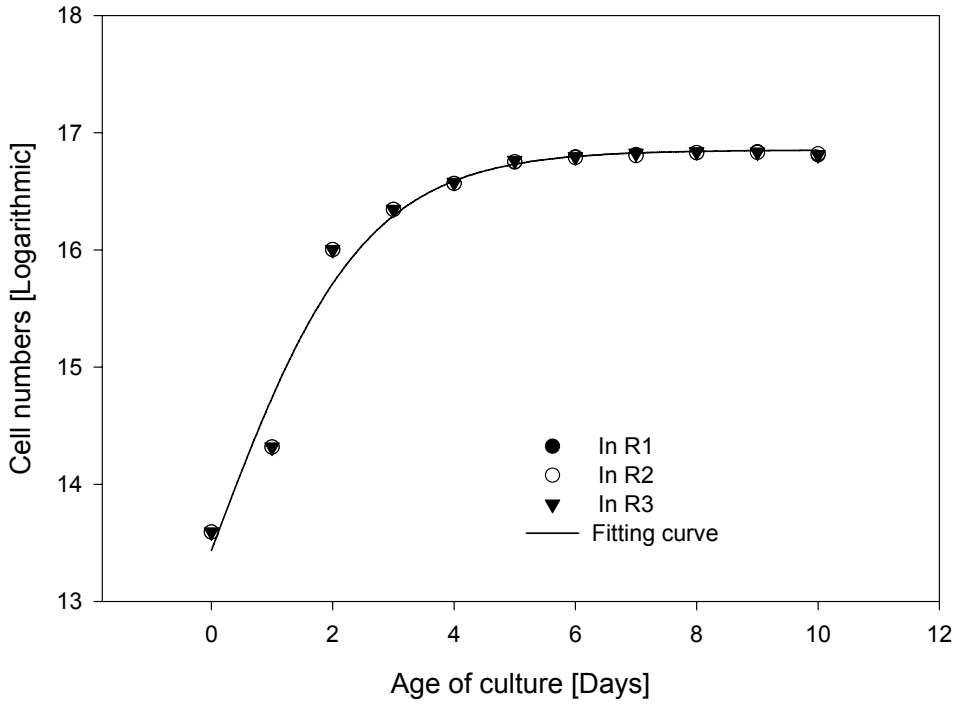

Appendix A.8 Table for non-linear regression parameters and graph showing Jassby and Platt's function fit to the growth curve of *Picochlorum* at 50 ppt in low phosphate for a replicate. This was used in obtaining the initial growth rates.

Parameter	Value	StdErr	CV(%)	Dependencies
CDm	3.347e+0	1.439e-1	4.300e+0	0.8326640
CDo	1.352e+1	1.369e-1	1.012e+0	0.8969783
μ	1.363e+0	1.384e-1	1.015e+1	0.6520586

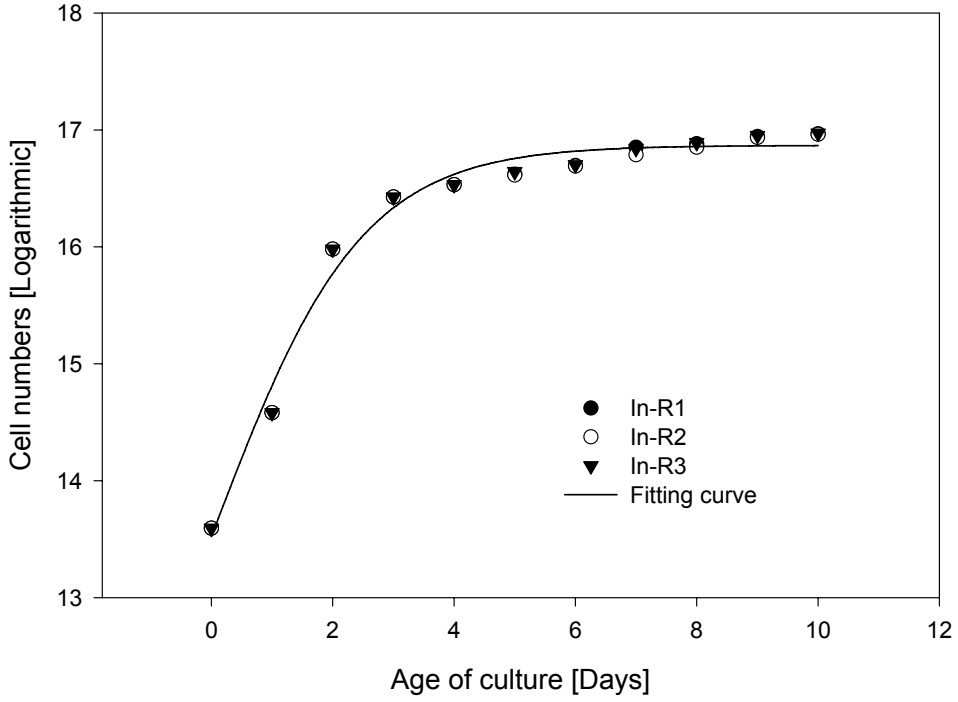

Appendix A.9 Table for non-linear regression parameters and graph showing Jassby and Platt's function fit to the growth curve of *Picochlorum* at 100 ppt in low phosphate for a replicate. This was used in obtaining the initial growth rates.

Parameter	Value	StdErr	CV(%)	Dependencies
CDm	3.368e+0	8.304e-2	2.466e+0	0.7080920
CDo	1.355e+1	7.598e-2	5.608e-1	0.8791384
μ	8.674e-1	5.045e-2	5.817e+0	0.7604466

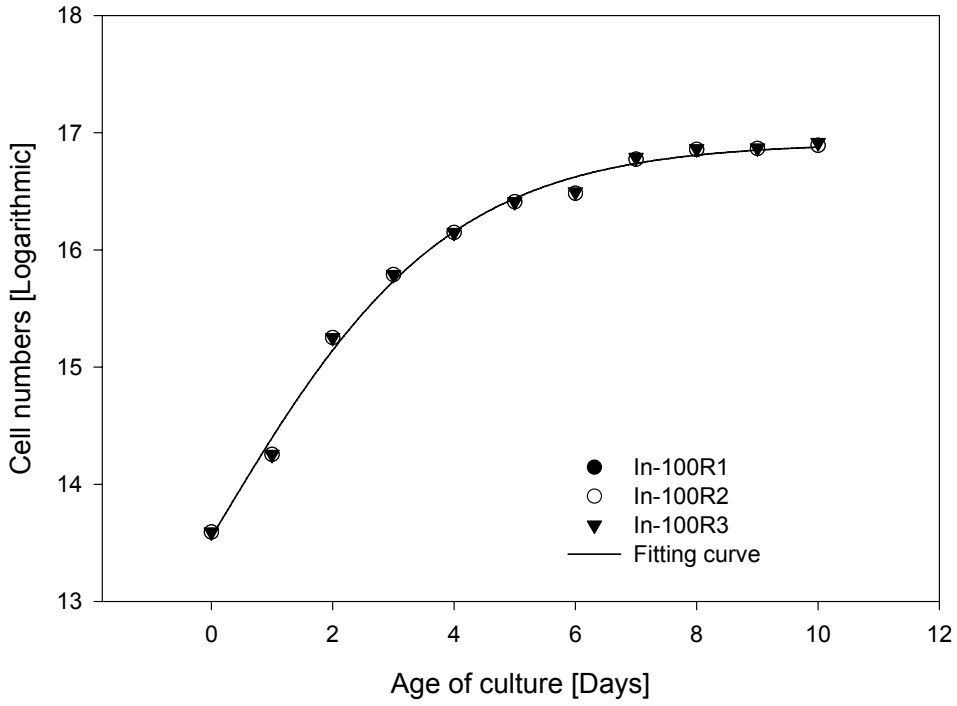

Appendix A.10 Table for non-linear regression parameters and graph showing Jassby and Platt's function fit to the growth curve of *Picochlorum* at 10 ppt in no added iron for a replicate. This was used in obtaining the initial growth rates.

Parameter	Value	StdErr	CV(%)	Dependencies
CDm	1.848e+0	8.902e-2	4.817e+0	0.5764223
CDo	1.370e+1	5.789e-2	4.225e-1	0.8581245
μ	3.040e-1	2.811e-2	9.248e+0	0.8520305

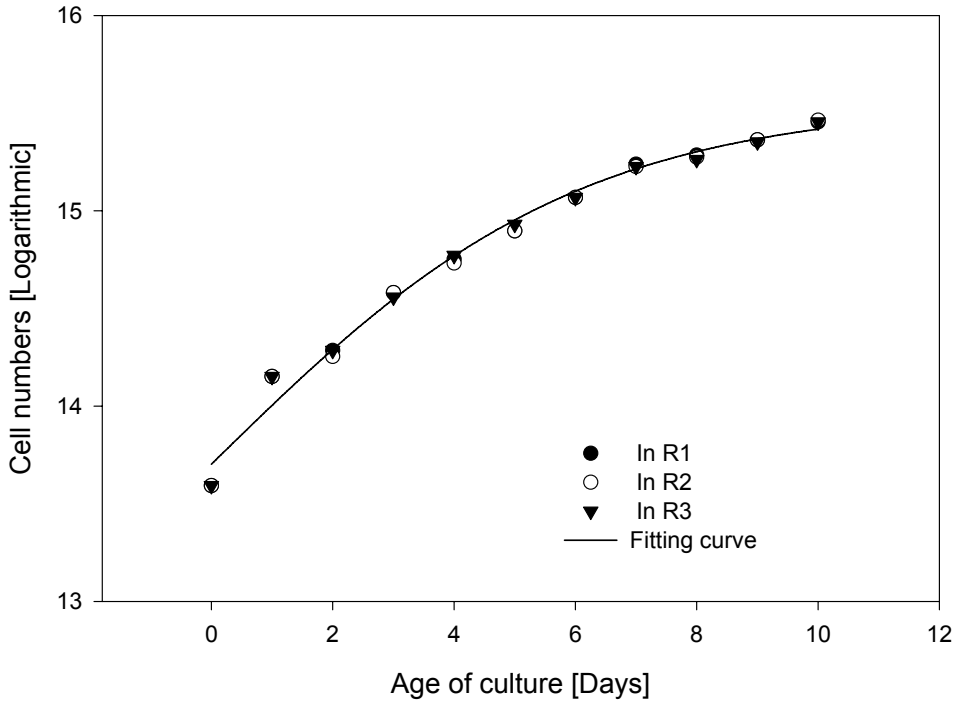

Appendix A.11 Table for non-linear regression parameters and graph showing Jassby and Platt's function fit to the growth curve of *Picochlorum* at 50 ppt in no added iron for a replicate. This was used in obtaining the initial growth rates.

Parameter	Value	StdErr	CV(%)	Dependencies
CDm	2.293e+0	1.332e-1	5.810e+0	0.5917021
CDo	1.370e+1	7.417e-2	5.413e-1	0.8540949
μ	3.452e-1	3.430e-2	9.937e+0	0.8663776

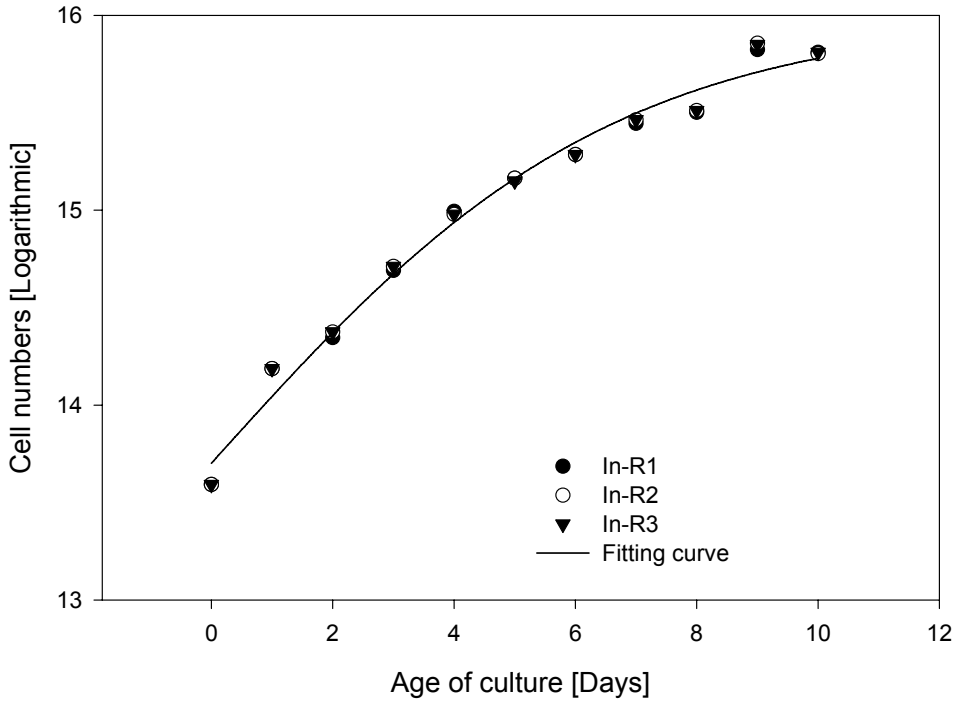

Appendix A.12 Table for non-linear regression parameters and graph showing Jassby and Platt's function fit to the growth curve of *Picochlorum* at 100 ppt in no added iron for a replicate. This was used in obtaining the initial growth rates.

Parameter	Value	StdErr	CV(%)	Dependencies
CDm	1.952e+4	4.348e+6	2.227e+4	0.0000000
CDo	1.369e+1	4.930e-2	3.600e-1	0.7142857
μ	1.369e-1	8.333e-3	6.088e+0	0.7142857

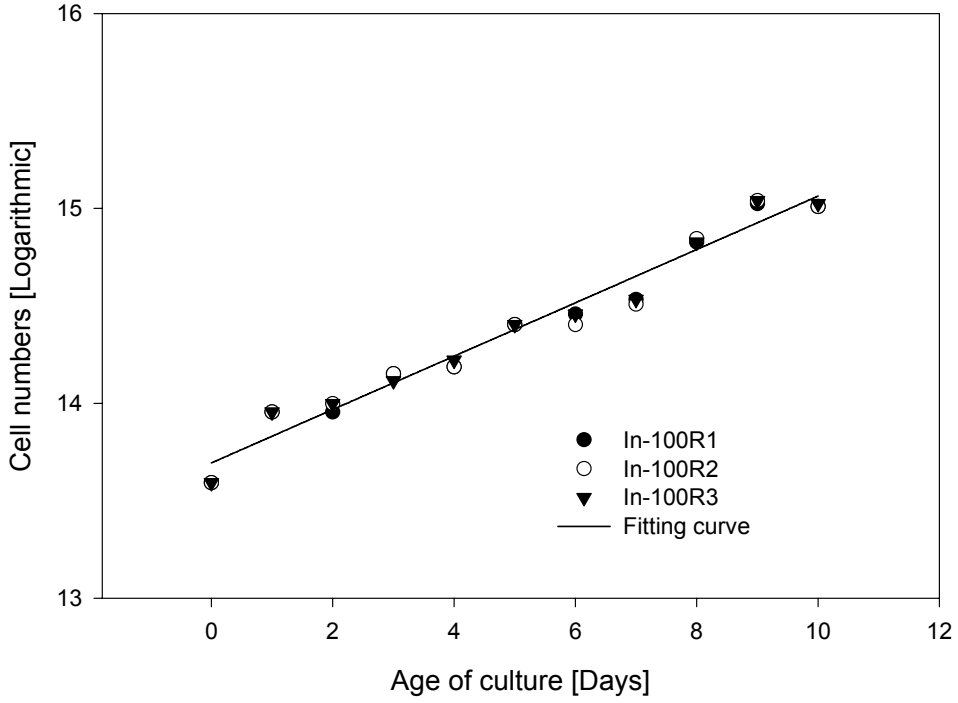

Appendix B.1 Table for non-linear regression parameters and graph showing Bannister's function fit to the growth curve of *Picochlorum* at 10 ppt in high carbon for a replicate. This was used in obtaining the convexity value.

$F = CDm \times (\mu \times d / \{CDm^c + (\mu \times d)^c)^{(1/c)}\} + CDo$

where CDm is increase In cell density, CDo is Initial In cell density, μ is growth rate (in d^{-1}, which is the initial slope), d is time in day and c is convexity.

$R = 0.99245806$ $R^2 = 0.98497300$

Standard Error of Estimate = 0.1981

	Coefficient	**Std. Error**	**t**	**P**
CDm	4.3916	0.5403	8.1281	<0.0001
μ	1.2353	0.3245	3.8072	0.0067
CDo	13.5924	0.1939	70.1100	<0.0001
c	1.8103	0.7850	2.3062	0.0545

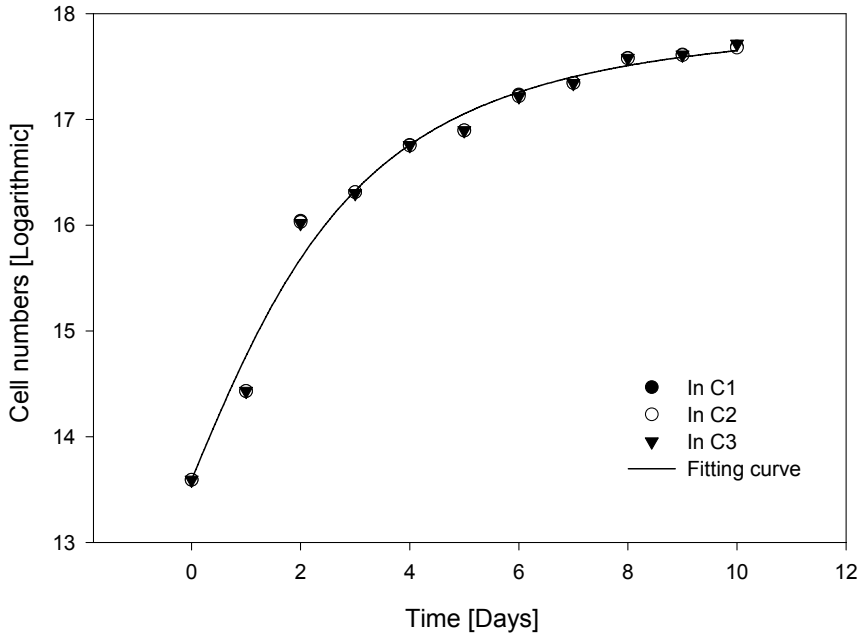

Appendix B.2 Table for non-linear regression parameters and graph showing Bannister's function fit to the growth curve of *Picochlorum* at 50 ppt in high carbon for a replicate. This was used in obtaining the convexity value.

$R = 0.99546344$ $R^2 = 0.99094745$

Standard Error of Estimate = 0.1479

	Coefficient	**Std. Error**	**t**	**P**
CDm	4.3344	0.4207	10.3033	<0.0001
μ	1.3151	0.2861	4.5968	0.0025
CDo	13.5924	0.1457	93.2763	<0.0001
c	1.6723	0.5452	3.0675	0.0181

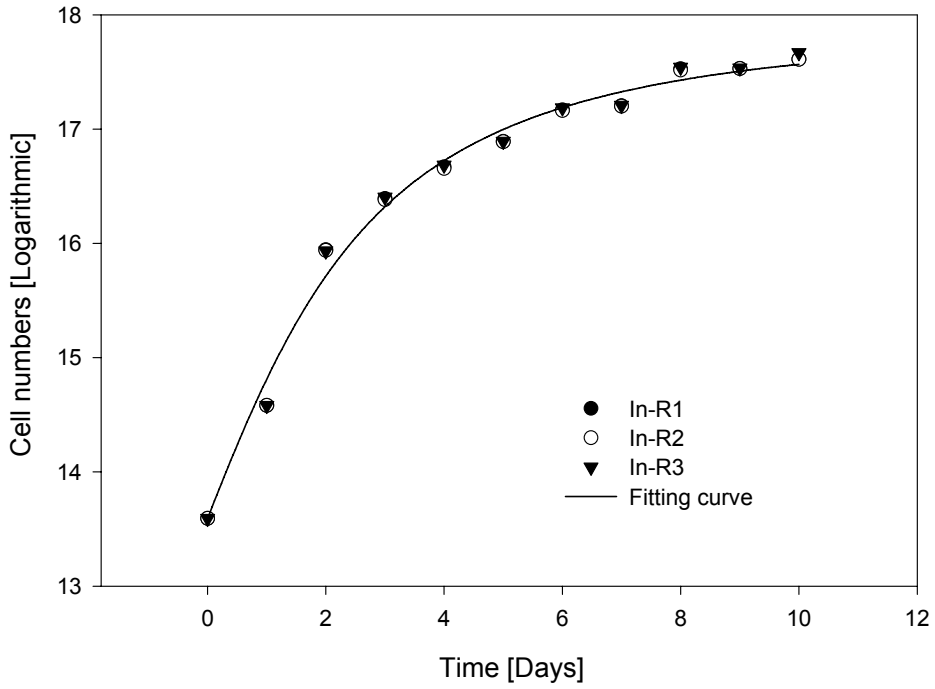

Appendix B.3 Table for non-linear regression parameters and graph showing Bannister's function fit to the growth curve of *Picochlorum* at 100 ppt in high carbon for a replicate. This was used in obtaining the convexity value.

$R = 0.99363407$ $R^2 = 0.98730866$

Standard Error of Estimate = 0.1648

	Coefficient	**Std. Error**	**t**	**P**
CDm	3.9067	0.6645	5.8791	0.0006
μ	0.6834	0.1414	4.8321	0.0019
CDo	13.5924	0.1518	89.5479	<0.0001
c	2.2531	1.2651	1.7810	0.1181

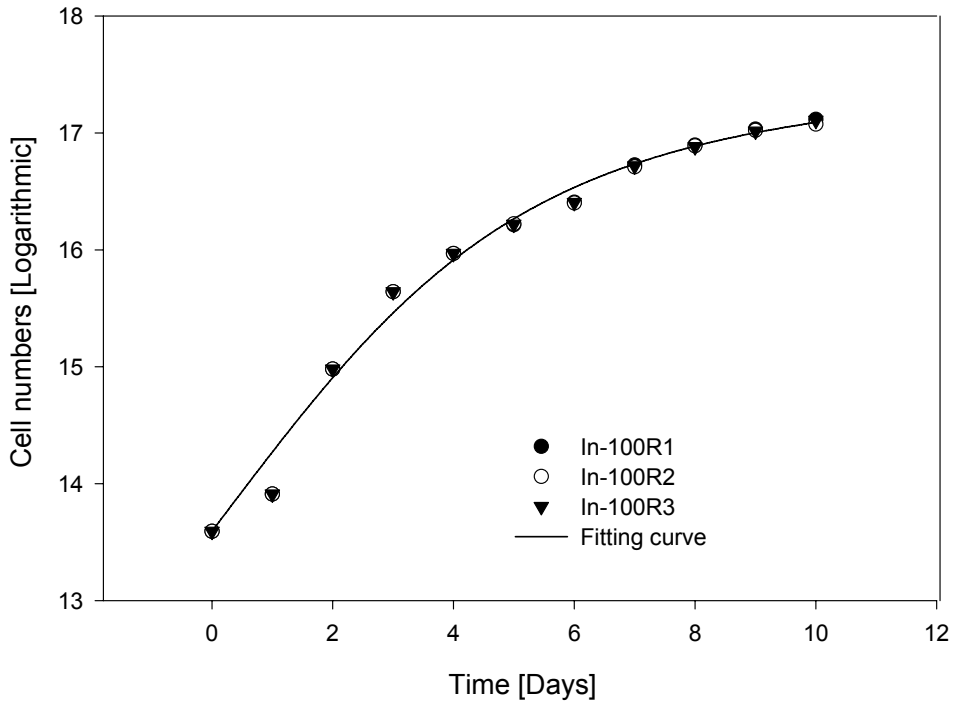

Appendix B.4 Table for non-linear regression parameters and graph showing Bannister's function fit to the growth curve of *Picochlorum* in low bicarbonate medium at 10 ppt for a replicate. This was used in obtaining the convexity value.

$R = 0.99898777$ $R^2 = 0.99797657$

Standard Error of Estimate = 0.0615

	Coefficient	**Std. Error**	**t**	**P**
CDm	21.9102	23.8645	0.9181	0.3891
μ	8.9628	12.5193	0.7159	0.4972
CDo	13.5924	0.0615	220.9781	<0.0001
c	0.2897	0.1618	1.7902	0.1165

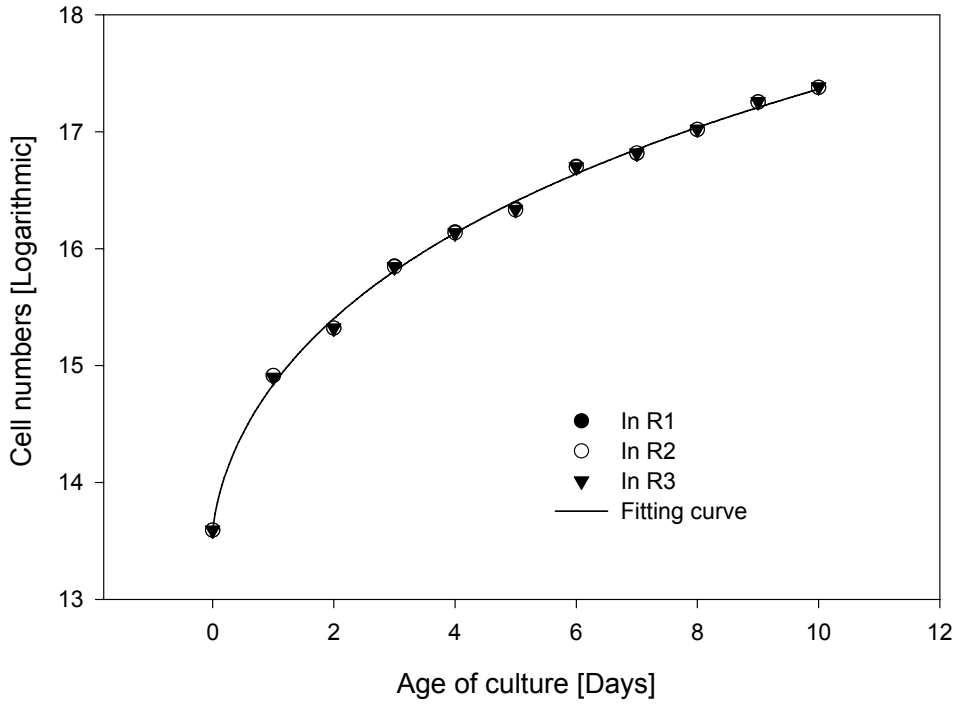

Appendix B.5 Table for non-linear regression parameters and graph showing Bannister's function fit to the growth curve of *Picochlorum* in low bicarbonate medium at 50 ppt for a replicate. This was used in obtaining the convexity value.

R = 0.99770484 R^2 = 0.99541495

Standard Error of Estimate = 0.0957

	Coefficient	**Std. Error**	**t**	**P**
CDm	9.1393	5.5753	1.6392	0.1452
μ	2.3195	1.6596	1.3976	0.2049
CDo	13.5924	0.0955	142.2944	<0.0001
c	0.5398	0.2769	1.9494	0.0922

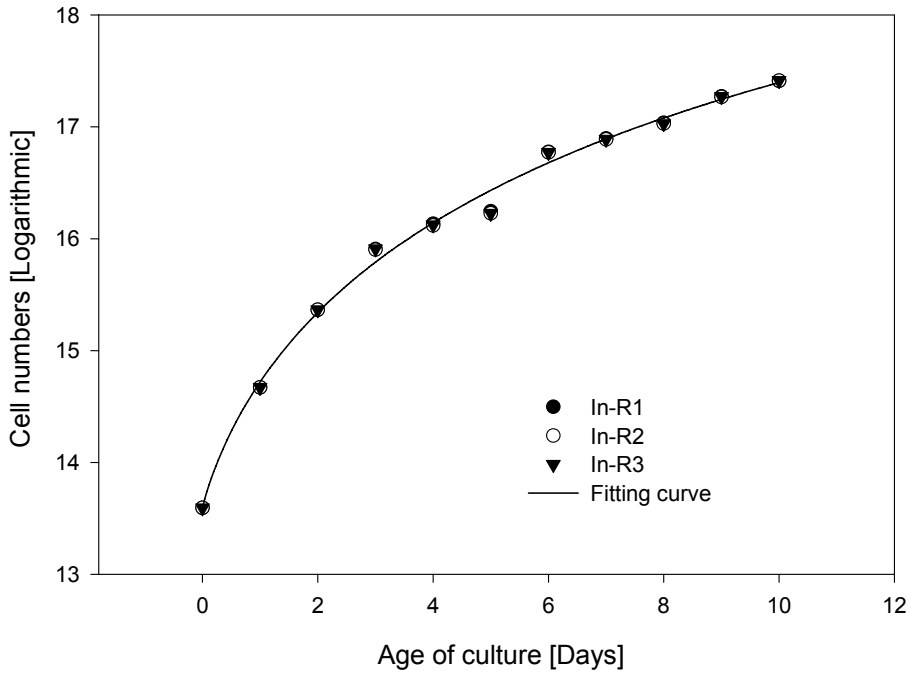

Appendix B.6 Table for non-linear regression parameters and graph showing Bannister's function fit to the growth curve of *Picochlorum* in low bicarbonate medium at 100 ppt for a replicate. This was used in obtaining the convexity value.

$R = 0.99853727$ $R^2 = 0.99707668$

Standard Error of Estimate = 0.0690

	Coefficient	**Std. Error**	**t**	**P**
CDm	10.0789	7.5682	1.3317	0.2247
μ	1.0007	0.4473	2.2373	0.0603
CDo	13.5924	0.0684	198.6128	<0.0001
c	0.6293	0.3246	1.9385	0.0937

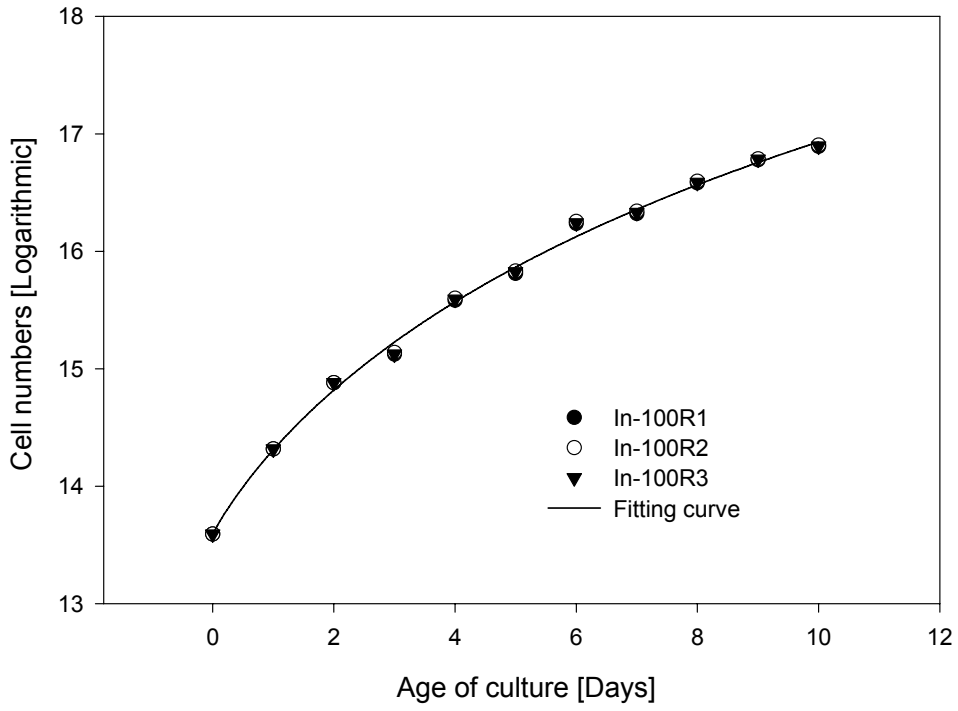

Appendix B.7 Table for non-linear regression parameters and graph showing Bannister's function fit to the growth curve of *Picochlorum* in low phosphate medium at 10 ppt for a replicate. This was used in obtaining the convexity value.

$R = 0.99079953$ $R^2 = 0.98168371$

Standard Error of Estimate = 0.1827

	Coefficient	**Std. Error**	**t**	**P**
CDm	3.2224	0.2030	15.8740	<0.0001
μ	1.0948	0.1773	6.1750	0.0005
CDo	13.5924	0.1733	78.4426	<0.0001
c	4.6946	2.7007	1.7383	0.1257

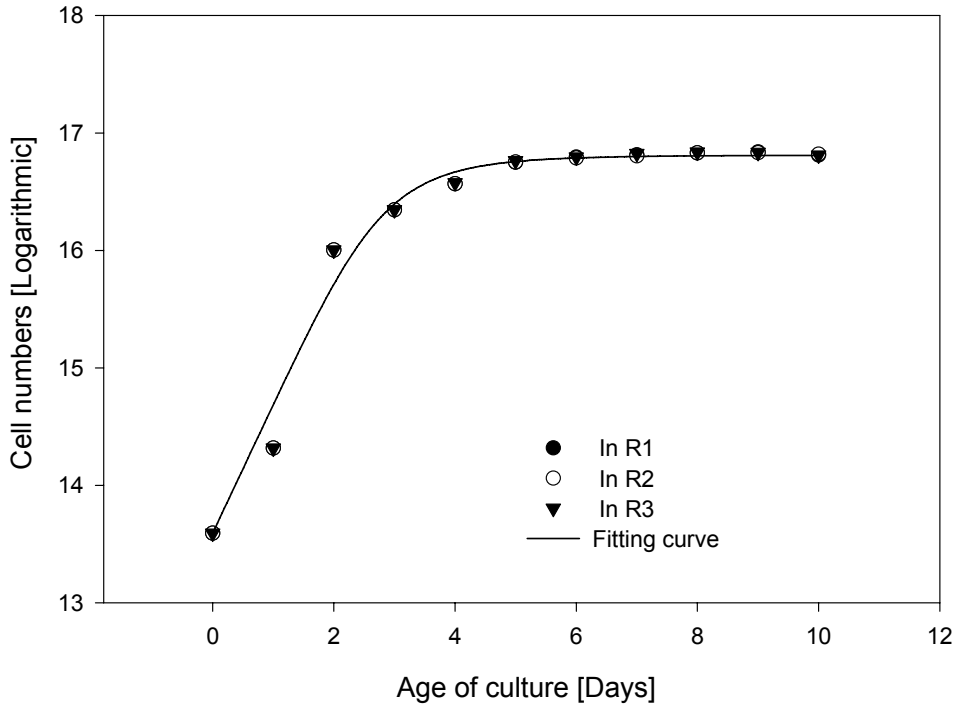

Appendix B.8 Table for non-linear regression parameters and graph showing Bannister's function fit to the growth curve of *Picochlorum* in low phosphate medium at 50 ppt for a replicate. This was used in obtaining the convexity value.

$R = 0.99408090$ $R^2 = 0.98819683$

Standard Error of Estimate = 0.1418

	Coefficient	**Std. Error**	**t**	**P**
CDm	3.2679	0.1744	18.7362	<0.0001
μ	1.2177	0.1873	6.5029	0.0003
CDo	13.5924	0.1385	98.1326	<0.0001
c	3.2201	1.1394	2.8261	0.0255

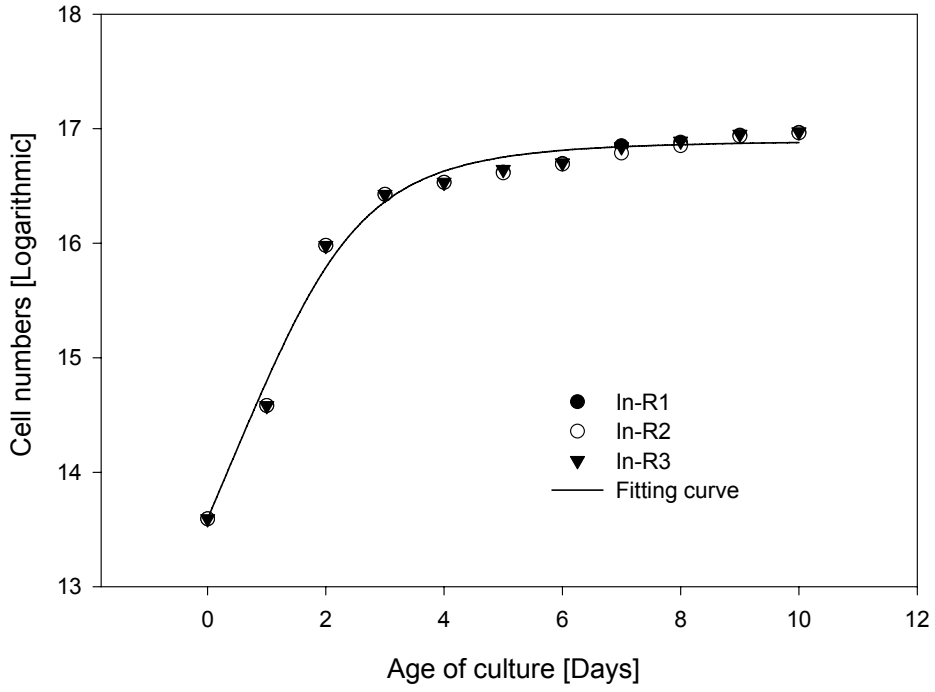

Appendix B.9 Table for non-linear regression parameters and graph showing Bannister's function fit to the growth curve of *Picochlorum* in low phosphate medium at 100 ppt for a replicate. This was used in obtaining the convexity value.

$R = 0.99777462$ $R^2 = 0.99555419$

Standard Error of Estimate = 0.0902

	Coefficient	**Std. Error**	**t**	**P**
CDm	3.4824	0.1972	17.6622	<0.0001
μ	0.8332	0.0943	8.8386	<0.0001
CDo	13.5924	0.0855	159.0288	<0.0001
c	2.4322	0.6016	4.0429	0.0049

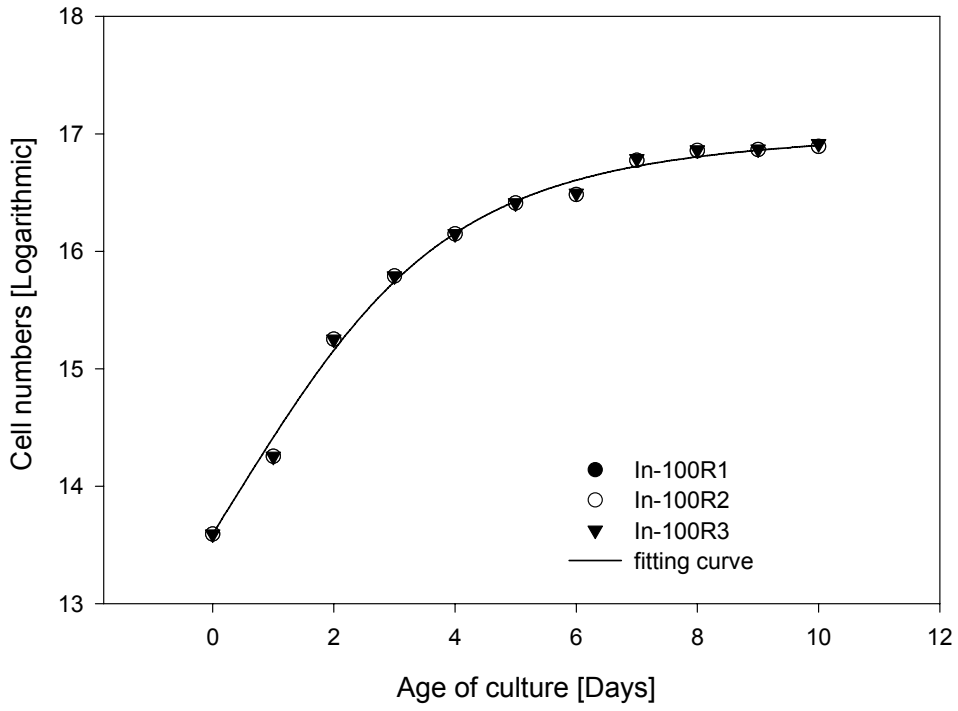

Appendix B.10 Table for non-linear regression parameters and graph showing Bannister's function fit to the growth curve of *Picochlorum* in no added medium at 10 ppt for a replicate. This was used in obtaining the convexity value.

R = 0.99687927 R^2= 0.99376828

Standard Error of Estimate = 0.0556

	Coefficient	**Std. Error**	**t**	**P**
CDm	11.6888	23.3868	0.4998	0.6325
μ	1.2848	1.9172	0.6702	0.5242
CDo	13.5924	0.0555	245.0191	<0.0001
c	0.3703	0.3649	1.0148	0.3440

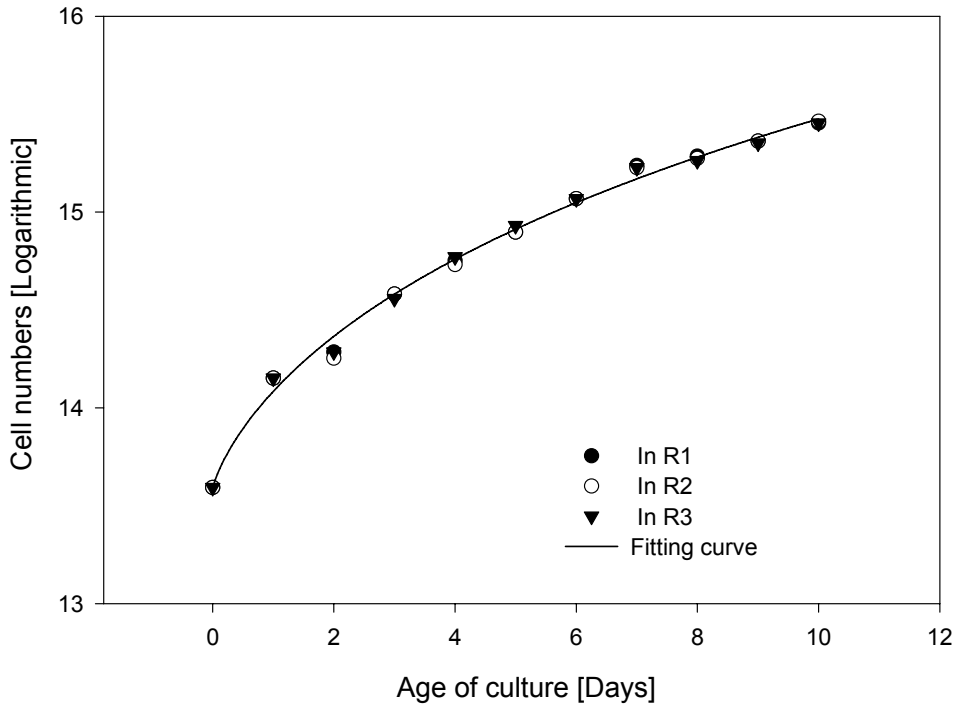

Appendix B.11 Table for non-linear regression parameters and graph showing Bannister's function fit to the growth curve of *Picochlorum* in no added medium at 50 ppt for a replicate. This was used in obtaining the convexity value.

R = 0.99609864 R^2 = 0.99221251

Standard Error of Estimate = 0.0752

	Coefficient	**Std. Error**	**t**	**P**
CDm	17.6562	50.5880	0.3490	0.7373
μ	1.3405	2.4021	0.5580	0.5942
CDo	13.5924	0.0750	181.2874	<0.0001
c	0.3623	0.4423	0.8190	0.4398

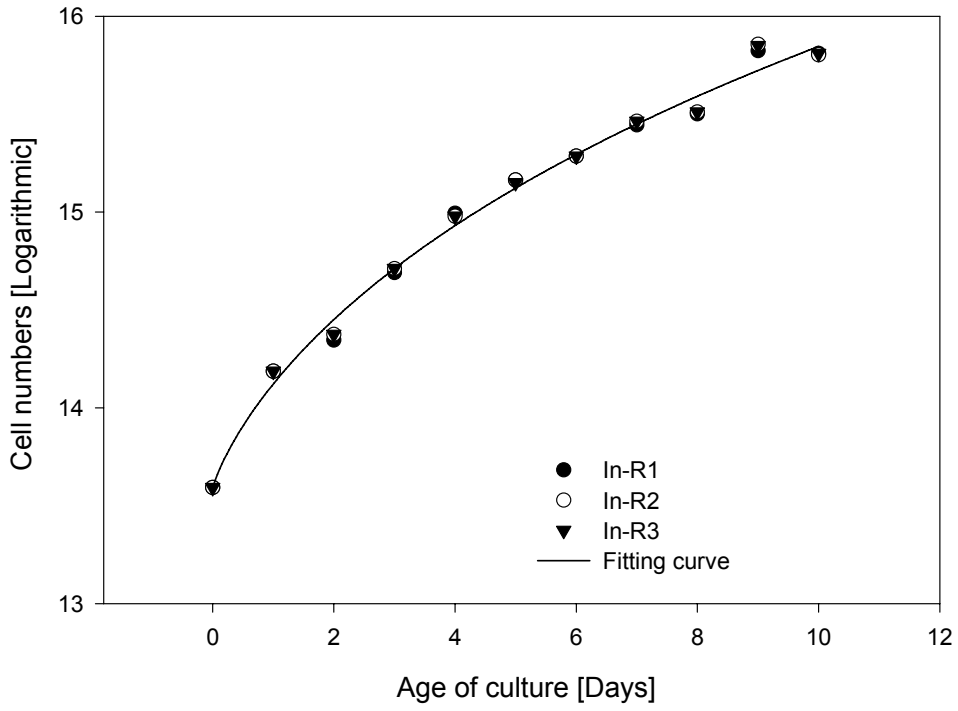

Appendix B.12 Table for non-linear regression parameters and graph showing Bannister's function fit to the growth curve of *Picochlorum* in no added medium at 100 ppt for a replicate. This was used in obtaining the convexity value.

R = 0.98270919 R^2 = 0.96571735

Standard Error of Estimate = 0.1019

	Coefficient	**Std. Error**	**t**	**P**
CDm	105.7465	2717.4034	0.0389	0.9700
μ	0.2466	0.8076	0.3054	0.7690
CDo	13.5924	0.1004	135.3321	<0.0001
c	0.3864	2.8521	0.1355	0.8961

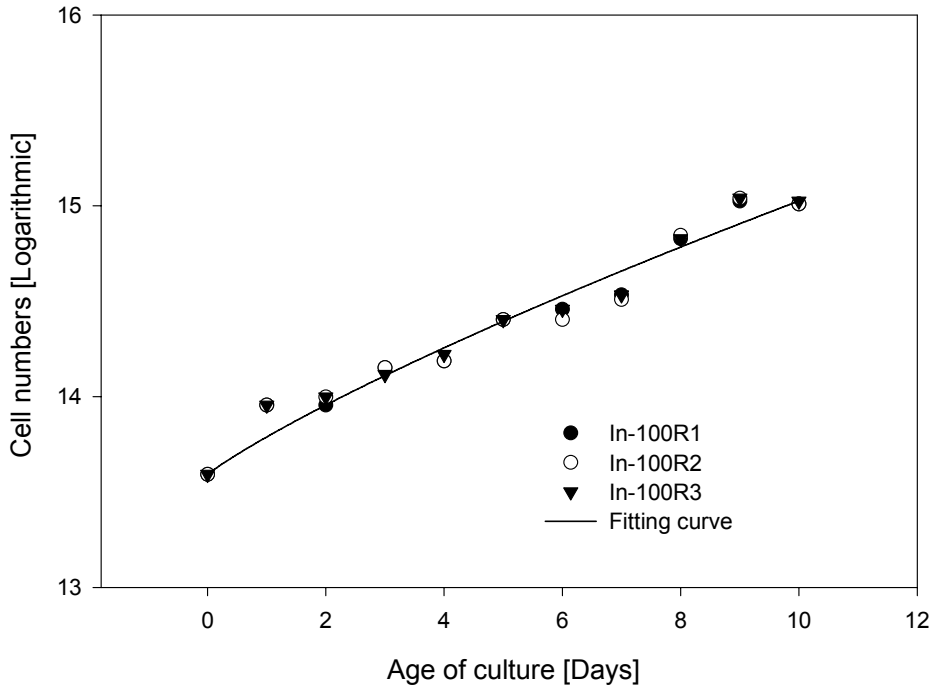

Appendix C.1 Analysis of variance (ANOVA) for cell yield at day 10

ANOVA for Salinity and Bicarbonate effect

Source	Sum-of-Squares	df	Mean-Square	F-ratio	P
Salinity	1.17655E+15	2	5.88273E+14	1016.210	0.000
Carbon	3.56890E+14	1	3.56890E+14	616.509	0.000
Salinity * Carbon	4.98203E+13	2	2.49101E+13	43.031	0.000
Error	6.94667E+12	12	5.78889E+11		

ANOVA for Salinity and Phosphate effect

Source	Sum-of-Squares	df	Mean-Square	F-ratio	P
Salinity	4.01092E+14	2	2.00546E+14	338.713	0.000
Phosphorus	1.51525E+15	1	1.51525E+15	2559.186	0.000
Salinity * Phosphorus	4.42403E+14	2	2.21201E+14	373.598	0.000
Error	7.10500E+12	12	5.92083E+11		

ANOVA for Salinity and Iron effect

Source	Sum-of-Squares	df	Mean-Square	F-ratio	P
Salinity	5.34455E+14	2	2.67228E+14	465.418	0.000
Iron	5.45838E+15	1	5.45838E+15	9506.619	0.000
Salinity * Iron	3.16910E+14	2	1.58455E+14	275.974	0.000
Error	6.89000E+12	12	5.74167E+11		

Appendix C.2 Analysis of variance (ANOVA) for Initial Growth Rate

ANOVA for Salinity and Bicarbonate effect

Source	Sum-of-Squares	df	Mean-Square	F-ratio	P
Salinity	0.330	2	0.165	7718.798	0.000
Carbon	0.537	1	0.537	25140.415	0.000
Salinity * Carbon	0.038	2	0.019	891.641	0.000
Error	0.000	12	0.000		

ANOVA for Salinity and Phosphate effect

Source	Sum-of-Squares	df	Mean-Square	F-ratio	P
Salinity	0.789	2	0.395	17654.729	0.000
Phosphorus	0.203	1	0.203	9088.248	0.000
Salinity * Phosphorus	0.015	2	0.007	326.170	0.000
Error	0.000	12	0.000		

ANOVA for Salinity and Iron effect

Source	Sum-of-Squares	df	Mean-Square	F-ratio	P
Salinity	0.330	2	0.165	8249.734	0.000
Iron	2.390	1	2.390	119589.639	0.000
Salinity * Iron	0.039	2	0.020	979.033	0.000
Error	0.000	12	0.000		

Appendix C.3 Analysis of variance (ANOVA) for Pmax

ANOVA for Salinity and Bicarbonate effect

Source	Sum-of-Squares	df	Mean-Square	F-ratio	P
Salinity	299.145	2	149.572	47.447	0.000
Carbon	33.320	1	33.320	10.570	0.007
Salinity * Carbon	2.913	2	1.457	0.462	0.641
Error	37.829	12	3.152		

ANOVA for Salinity and Phosphate effect

Source	Sum-of-Squares	df	Mean-Square	F-ratio	P
Salinity	188.131	2	94.065	27.798	0.000
Phosphorus	55.020	1	55.020	16.259	0.002
Salinity * Phosphorus	4.706	2	2.353	0.695	0.518
Error	40.607	12	3.384		

ANOVA for Salinity and Iron effect

Source	Sum-of-Squares	df	Mean-Square	F-ratio	P
Salinity	149.791	2	74.896	92.996	0.000
Iron	306.942	1	306.942	381.123	0.000
Salinity * Iron	13.708	2	6.854	8.510	0.005
Error	9.664	12	0.805		

Appendix C.4 Analysis of variance (ANOVA) for α

ANOVA for Salinity and Bicarbonate effect

Source	Sum-of-Squares	df	Mean-Square	F-ratio	P
Salinity	0.011	2	0.005	4.115	0.044
Carbon	0.000	1	0.000	0.106	0.750
Salinity * Carbon	0.003	2	0.001	1.051	0.380
Error	0.016	12	0.001		

ANOVA for Salinity and Phosphate effect

Source	Sum-of-Squares	df	Mean-Square	F-ratio	P
Salinity	0.004	2	0.002	0.238	0.792
Phosphorus	0.004	1	0.004	0.462	0.510
Salinity * Phosphorus	0.014	2	0.007	0.853	0.450
Error	0.098	12	0.008		

ANOVA for Salinity and Iron effect

Source	Sum-of-Squares	df	Mean-Square	F-ratio	P
Salinity	0.004	2	0.002	0.499	0.619
Iron	0.010	1	0.010	2.208	0.163
Salinity * Iron	0.000	2	0.000	0.011	0.989
Error	0.053	12	0.004		

Appendix C.5 Analysis of variance (ANOVA) for R_d

ANOVA for Salinity and Bicarbonate effect

Source	Sum-of-Squares	df	Mean-Square	F-ratio	P
Salinity	0.134	2	0.067	0.258	0.777
Carbon	0.001	1	0.001	0.002	0.964
Salinity * Carbon	0.053	2	0.026	0.102	0.904
Error	3.109	12	0.259		

ANOVA for Salinity and Phosphate effect

Source	Sum-of-Squares	df	Mean-Square	F-ratio	P
Salinity	0.729	2	0.364	1.441	0.275
Phosphorus	0.076	1	0.076	0.301	0.594
Salinity * Phosphorus	0.429	2	0.214	0.848	0.452
Error	3.035	12	0.253		

ANOVA for Salinity and Iron effect

Source	Sum-of-Squares	df	Mean-Square	F-ratio	P
Salinity	0.055	2	0.027	0.059	0.943
Iron	0.005	1	0.005	0.010	0.922
Salinity * Iron	0.024	2	0.012	0.026	0.974
Error	5.592	12	0.466		

Appendix C.6 Analysis of variance for Salinity and Bicarbonate on pigments analysis

ANOVA for Total chlorophyll

Source	Sum-of-Squares	df	Mean-Square	F-ratio	P
Salinity	4988.273	2	2494.136	111.879	0.000
Carbon	27.421	1	27.421	1.230	0.289
Salinity * Carbon	348.790	2	174.395	7.823	0.007
Error	267.518	12	22.293		

ANOVA for Chlorophyll a/b ratio

Source	Sum-of-Squares	df	Mean-Square	F-ratio	P
Salinity	0.025	2	0.012	0.268	0.770
Carbon	0.034	1	0.034	0.735	0.408
Salinity * Carbon	0.101	2	0.050	1.092	0.367
Error	0.553	12	0.046		

ANOVA for Total Carotenoids

Source	Sum-of-Squares	df	Mean-Square	F-ratio	P
Salinity	323.967	2	161.983	58.312	0.000
Carbon	15.097	1	15.097	5.435	0.038
Salinity * Carbon	22.998	2	11.499	4.139	0.043
Error	33.335	12	2.778		

ANOVA for Chlorophyll/Carotenoids ratio

Source	Sum-of-Squares	df	Mean-Square	F-ratio	P
Salinity	0.456	2	0.228	39.723	0.000
Carbon	0.027	1	0.027	4.683	0.051
Salinity * Carbon	0.612	2	0.306	53.376	0.000
Error	0.069	12	0.006		

Appendix C.7 Analysis of variance for Salinity and Phosphate on pigments analysis

ANOVA for Total Chlorophyll

Source	Sum-of-Squares	df	Mean-Square	F-ratio	P
Salinity	1236.230	2	618.115	47.948	0.000
Phosphorus	372.561	1	372.561	28.900	0.000
Salinity * Phosphorus	303.453	2	151.727	11.770	0.001
Error	154.696	12	12.891		

ANOVA for Chlorophyll a/b ratio

Source	Sum-of-Squares	df	Mean-Square	F-ratio	P
Salinity	0.171	2	0.086	3.841	0.051
Phosphorus	0.016	1	0.016	0.705	0.417
Salinity * Phosphorus	0.047	2	0.024	1.060	0.377
Error	0.267	12	0.022		

ANOVA for Total Carotenoids

Source	Sum-of-Squares	df	Mean-Square	F-ratio	P
Salinity	95.769	2	47.885	21.933	0.000
Phosphorus	57.899	1	57.899	26.520	0.000
Salinity * Phosphorus	51.832	2	25.916	11.871	0.001
Error	26.199	12	2.183		

ANOVA for Chlorophyll/Carotenoid ratio

Source	Sum-of-Squares	df	Mean-Square	F-ratio	P
Salinity	0.400	2	0.200	45.753	0.000
Phosphorus	0.038	1	0.038	8.740	0.012
Salinity * Phosphorus	0.055	2	0.027	6.285	0.014
Error	0.052	12	0.004		

Appendix C.8 Analysis of variance for Salinity and Iron on pigments analysis

ANOVA for Total Chlorophyll

Source	Sum-of-Squares	df	Mean-Square	F-ratio	P
Salinity	479.479	2	239.740	6.605	0.012
Iron	477.798	1	477.798	13.164	0.003
Salinity * Iron	2505.014	2	1252.507	34.508	0.000
Error	435.549	12	36.296		

ANOVA for Chlorophyll a/b ratio

Source	Sum-of-Squares	df	Mean-Square	F-ratio	P
Salinity	0.320	2	0.160	1.814	0.205
Iron	10.102	1	10.102	114.660	0.000
Salinity * Iron	0.301	2	0.151	1.710	0.222
Error	1.057	12	0.088		

ANOVA for Total Carotenoids

Source	Sum-of-Squares	df	Mean-Square	F-ratio	P
Salinity	129.048	2	64.524	21.162	0.000
Iron	85.945	1	85.945	28.188	0.000
Salinity * Iron	192.542	2	96.271	31.575	0.000
Error	36.588	12	3.049		

ANOVA for Chlorophyll/Carotenoids

Source	Sum-of-Squares	df	Mean-Square	F-ratio	P
Salinity	0.418	2	0.209	1.420	0.279
Iron	0.162	1	0.162	1.102	0.315
Salinity * Iron	0.022	2	0.011	0.075	0.928
Error	1.764	12	0.147		

Appendix C.9 Analysis of variance for Salinity and Bicarbonate on fluorescence analysis

ANOVA for Fv/Fm

Source	Sum-of-Squares	df	Mean-Square	F-ratio	P
Salinity	0.003	2	0.002	10.043	0.003
Carbon	0.001	1	0.001	3.630	0.081
Salinity * Carbon	0.001	2	0.000	2.852	0.097
Error	0.002	12	0.000		

ANOVA for ΦPSII

Source	Sum-of-Squares	df	Mean-Square	F-ratio	P
Salinity	0.011	2	0.006	9.824	0.003
Carbon	0.011	1	0.011	19.525	0.001
Salinity * Carbon	0.000	2	0.000	0.173	0.843
Error	0.007	12	0.001		

ANOVA for qP

Source	Sum-of-Squares	df	Mean-Square	F-ratio	P
Salinity	0.059	2	0.030	12.703	0.001
Carbon	0.033	1	0.033	14.311	0.003
Salinity * Carbon	0.002	2	0.001	0.535	0.599
Error	0.028	12	0.002		

ANOVA for NPQ

Source	Sum-of-Squares	df	Mean-Square	F-ratio	P
Salinity	0.075	2	0.038	2.581	0.117
Carbon	0.064	1	0.064	4.419	0.057
Salinity * Carbon	0.012	2	0.006	0.424	0.664
Error	0.175	12	0.015		

Appendix C.10 Analysis of variance for Salinity and Phosphate on fluorescence analysis

ANOVA for Fv/Fm

Source	Sum-of-Squares	df	Mean-Square	F-ratio	P
Salinity	0.005	2	0.003	22.139	0.000
Phosphorus	0.006	1	0.006	50.275	0.000
Salinity * Phosphorus	0.006	2	0.003	25.248	0.000
Error	0.001	12	0.000		

ANOVA for ΦPSII

Source	Sum-of-Squares	df	Mean-Square	F-ratio	P
Salinity	0.001	2	0.001	5.331	0.022
Phosphorus	0.017	1	0.017	123.077	0.000
Salinity * Phosphorus	0.006	2	0.003	23.012	0.000
Error	0.002	12	0.000		

ANOVA for qP

Source	Sum-of-Squares	df	Mean-Square	F-ratio	P
Salinity	0.076	2	0.038	28.883	0.000
Phosphorus	0.005	1	0.005	3.459	0.088
Salinity * Phosphorus	0.001	2	0.000	0.251	0.782
Error	0.016	12	0.001		

ANOVA for NPQ

Source	Sum-of-Squares	df	Mean-Square	F-ratio	P
Salinity	0.345	2	0.172	15.847	0.000
Phosphorus	1.107	1	1.107	101.714	0.000
Salinity * Phosphorus	0.109	2	0.055	5.030	0.026
Error	0.131	12	0.011		

Appendix C.11 Analysis of variance for Salinity and Iron on fluorescence analysis

ANOVA for Fv/Fm

Source	Sum-of-Squares	df	Mean-Square	F-ratio	P
Salinity	0.048	2	0.024	8.064	0.006
Iron	0.725	1	0.725	244.748	0.000
Salinity * Iron	0.029	2	0.014	4.829	0.029
Error	0.036	12	0.003		

ANOVA for ΦPSII

Source	Sum-of-Squares	df	Mean-Square	F-ratio	P
Salinity	0.002	2	0.001	2.070	0.169
Iron	0.113	1	0.113	223.352	0.000
Salinity * Iron	0.004	2	0.002	3.893	0.050
Error	0.006	12	0.001		

ANOVA for qP

Source	Sum-of-Squares	df	Mean-Square	F-ratio	P
Salinity	0.019	2	0.009	0.564	0.583
Iron	0.459	1	0.459	27.407	0.000
Salinity * Iron	0.023	2	0.011	0.676	0.527
Error	0.201	12	0.017		

NPQ

Source	Sum-of-Squares	df	Mean-Square	F-ratio	P
Salinity	2.675	2	1.337	18.762	0.000
Iron	0.989	1	0.989	13.875	0.003
Salinity * Iron	1.831	2	0.915	12.841	0.001
Error	0.855	12	0.071		

Appendix C.12 Analysis of variance (ANOVA) for convexity values

ANOVA for Salinity and Bicarbonate effect

Source	Sum-of-Squares	df	Mean-Square	F-ratio	P
Salinity	0.667	2	0.333	501.583	0.000
Carbon	9.354	1	9.354	14068.519	0.000
Salinity * Carbon	0.229	2	0.115	172.580	0.000
Error	0.008	12	0.001		

ANOVA for Salinity and Phosphate effect

Source	Sum-of-Squares	df	Mean-Square	F-ratio	P
Salinity	2.872	2	1.436	1120.826	0.000
Phosphorus	10.273	1	10.273	8017.525	0.000
Salinity * Phosphorus	5.525	2	2.762	2155.997	0.000
Error	0.015	12	0.001		

ANOVA for Salinity and Iron effect

Source	Sum-of-Squares	df	Mean-Square	F-ratio	P
Salinity	0.287	2	0.143	123.513	0.000
Carbon	11.024	1	11.024	9499.627	0.000
Salinity * Carbon	0.398	2	0.199	171.551	0.000
Error	0.014	12	0.001		

Appendix D.1 Table for non-linear regression parameters and graph showing Jassby and Platt's function fit to the P-I curve of *Picochlorum* at 10 ppt in high carbon for a replicate.

$F = Pm \times \tanh \{(\alpha \times I)/Pm\} + R_d$

where P_{max} is light saturated photosynthetic rate , R_d is dark respiration, α is the initial slope and I is the light intensity.

Parameter	Value	StdErr	CV(%)	Dependencies
P_{max}	2.130e+1	1.819e+0	8.539e+0	0.5357220
R_d	5.239e-1	1.413e+0	2.696e+2	0.7191460
α	1.523e-1	3.777e-2	2.479e+1	0.5106309

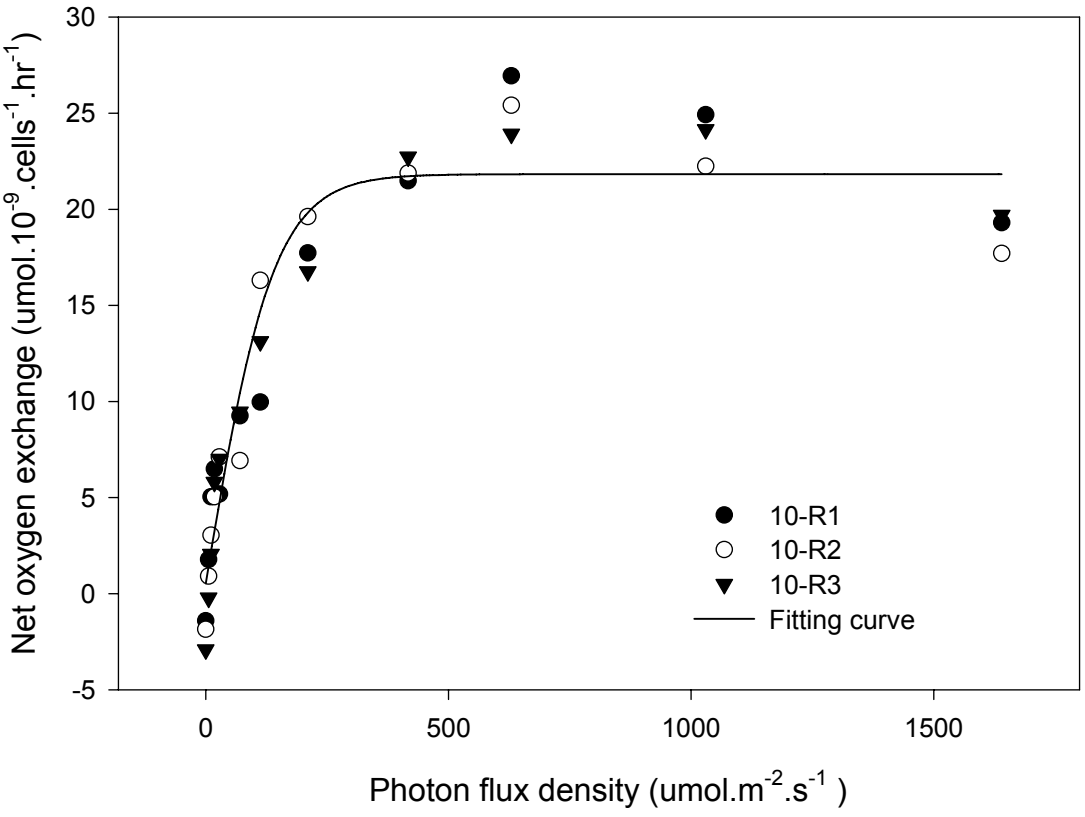

Appendix D.2 Table for non-linear regression parameters and graph showing Jassby and Platt's function fit to the P-I curve of *Picochlorum* at 50 ppt in high carbon for a replicate.

Parameter	Value	StdErr	CV(%)	Dependencies
P_{max}	2.203e+1	1.189e+0	5.400e+0	0.5025115
R_d	-6.028e-1	8.969e-1	1.488e+2	0.7004436
α	1.323e-1	2.065e-2	1.561e+1	0.5007885

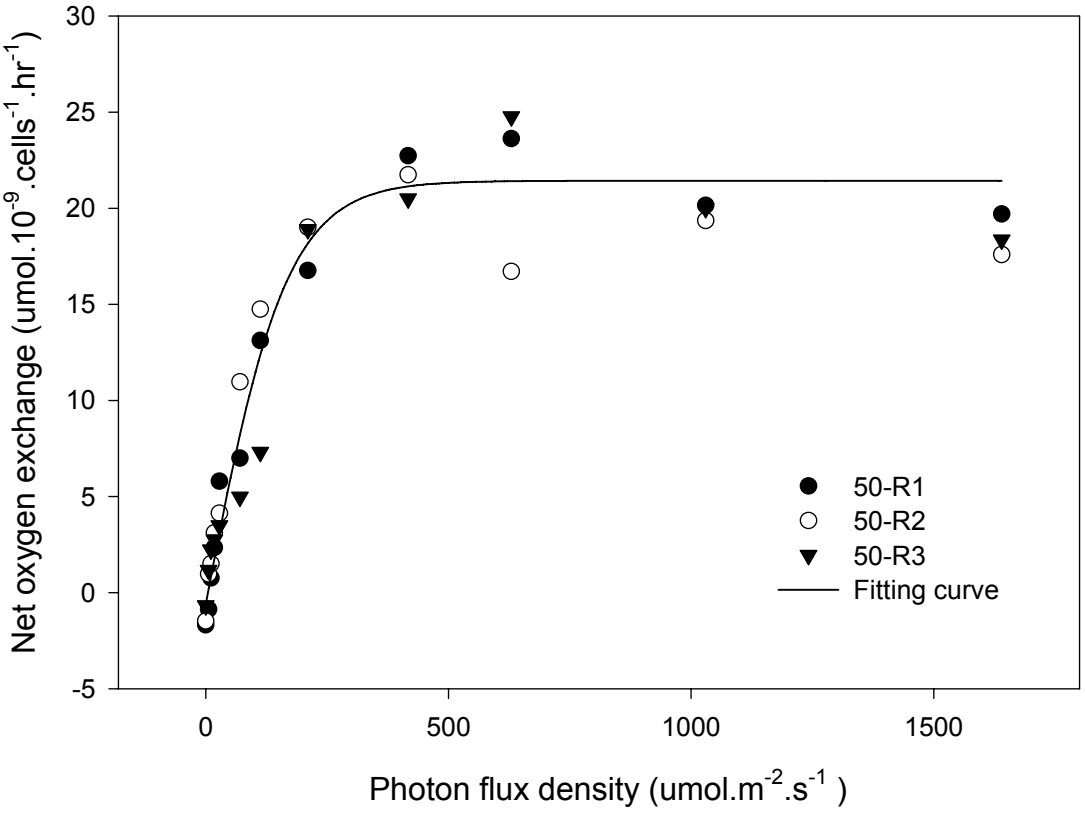

Appendix D.3 Table for non-linear regression parameters and graph showing Jassby and Platt's function fit to the P-I curve of *Picochlorum* at 100 ppt in high carbon for a replicate.

Parameter	Value	StdErr	CV(%)	Dependencies
P_{max}	1.387e+1	7.684e-1	5.540e+0	0.4632024
R_d	1.018e+0	5.595e-1	5.498e+1	0.6798591
α	6.870e-2	1.098e-2	1.599e+1	0.4928269

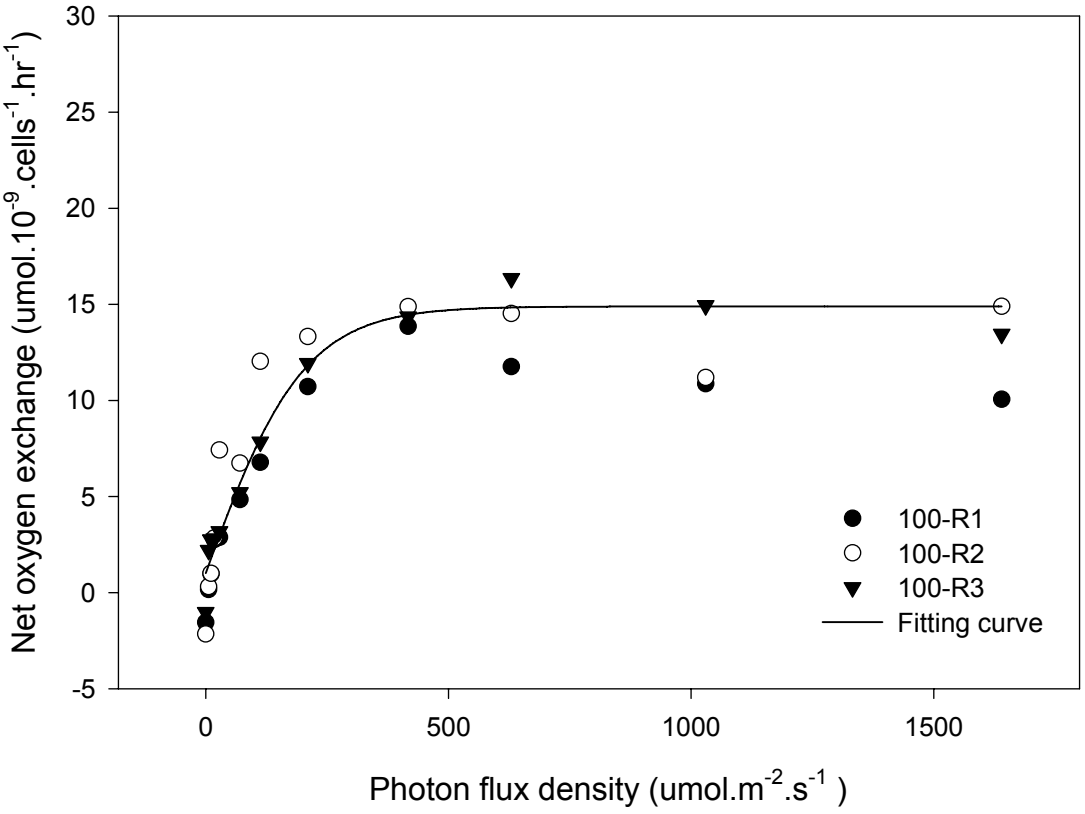

Appendix D.4 Table for non-linear regression parameters and graph showing Jassby and Platt's function fit to the P-I curve of *Picochlorum* at 10 ppt in low bicarbonate (LC) for a replicate.

Parameter	Value	StdErr	CV(%)	Dependencies
P_{max}	2.441e+1	1.614e+0	6.613e+0	0.4514992
R_d	-6.980e-1	1.163e+0	1.666e+2	0.6740419
α	1.145e-1	2.184e-2	1.907e+1	0.4912931

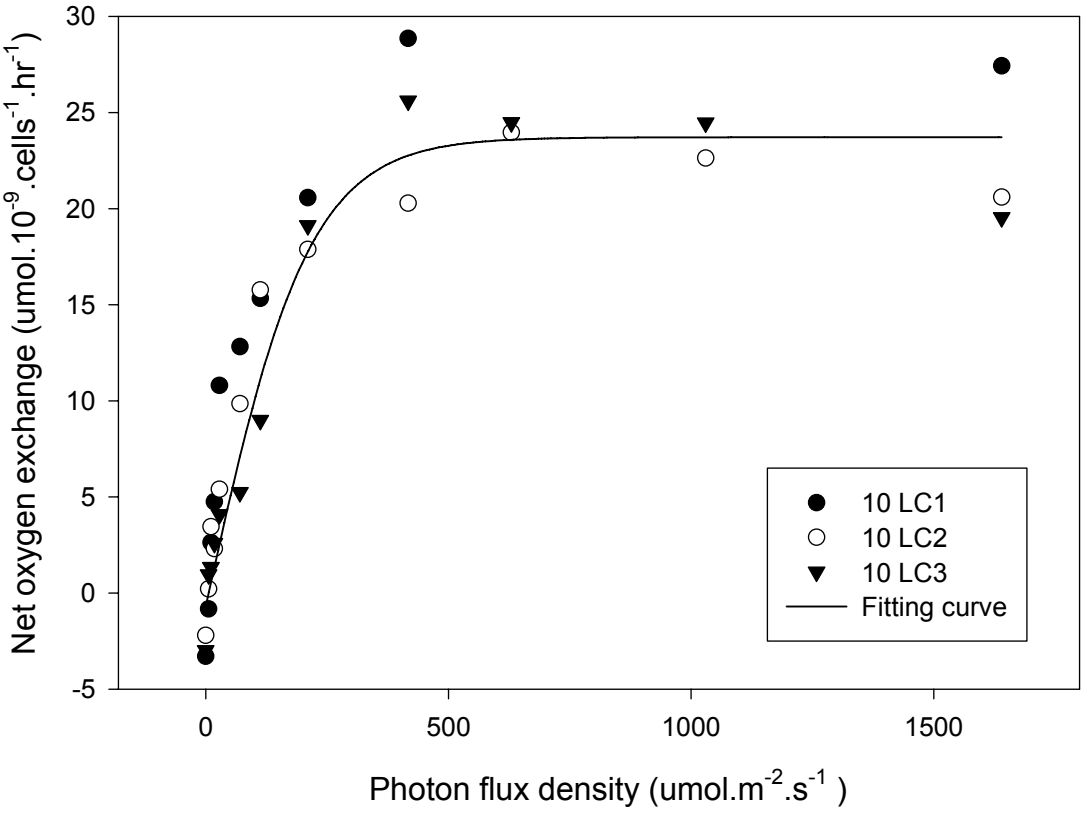

Appendix D.5 Table for non-linear regression parameters and graph showing Jassby and Platt's function fit to the P-I curve of *Picochlorum* at 50 ppt in low bicarbonate (LC) for a replicate.

Parameter	Value	StdErr	CV(%)	Dependencies
P_{max}	2.331e+1	2.611e+0	1.120e+1	0.5348006
R_d	-9.308e-1	2.026e+0	2.177e+2	0.7186153
α	1.654e-1	5.395e-2	3.261e+1	0.5103264

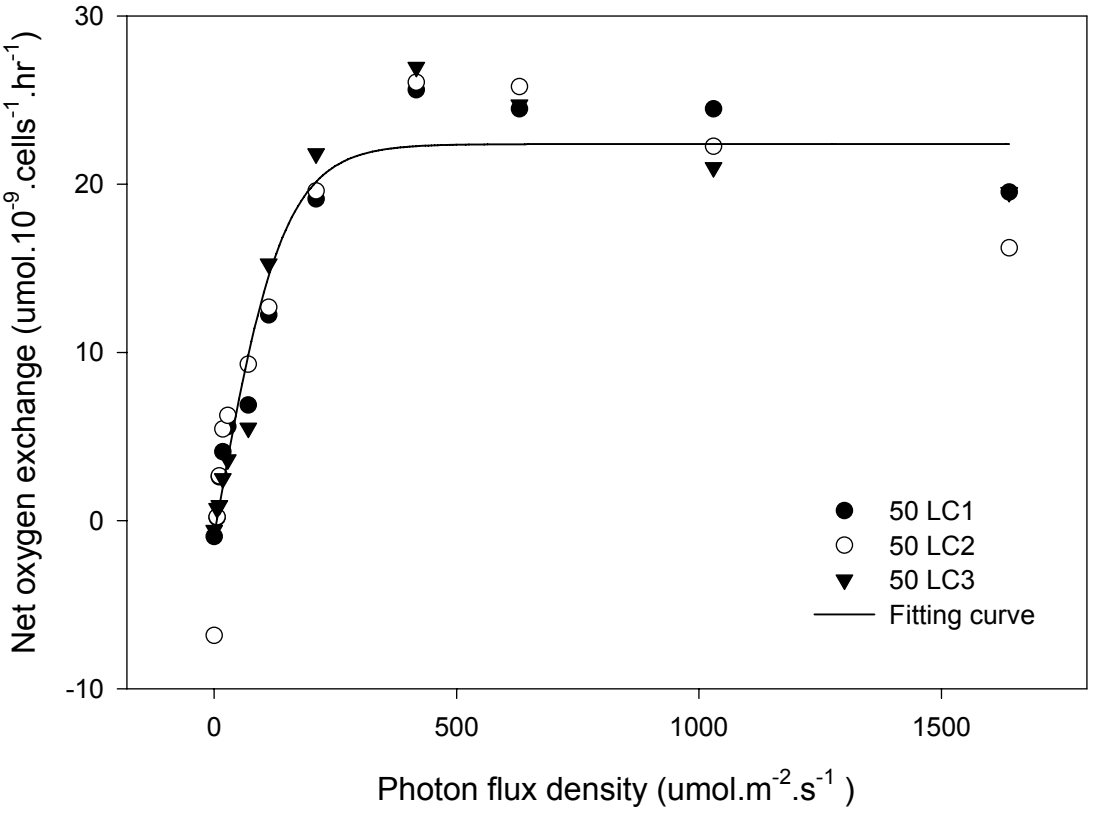

Appendix D.6 Table for non-linear regression parameters and graph showing Jassby and Platt's function fit to the P-I curve of *Picochlorum* at 100 ppt in low bicarbonate (LC) for a replicate.

Parameter	Value	StdErr	CV(%)	Dependencies
P_{max}	1.511e+1	1.209e+0	8.002e+0	0.4825794
R_d	1.620e-1	8.959e-1	5.530e+2	0.6897774
α	8.229e-2	1.898e-2	2.306e+1	0.4962012

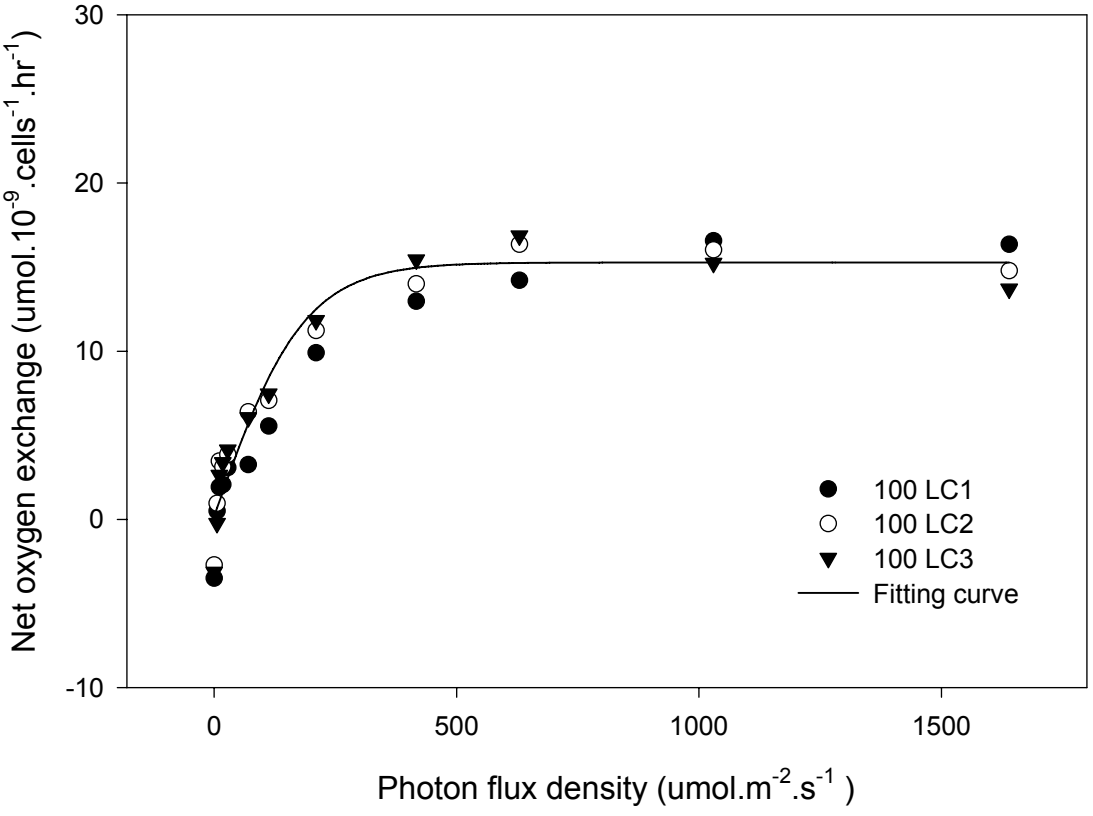

Appendix D.7 Table for non-linear regression parameters and graph showing Jassby and Platt's function fit to the P-I curve of *Picochlorum* at 10 ppt in low phosphate (LP) for a replicate.

Parameter	Value	StdErr	CV(%)	Dependencies
P_{max}	1.639e+1	9.584e-1	5.849e+0	0.5673629
R_d	7.541e-2	7.657e-1	1.015e+3	0.7376853
α	1.385e-1	2.380e-2	1.719e+1	0.5221345

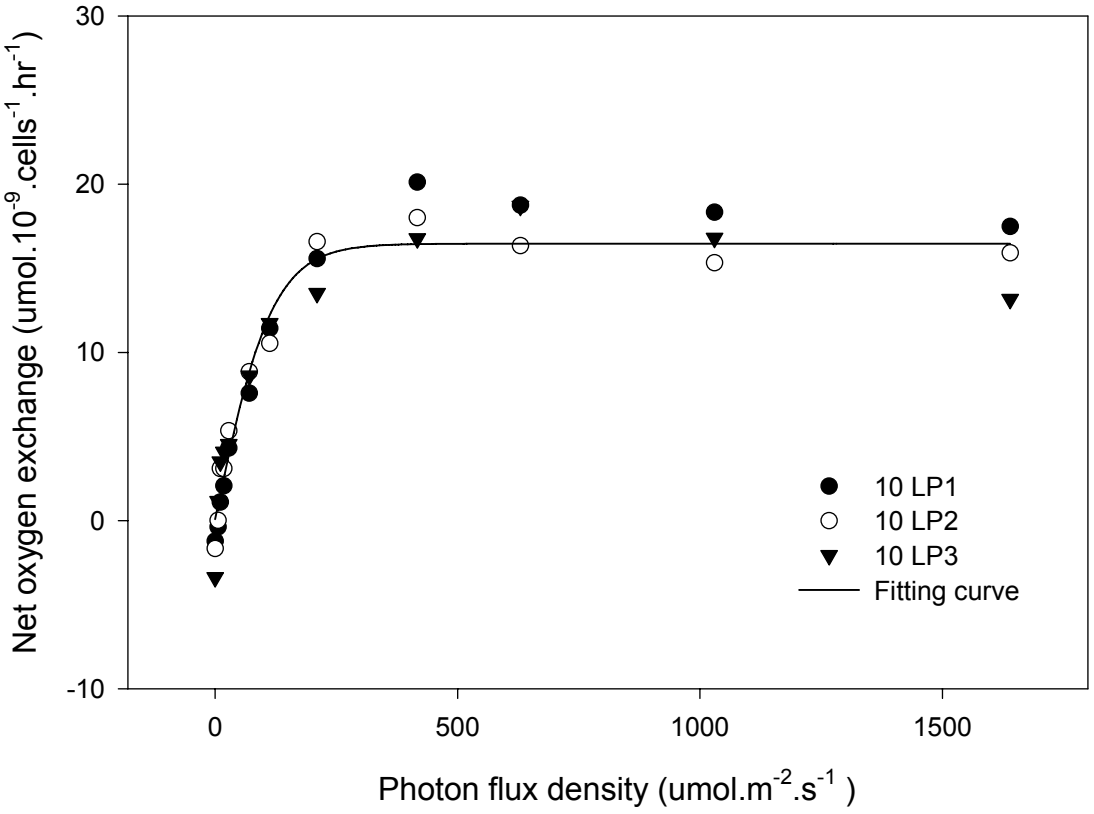

Appendix D.8 Table for non-linear regression parameters and graph showing Jassby and Platt's function fit to the P-I curve of *Picochlorum* at 50 ppt in low phosphate (LP) for a replicate.

Parameter	Value	StdErr	CV(%)	Dependencies
P_{max}	1.725e+1	1.550e+0	8.985e+0	0.5983775
R_d	-1.915e+0	1.273e+0	6.648e+1	0.7565408
α	1.722e-1	4.608e-2	2.676e+1	0.5360453

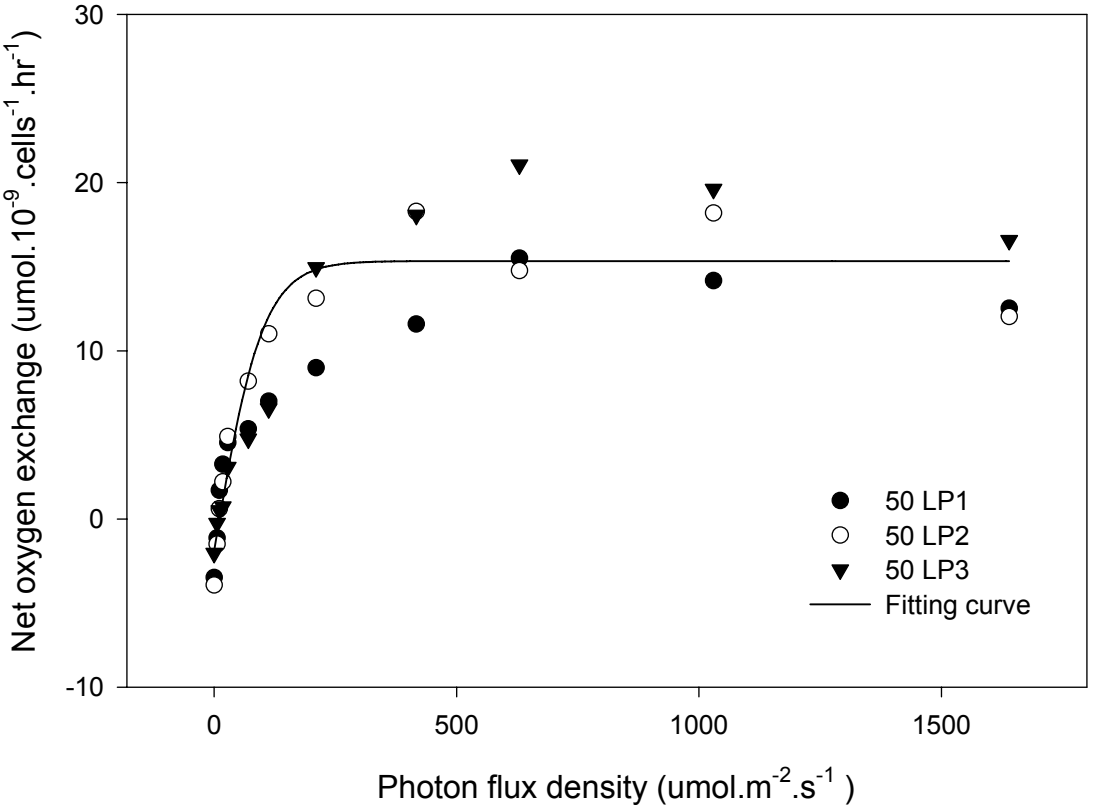

Appendix D.9 Table for non-linear regression parameters and graph showing Jassby and Platt's function fit to the P-I curve of *Picochlorum* at 100 ppt in low phosphate (LP) for a replicate.

Parameter	Value	StdErr	CV(%)	Dependencies
P_{max}	1.080e+1	3.672e-1	3.399e+0	0.5975630
R_d	-7.910e-1	3.014e-1	3.810e+1	0.7560352
α	1.072e-1	1.086e-2	1.013e+1	0.5356355

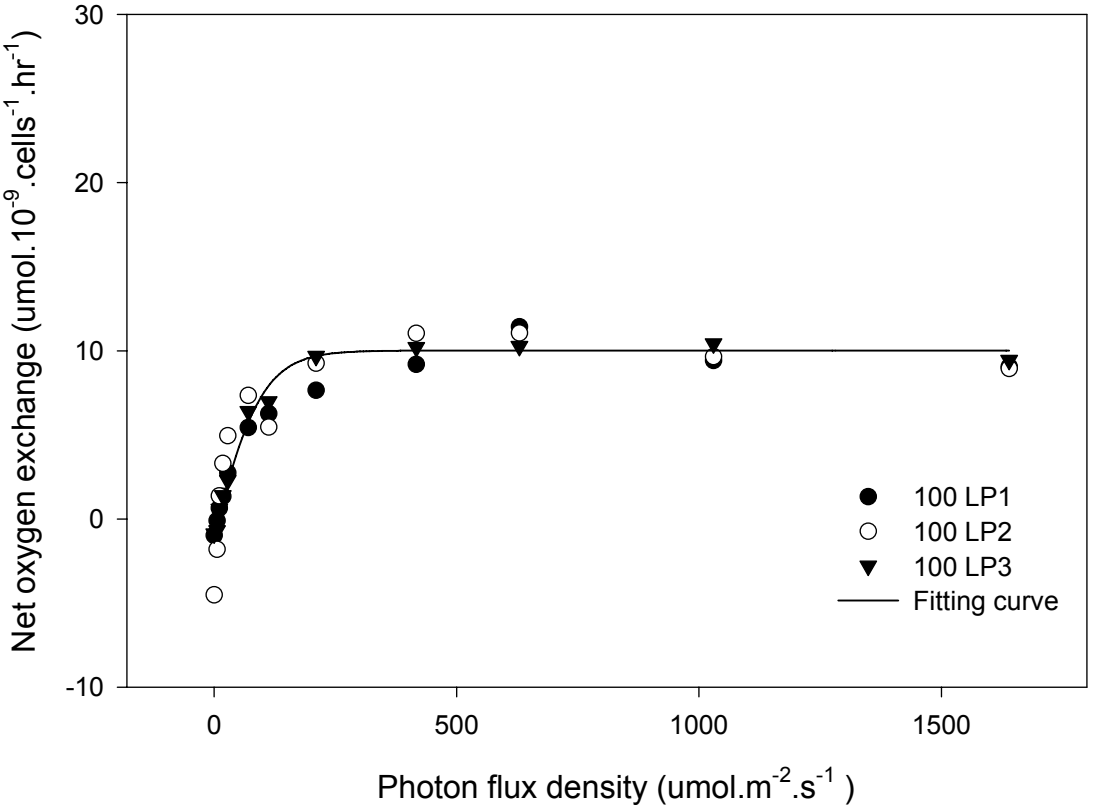

Appendix D.10 Table for non-linear regression parameters and graph showing Jassby and Platt's function fit to the P-I curve of *Picochlorum* at 10 ppt in no added iron (-Fe) medium for a replicate.

Parameter	Value	StdErr	CV(%)	Dependencies
P_{max}	1.178e+1	1.072e+0	9.100e+0	0.7727544
R_d	-1.487e+0	9.876e-1	6.642e+1	0.8576216
α	2.766e-1	7.594e-2	2.745e+1	0.6473311

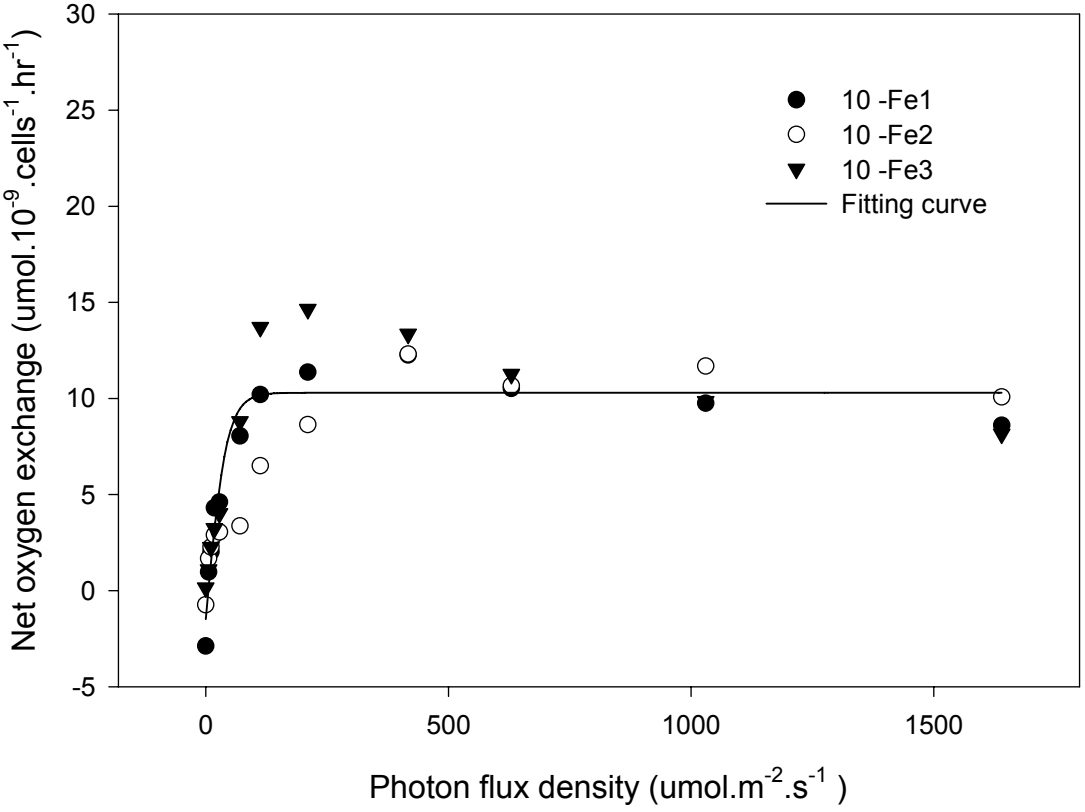

Appendix D.11 Table for non-linear regression parameters and graph showing Jassby and Platt's function fit to the P-I curve of *Picochlorum* at 50 ppt in no added iron (-Fe) medium for a replicate.

Parameter	Value	StdErr	CV(%)	Dependencies
P_{max}	1.279e+1	1.548e+0	1.211e+1	0.7009229
R_d	-7.735e-1	1.385e+0	1.790e+2	0.8205483
α	2.101e-1	8.067e-2	3.840e+1	0.6039127

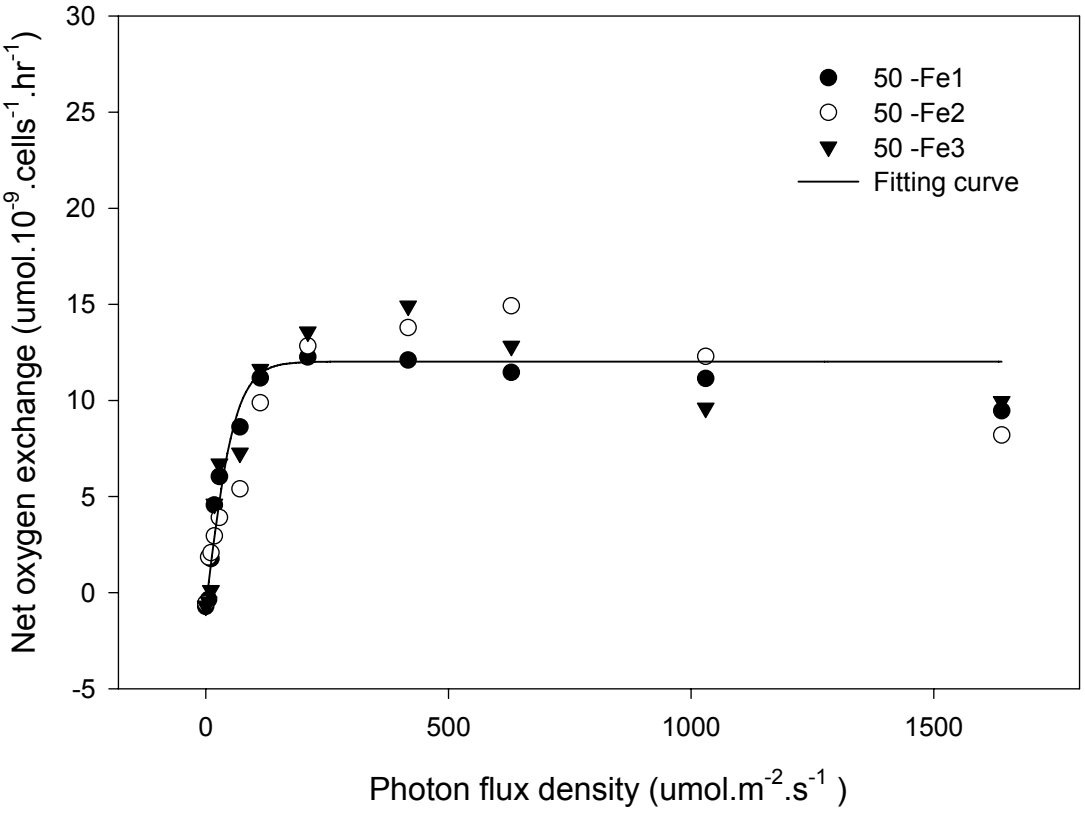

Appendix D.12 Table for non-linear regression parameters and graph showing Jassby and Platt's function fit to the P-I curve of *Picochlorum* at 100 ppt in no added iron (-Fe) medium for a replicate.

Parameter	Value	StdErr	CV(%)	Dependencies
P_{max}	8.078e+0	4.890e-1	6.054e+0	0.7503222
R_d	-5.043e-1	4.480e-1	8.884e+1	0.8469803
α	1.671e-1	3.158e-2	1.890e+1	0.6359717

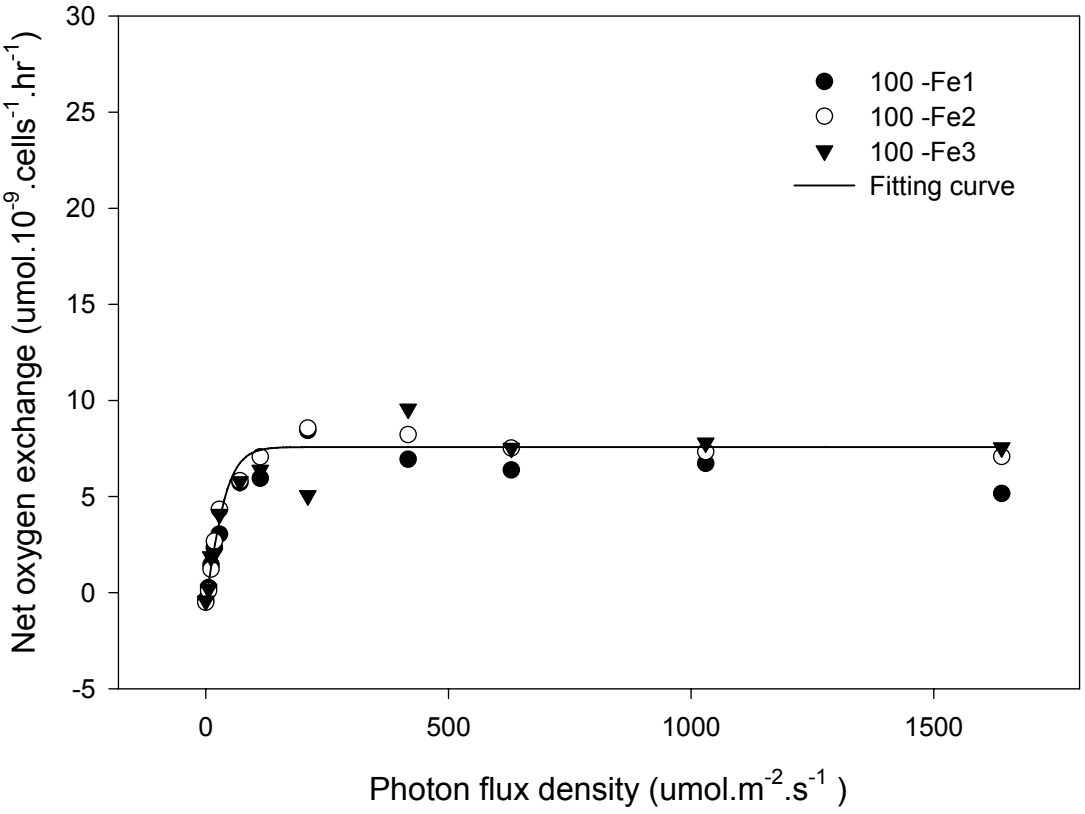

VITA

Joseph Nana Annan

Candidate for the Degree of

Doctor of Philosophy

Thesis: GROWTH RESPONSE OF THE GREEN ALGA *PICOCHLORUM OKLAHOMENSIS* TO NUTRIENT LIMITATION AND SALINITY STRESS

Major Field: Plant Science

Biographical:

Personal Data: Born in Sekondi, Western Region, Ghana, on October 12, 1966, to Samuel A. Annan and Emma Kwofie.

Education: Graduated from Ghana National College, Cape Coast with General Certificate of Education Ordinary and Advanced levels in 1985 and 1987 respectively; Received Bachelor of Science degree in Botany and Zoology and Diploma in Education in 1992 and Master of Philosophy in Botany in 1999 from the University of Cape Coast, Ghana; Completed the requirements for the Doctor of Philosophy degree in Plant Science at Oklahoma State University, Stillwater, Oklahoma in May, 2008.

Experience: Assistant Lecturer, Department of Science Edu., University College of Education (UCEW), Winneba, Ghana, September 1999 to September 2001; Lecturer, Department of Science Education, UCEW/ University of Education, Winneba, Ghana, October 2001 to date; Research Assistant and/or Teaching Assistant/ Associate, Department of Botany, Oklahoma State University, June 2002 to August 2007; Lecturer, Department of Botany, Oklahoma State University, August 2007 to mid-May 2008.

Publication: Annan, J. N., Galyuon, I. K. A. and Donkor, V. A. 2007. Effects of solar radiation on photosynthesis and pigmentation in the cyanobacterium, *Microcoleus chthonoplastes*. *Journal of Ghana Science Association*. 9(1): 135-150.

Professional Memberships: Ghana Science Association, January 2001 to December 2002; Phycological Society of America, January 2004 to December 2008; American Society of Plant Biologists, January 2004 to December 2008.

Name: Joseph Nana Annan Date of Degree: July, 2008

Institution: Oklahoma State University Location: Stillwater, Oklahoma

Title of Study: GROWTH RESPONSE OF THE GREEN ALGA *PICOCHLORUM OKLAHOMENSIS* TO NUTRIENT LIMITATION AND SALINITY STRESS

Pages in Study: 142 Candidate for the Degree of Doctor of Philosophy

Major Field: Plant Science

Abstract: Photosynthetic organisms rarely experience optimal growth conditions in their natural habitat, and at any given time, two or more physical and chemical variables are likely to be suboptimal. It has been previously established that the extreme environment of the Great Salt Plains (GSP) results in low algal biomass, such that natural selection is likely driven by survival of multiple abiotic stresses rather than rapid growth and biotic interactions. The purpose of this study is to determine the effect of combined abiotic stress factors on growth and photosynthesis in the green alga *Picochlorum oklahomensis* isolated from the GSP habitat, specifically salinity and the inorganic nutrients phosphorus (P), iron (Fe) and carbon (C).

Algal cells were grown in batch cultures under high or limited P, Fe and C at salinities of 10, 50 and 100 ppt in artificial seawater (AS 100) medium. Cells were physiologically characterized by initial growth rates and cell yields, photosynthetic light-response curves (oxygen evolution), pigment composition, and the chlorophyll fluorescence parameters F_v/F_m , Φ_{PSII}, qP and NPQ.

In general, low P and low Fe resulted in significant primary effects and interaction with salinity for the majority of variables; a significant primary effect of C and C-salinity interaction were less common among the physiological variables, probably because cultures are open to atmospheric CO_2 but not to P or Fe. The chlorophyll fluorescence parameters F_v/F_m, Φ_{PSII} and NPQ all exhibit smaller responses to limitation by phosphorus or iron when grown at 100 ppt compared to 10 ppt. Similarly, with respect to pigment content and most fluorescence parameters, *P. oklahomensis* cultured in low P or Fe exhibit smaller inhibition by 100 ppt salinity relative to 10 ppt. Thus high salinity stress appears to be reduced under low nutrient conditions. P and Fe stress resulted in qualitative differences in physiological response. The overall P stress response indicates reversible photoprotection, whereas Fe stress response indicates chronic inhibition of PSII.

The interaction between salinity and P or Fe, together with previous reports of salinity-temperature interaction, are consistent with a general stress response that concurrently protects against several abiotic stress factors.

ADVISER'S APPROVAL: Dr. William J. Henley